

CR 151098

MC-76-476
. AS9-14653

FINAL REPORT

September, 1976

Detection of Tightly Closed Flaws by Nondestructive Testing (NDT) Methods in Steel and Titanium

Ward D. Rummel, Richard A. Rathke,
Paul H. Todd, Jr., Thomas L. Tedrow,
and Steve J. Mullen

Mr. W. L. Castner
NASA Technical Monitor

(NASA-CR-151098) DETECTION OF TIGHTLY
CLOSED FLAWS BY NONDESTRUCTIVE TESTING (NDT)
METHODS IN STEEL AND TITANIUM Final Report,
Jul. 1975 - Sep. 1976 (Martin Marietta
Aerospace, Denver, Colo.) 109 p

N77-15133
MC A06
MF A01
Unclassified
G3/20 59651

Final Report of Research Performed
under Contract NAS9-14653
for the

National Aeronautics and Space Administration
Lyndon B. Johnson Space Center
Houston, Texas 77058



MARTIN MARIETTA

1. Report No.	2. Government Accession No.	3. Recipient's Catalog No.	
4. Title and Subtitle DETECTION OF TIGHTLY CLOSED FLAWS BY NONDESTRUCTIVE TESTING (NDT) METHODS IN STEEL AND TITANIUM		5. Report Date September 1976	
7. Author(s) Ward D. Rummel, Richard A. Rathke, Paul H. Todd, Jr., Thomas L. Tedrow and		6. Performing Organization Code	
9. Performing Organization Name and Address Martin Marietta Aerospace Denver Division Denver, Colorado 80201		8. Performing Organization Report No. MCR-76-476	
12. Sponsoring Agency Name and Address National Aeronautics and Space Administration Washington, D.C. 20546		10. Work Unit No.	
		11. Contract or Grant No. NAS9-14653	
		13. Type of Report and Period Covered Contractor Report July 1975 - September 1976	
15. Supplementary Notes			
16. Abstract X-radiographic, liquid penetrant, ultrasonic, eddy current and magnetic particle testing techniques were optimized and applied to the evaluation of 4340 steel (180 KSI-UTS) and 6Al-4V titanium (STA) alloy specimens. Sixty steel specimens containing a total of 176 fatigue cracks and sixty titanium specimens containing a total of 135 fatigue cracks were evaluated. The crack ranged in length from .043 cm (.017 inch) to 1.02 cm (.400 inch) and in depth from .005 cm (.002 inch) to .239 cm (.094 inch) for steel specimens. Lengths ranged from .48 cm (0.019 inch) to 1.03 cm (.407 inch) and depths from 0.010 cm (.004 inch) to .261 cm (0.103 inch) for titanium specimens. Specimen thicknesses were nominally .152 cm (0.060 inch) and 0.635 cm (0.250 inch) and surface finishes were nominally 125 rms. Specimens were evaluated in the "as machined" surface condition, after etch surface and after proof loading in a randomized inspection sequence. Specimens were fractured and the actual crack sizes determined by measurement. Inspection data were then analyzed and plotted at 95% confidence by a sequential overlapping data grouping method. Lower confidence limits were calculated and plotted for each data group.			
17. Key Words Nondestructive Testing Flaw Detection Reliability Liquid Penetrant Ultrasonic Eddy Current X-radiography	Magnetic Particle Steel Titanium Fracture Cont. Fatigue Crack	18. Distribution Statement Unclassified - Unlimited Cat. 26	
19. Security Classif. (of this report) Unclassified	20. Security Classif. (of this page) Unclassified	21. No. of Pages 109	22. Price

PREFACE

This report was prepared by Martin Marietta Aerospace under Contract NAS9-14653. The study was initiated by the National Aeronautics and Space Administration, Lyndon B. Johnson Space Center to determine the ability of current, state-of-the-art, nondestructive testing techniques to detect surface cracks in high strength steel and titanium alloys. The work described herein was completed between July 1975 and September 1976. Mr. W. L. Castner of the Lyndon B. Johnson Space Center provided technical direction and monitor for this work.

At Martin Marietta Aerospace, Mr. Ward D. Rummel provided technical direction and program management. Mr. Richard A. Rathke was the principle investigator for eddy current testing and statistical data analysis techniques. Messrs. Paul H. Todd, Jr. and Steve J. Mullen were principle investigators for ultrasonic, magnetic particle and liquid penetrant testing techniques. Mr. Thomas L. Tedrow was the principle investigator for X-radiographic testing techniques. The inspection and analysis studies were supported by Messrs. H. D. Brinkerhoff, and S. R. Marston. Specimen preparation was supported by Mr. W. Arbegast, Dr. Conrad F. Fiftal, Mr. John Shepic and Mr. W. Post.

Management support was provided by Messrs. G. McGee, C. Danstedt, J. Seidl and R. Daum.

Editing and typing were done by Ms. M. Losey.

The assistance and cooperation of all contributing personnel are appreciated and gratefully acknowledged. We also appreciate the program direction, support and numerous contributions of Mr. W. L. Castner and gratefully acknowledge his continuing support.

CONTENTS

	Page
PREFACE	iii
SUMMARY	ix
I. INTRODUCTION	1
Program Orientation	2
Experimental Test Program Approach	2
II. TEST SPECIMEN PREPARATION	5
Preparation of Specimen Blanks	5
Fatigue Crack Growth Procedures	5
Preparation of Test Specimens	8
Test Specimens	9
Flaw Location	9
Specimen Machining	11
III. NDT METHODS OPTIMIZATION AND PROCEDURES	
DEVELOPMENT	12
Nondestructive Test Evaluation	12
X-Radiography Optimization	12
Liquid Penetrant Optimization	13
Ultrasonic Test Optimization	16
Eddy Current Test Optimization	16
Magnetic Particle Test Optimization	20
IV. NDT EVALUATION OF TEST SPECIMENS	21
Sequence 1 - Evaluation of Specimens in the As Machined Condition	21
Sequence 2 - Evaluation of Specimens in the Post-Etched Condition	23
Sequence 3 - Evaluation of Specimens in the Post-Proof Loaded Condition	23
V. SPECIMEN FRACTURE AND CRACK MEASUREMENT	25
VI. DATA ANALYSIS	26
Actual Crack Data	26
Nondestructive Test Data	26
Data Ordering	26
Statistical Analysis	26
Data Plotting	48
VII. RESULTS, CONCLUSIONS AND RECOMMENDATIONS	68
References	71

APPENDIX

	Page
A. DETECTION OF TIGHTLY CLOSED FLAWS BY RADIOGRAPHIC INSPECTION IN STEEL AND TITANIUM	73
B. LIQUID PENETRANT INSPECTION PROCEDURE FOR FATIGUE CRACK DETECTION	80
C. ULTRASONIC INSPECTION FOR FATIGUE CRACK PROGRAM PANELS	83
D. EDDY CURRENT INSPECTION AND C-SCAN RECORDING OF TITANIUM PANELS	90
E. EDDY CURRENT INSPECTION AND C-SCAN RECORDING OF STEEL PANELS	94
F. FLUORESCENT MAGNETIC PARTICLE INSPECTION FOR FATIGUE CRACK DETECTION	97

Figure

	<u>Page</u>
1. Sequence of the Test Program	4
2. Side View of Crack Starter and Final Crack Configuration, Cases 1 and 2	6
3. Side View of Crack Starter and Final Crack Configuration, Cases 3 and 4	7
4. Grid Pattern Layout	10
5. NDT Specimen Configuration	11
6. Comparison of P-149 and I-319 Fluorescent Penetrants by the Meniscus Method (P-149 on the Left has Superior Thin Film Sensitivity)	14
7. Comparison of P-149 and P6F-4 Fluorescent Penetrants by the Meniscus Method (P6F-4 on the Right has Superior Thin Film Sensitivity)	14
8. Ultrasonic Shear Wave, Pulse-Echo Reflected Signal Amplitude from a Case 1 Crack as a Function of Incident Angle	17
9. Spring-Loaded Flat Block, Eddy Current Scanning Probe Holder	18
10. Spring-Loaded Eddy Current Scanning Probe Holder Used on Warped Panels	19
11. Intentional and Unintentional Cracks Revealed by Penetrant (Actual Size)	22
12. Crack Detection Probability of the X-radiographic Inspection Method for Titanium Specimens Plotted by Actual Crack Length at 95% Confidence	50
13. Crack Detection Probability of the X-radiographic Inspection Method for Titanium Specimens Plotted by Actual Crack Depth at 95% Confidence	51
14. Crack Detection Probability of the Penetrant Inspection Method for Titanium Specimens Plotted by Actual Crack Length at 95% Confidence	52
15. Crack Detection Probability of the Penetrant Inspection Method for Titanium Specimens Plotted by Actual Crack Depth at 95% Confidence	53
16. Crack Detection Probability of the Ultrasonic Inspection Method for Titanium Specimens Plotted by Actual Crack Length at 95% Confidence	54

17.	Crack Detection Probability of the Ultra- sonic Inspection Method for Titanium Specimens Plotted by Actual Crack Depth at 95% Confidence	55
18.	Crack Detection Probability of the Eddy Current Inspection Method for Titanium Specimens Plotted by Actual Crack Length at 95% Confidence	56
19.	Crack Detection Probability of the Eddy Current Inspection Method for Titanium Specimens Plotted by Actual Crack Depth at 95% Confidence	57
20.	Crack Detection Probability of the X- radiographic Inspection Method for Steel Specimens Plotted by Actual Crack Length at 95% Confidence	58
21.	Crack Detection Probability of the X- radiographic Inspection Method for Steel Specimens Plotted by Actual Crack Depth at 95% Confidence	59
22.	Crack Detection Probability of the Penetrant Inspection Method for Steel Specimens Plotted by Actual Crack Length at 95% Confidence	60
23.	Crack Detection Probability of the Penetrant Inspection Method for Steel Specimens Plotted by Actual Crack Depth at 95% Confidence	61
24.	Crack Detection Probability of the Ultra- sonic Inspection Method for Steel Specimens Plotted by Actual Crack Length at 95% Confidence	62
25.	Crack Detection Probability of the Ultrasonic Inspection Method for Steel Specimens Plotted by Actual Crack Depth at 95% Con- fidence	63
26.	Crack Detection Probability of the Eddy Current Inspection Method for Steel Specimens Plotted by Actual Crack Length at 95% Confidence	64
27.	Crack Detection Probability of the Eddy Current Inspection Method for Steel Specimens Plotted by Actual Crack Depth at 95% Confidence	65
28.	Crack Detection Probability of the Magnetic Particle Inspection Method for Steel Specimens Plotted by Actual Crack Length at 95% Confidence	66

29. Crack Detection Probability of the Magnetic
Particle Inspection Method for Steel Specimens
Plotted by Actual Crack Depth at 95%
Confidence 67

Table

	<u>Page</u>
1. Factors in Test Specimen Preparation	5
2. EDM Notch and Fatigue Flaw Sizes for Bending Fatigue of 4340 Steel ($u = 180$ KSI) and 6Al-4V Titanium STA	8
3. Flaw Distribution in Steel and Titanium Specimens	9
4. Results of Penetrant Evaluation by the Meniscus Method	15
5. Actual Crack Data - Titanium	27
6. Tabulation of Nondestructive Test Observations for Titanium, Sequence 1	30
7. Tabulation of Nondestructive Test Observations for Titanium, Sequence 2	33
8. Tabulation of Nondestructive Test Observations for Titanium, Sequence 3	34
9. Actual Crack Data - Steel	37
10. Tabulation of Nondestructive Test Observations for Steel, Sequence 1	40
11. Tabulation of Nondestructive Test Observations for Steel, Sequence 2	43
12. Tabulation of Nondestructive Test Observations for Steel, Sequence 3	44

THE DETECTION OF TIGHTLY CLOSED FLAWS
BY NONDESTRUCTIVE TESTING (NDT) METHODS
IN STEEL AND TITANIUM

By Ward D. Rummel, Richard A. Rathke,
Paul H. Todd, Jr., and Steve J. Mullen
Martin Marietta Aerospace

SUMMARY

This program was conducted to investigate the reliability of state-of-the-art production nondestructive testing (NDT) techniques to detect tightly closed fatigue cracks in high strength steel (4340 - 180 KSI) and titanium 6Al-4V - STA alloys. X-radiography, liquid penetrant, ultrasonic, eddy current and magnetic particle (steel only) techniques were evaluated and analyzed to determine detection sensitivities.

176 fatigue cracks in 60 steel specimens and 135 fatigue cracks in 60 titanium specimen were evaluated with specimens in the "as machined" surface condition, after etching to remove flowed material due to machining and after proof loading. Specimen thicknesses were 0.152 cm (0.060 inch) and 0.635 cm (0.250 inch) for both materials. After all specimens were fractured to evaluate and measure actual crack size.

Comparison and statistical analysis of all NDT data was performed with respect to actual measured crack size. Analyses were performed to determine detection reliabilities at the 95% confidence level using a data grouping and "count down" method based on actual crack dimensions. Overlapping of data groups (independent observations) was used to smooth data for graphical presentations. Plots of detection reliabilities as a function of crack factors variables were minimized by consistent and rigid application of inspection procedures and by use of experienced and dependable personnel. Strict application of this data can be made only for the materials and test conditions described. Improved reliabilities may be obtained by application of different procedures or by application of procedures to more rigorous controlled test specimens (i.e., polished, length and crack depth are reported as well as the actual data files used in analysis and plotting. Lower confidence limits for each data group were estimated by binomial distribution analysis

and plotted with the reliability data. Results show an increase in detection reliability for the liquid penetrant inspection method after etching the specimen surfaces. An increase in detection reliability for all methods was obtained after proof loading the specimens. The results reflect capabilities of state-of-the-art production methods when, properly applied and human factors, test condition and other procedural variables are minimized.

I. INTRODUCTION

Nondestructive testing (NDT) is a major tool in modern engineering structures technology. Structural integrity, reliability and maintainability are direct functions of the NDT program applied during manufacture. The safety, reliability and life cycle costs of a structure are dependent on the capabilities and reliabilities of the NDT applied to it during manufacture and field maintenance operations. Recent analyses have shown that a greater impact on structures life can be gained by improvement of NDT capabilities than by improvement in all other tangible life cycle design elements (i.e., stress analysis, fracture toughness, fatigue life).¹.

A critical element in an NDT technology improvement program is an understanding of current capabilities of NDT techniques. A review of NDT literature reveals a wide range of descriptions of methods applied and flaws (or material anomalies) detected. Little statistically reliable flaw detection data for various nondestructive test (NDT) methods are available.^{2,3} In seeking and establishing NDT reliability data, it is necessary to understand and separate the elements of an NDT process as applied in current state-of-the-art production processes. These elements include:

1. Flaw detection
2. Flaw description - size, orientation, geometry, etc., and
3. Flaw location.

The primary thrust of NDT technology has been in flaw detection or more generally in establishing "how small a flaw can be detected?" In establishing the flaw detection reliability of a technique, the thrust must be shifted to determining "how large a flaw can be missed?" Flaw detection reliability (i.e., "how large a flaw can be missed?") is a key factor in the application of linear elastic fracture mechanics and fracture control principles in design acceptance. The program described herein was conducted to investigate the reliability of various NDT methods to detect tightly closed flaws in titanium and steel alloy sheet and plate. Controlled application of state-of-the-art NDT methods were made to test specimens of varying surface conditions and proof stress load exposure to establish

and plot respective flaw detection reliabilities as a function of flaw size and test specimen condition.

Program Orientation

In the NASA Space Shuttle and other advanced spacecraft programs, fracture control will be assured by a combination of (1) linear elastic fracture mechanics in design and analysis and (2) nondestructive testing in structural assessment and verification. The detectable flaw size, as determined by nondestructive testing, will be used as a basis for establishing design allowables. A program to determine the detectable flaw size was required to provide preliminary design data.

High strength titanium and steel alloys are used in critical hardware assemblies and must be assessed by nondestructive testing methods for soundness. These materials differ from other structural materials in flaw growth, flaw tolerance and in physical response to nondestructive interrogation (test) methods. Criticality of application and unique NDT method interaction make specific evaluation of NDT flaw detection reliability for these materials necessary.

Related NDT flaw detection reliability programs were used to select the range of flaw sizes evaluated, the test methods evaluated, the general program approach, the format for the data generated and the data analysis methods applied.

Experimental Test Program Approach

Experience has shown that small, tightly closed cracks are one of the most difficult types of flaws to detect and are one of the flaw types most detrimental to load-carrying structures. Tightly closed flaws may be simulated by artificially induced fatigue cracks. The size and shape of an artificially induced fatigue crack may be varied and controlled over a wide range of conditions and thus making it a good selection for experimentally evaluating NDT flaw detection reliability. Artificially induced fatigue cracks in flat titanium and steel sheet and plate test specimens were chosen for evaluating NDT reliability.

Many variables in the nondestructive testing method to be applied are possible. To meet the objective of the program, (i.e., to establish preliminary design data) nondestructive

testing methods were selected which are representative of current state-of-the-art production practices. Details of the method and the procedure for application were documented and described in sufficient detail to (1) enable duplication of the results by independent investigators and (2) to enable objective comparison of results obtained by variations in the methods. Details of the methods and procedures are included in the appendix of this report. These methods were applied by NDT personnel using conventional equipment which is routinely used in production inspection. Since the primary objective of the program was to determine the ability of nondestructive testing (NDT) methods to reliably detect small, tightly closed flaws in titanium and steel, efforts were made to minimize human factors. Experienced and dependable NDT personnel were employed for all evaluations. Production part test conditions were simulated as closely as possible by evaluation of the test specimens in the "as machined" condition by X-radiographic, liquid penetrant, ultrasonic, eddy current and magnetic particle (steel only) techniques; evaluation of all specimens by the liquid penetrant technique after etching the test specimen surfaces; and evaluation by all techniques after the specimen had been proof loaded. Each evaluation was performed by three independent NDT operators to provide an internal check of detectability and to randomize test results.

With the objectives, required data, test conditions and analysis methods defined an experimental test program was planned and completed. The test program was divided into the following elements:

1. Test specimen preparation;
2. NDT method optimization and procedure development;
3. NDT evaluations;
4. Specimen fracture and flaw measurement;
5. Data correlation and analysis.

The sequence of the program is shown in Figure 1.

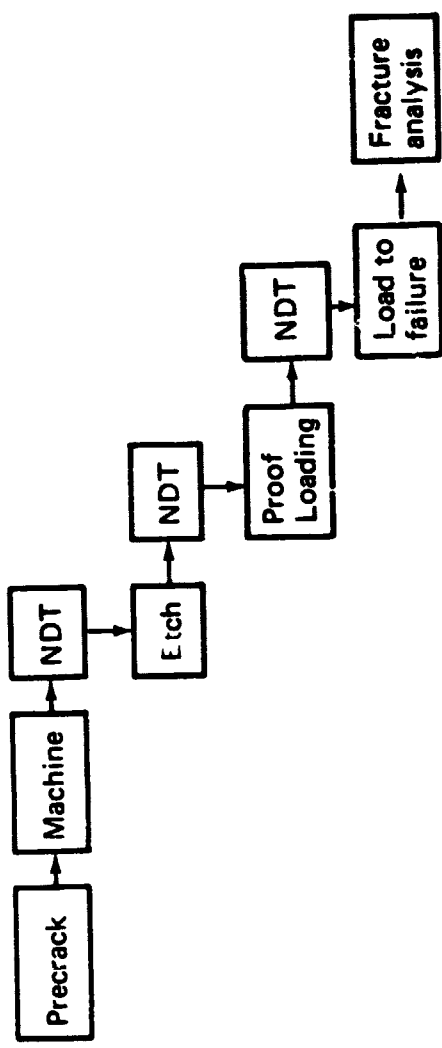


Figure 1. Sequence of the Test Program

II. TEST SPECIMEN PREPARATION

Preparation of test specimens used in reliability demonstration programs is a critical program step. Factors which must be considered in specimen preparation are summarized in Table 1.

Table 1. Factors in Test Specimen Preparation

Specimen Material - type, alloy condition and thickness
Specimen Size and configuration
Flaw Types - size, shape, orientation and location
Flaw Initiation Method and Conditions of Growth
Flaw Starter Notch Removal - Method, depth
Final Specimen - Configuration, thickness and surface condition

Preparation of Specimen Blanks

For this program, high strength steel and titanium alloys were to be evaluated in 0.152 cm (0.060 inch) and 0.635 cm (.250 inch) thicknesses. 6 Al-4V titanium alloy and 4340 steel ($\sigma_u = 180$ KSI). Initial material thicknesses of 0.317 cm (0.125 inch) and 0.792 cm (0.312 inch) were procured for specimen preparation. Material sheets were cut into 40.64 cm (16 inches) by 15.24 cm (6 inches) specimen blanks with the sheet grain direction oriented along the length of the specimen. 6 Al-4V titanium was procured in the solution heat treated and aged condition as required 4340 specimen blanks were heat treated to 180 KSI ultimate tensile strength before introducing flaws.

Fatigue Crack Growth Procedures

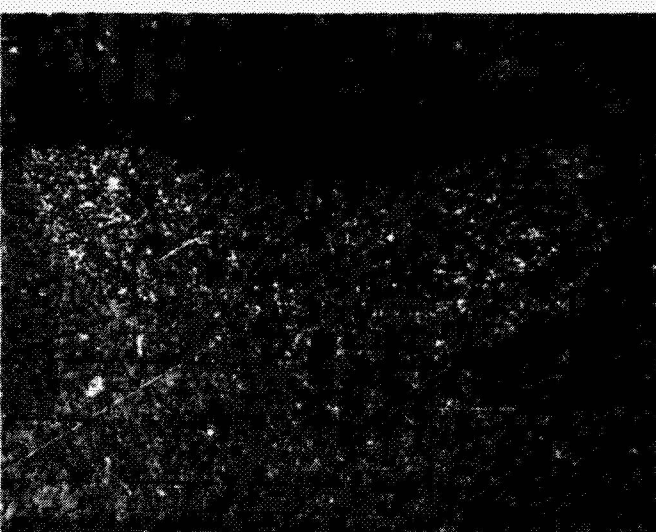
Flaws of four different sizes and shapes were selected for evaluation. Two specimens in each material and thickness were used to establish flaw initiation and growth parameters. Fatigue cracks that have aspect ratios of 0.5 and 0.1 may be produced by the use of shaped electro-discharge machined (EDM) starter notches, extension of the crack in bending fatigue, and removal of the starter notch. Figures 2 and 3 are cross-sectional

$a/2c = 0.5$ $a/t = 0.25$
Case 1 



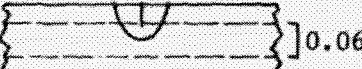
Case 1, $a/2c = 0.5$, 0.310-in. thick Specimen

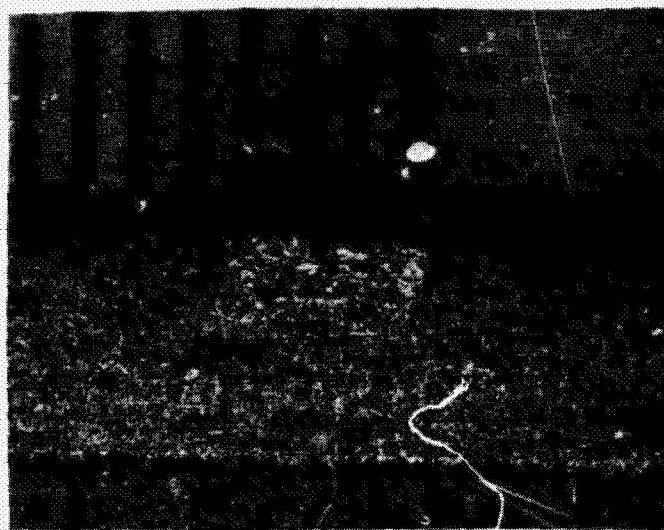
$a/2c = 0.1$ $a/t = 0.2$
Case 2 



Case 2, $a/2c = 0.1$, 0.310-in. thick Specimen

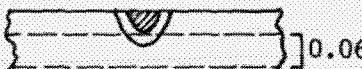
Note: t = thickness of material; a = depth of crack; $2c$ = length of crack; shaded area = EDM starter notch shape;] = final machined thickness.

$a/2c = 0.5$ $a/t = 0.5$
Case 3 ] 0.060"



Note: t = thickness of material; a = depth of crack; $2c$ = length of crack; shaded area = EDM starter notch shape;] = final machined thickness.

Case 3, $a/2c = 0.5$, 0.060-in. thick specimen

$a/2c = 0.25$ $a/t = 0.25$
Case 4 ] 0.060"



Case 4, $a/2c = 0.1$, 0.060-in. thick specimen

Figure 3.
Side View of Crack Starter and Final Crack Configuration, Cases 3 and 4

photographs of typical starter notches and fatigue flaw extension to the required surface length. The maximum fatigue stress must be no greater than one-half of the yield stress in order to preserve flaw tightness. After initial work to establish procedures, flaws of a desired shape and size may be produced by controlling the EDM starter notch shape and depth and by visual monitoring of the surface crack length.

Flaw growth procedures were verified by fracturing trial specimens and measuring actual flaw dimensions. Starter flaw sizes and growth dimensions are shown in Table 2.

Table 2.
EDM Notch and Fatigue Flaw Sizes for Bending Fatigue of 4340 Steel ($\sigma_y = 180$ KSI) and 6 Al-4V Titanium - STA

	Stock Thickness t_0 (in.)	Notch Depth a_0 (in.)	Notch Length $2C_0$ (in.)	Approx. Growth Ratio Δ_a/C	Depth Growth Δ_a (in.)	Length Growth $\Delta(2C)$ (in.)	Total Depth a_1 (in.)	Total Length $2C_1$ (in.)	Machined Thickness t_1 (in.)	Final Depth a_f (in.)	Final length $2C_f$ (in.)	Material Removed Flaw Side
Case 1	0.312 and 0.125	0.010	0.100	3	0.025	0.020	.035	0.170	0.250 and 0.060	0.010	0.100	0.025
Case 2	0.312 and 0.125	0.015	0.020	1	0.030	0.070	.045	0.090	0.250 and 0.060	0.025	0.050	0.020
Case 3	0.312 and 0.125	0.020	0.225	3	0.030	0.250	0.050	0.325	0.250 and 0.060	0.025	0.250	0.025
Case 4	0.312	0.015	0.020	1	0.080	0.160	0.095	0.185	0.250	0.075	0.150	0.020

The maximum fatigue stress during flaw extension was no greater than half the yield stress. The fatigue stress was ≤ 80 KSI for 4340 steel ($\sigma_y = 160$ KSI) and ≤ 70 KSI for 6 Al-4V titanium STA ($\sigma_y = 145$ KSI).

Preparation of Test Specimens

Several calibration test specimens in each material were prepared containing each of the flaw (Case) types. Case 1, 2 and 3 flaws were grown in the thin (0.125 inch) material and Case 1, 2, 3 and 4 flaws were grown in the thick (0.312 inch) material. These specimens were used to optimize NDT techniques and were initially used for set up and calibration of equipment before starting the NL evaluation cycle.

Test Specimens

Thirty specimen blanks from each material and each thickness were locally polished and electrodischarge-machined starter notches introduced at planned locations. Flaws were randomly distributed among the specimens so some specimens contain no flaws and some specimens contain up to six flaws. The flaws were randomly distributed on both sides of the specimens. All of the 0.075-inch deep flaws were introduced in the 0.250-inch (0.312-inch blank) thick specimens and the other flaws were randomly distributed in both thicknesses. The desired number and distribution of flaws for each material is summarized in Table 3.

Table 3. Flaw Distribution in Steel and Titanium Specimens

Number of Flaws Each Material	Flaw Depth (inch)	Flaw Length (inch)	a/2c
30	0.010	0.100	0.1
30	0.025	0.050	0.5
30	0.025	0.250	0.1
30	0.075	0.150	0.5

Allowance was made for flaws which failed to grow and for those inadvertently removed during machining. 161 flaws were initiated in titanium specimens and 128 flaws were initiated in steel specimens.

Flaw Location

To reduce inspection time in describing flaw location and to reduce the subsequent confusion in flaw analysis, the following grid location scheme will be used for flaw initiation. The panel surface will be divided into a one inch grid network. The panel identification (A side) will be located in the lower left hand corner. The short dimension (width) will be designated as the X-dimension and points along the panel length direction will be designated by the Y dimension. Grid location will be by location of the intersection of an X and Y grid and proceeding to

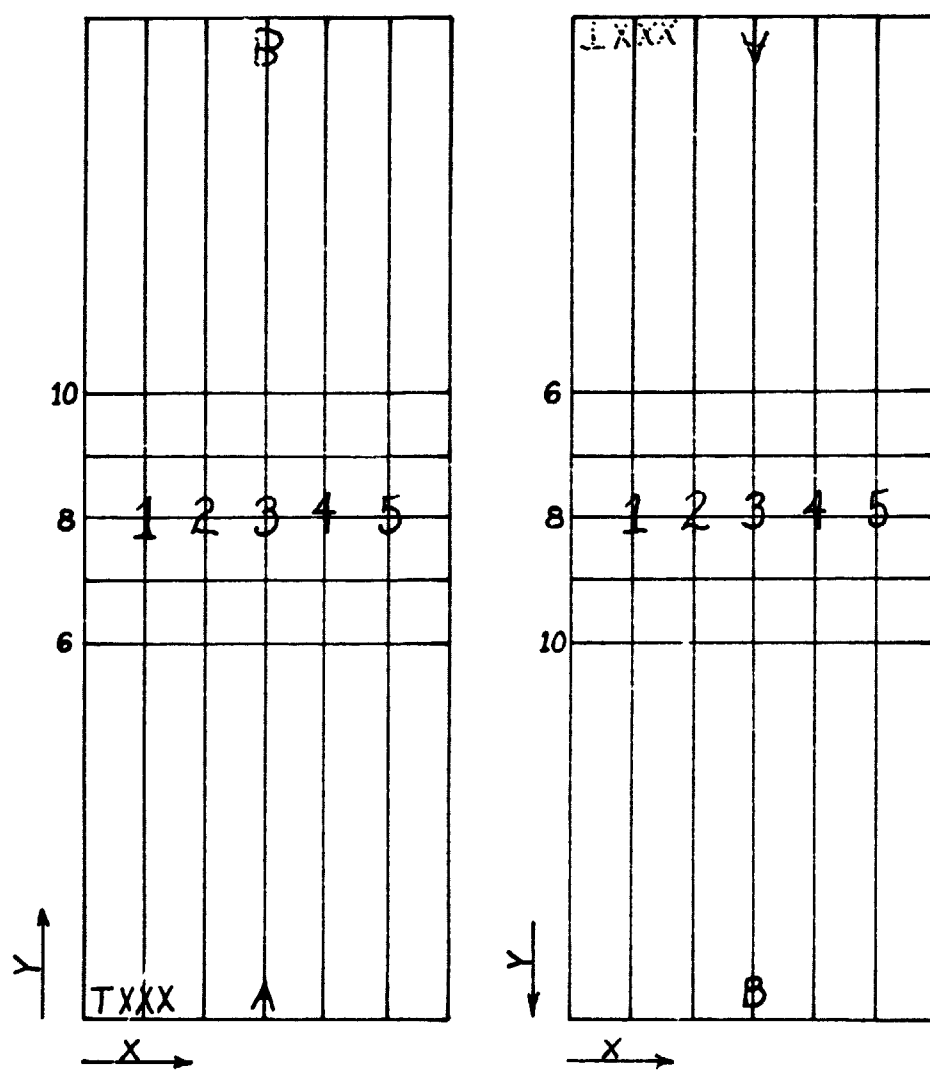


Figure 4 - Grid Pattern Layout

the next highest number in both the X and Y directions. On the reverse (B) side the X direction remains the same and the Y direction is from the top of the panel toward the bottom of the panel as shown in Figure 4.

Specimen Machining

Following fatigue flaw growth the EFM starter notches were removed by machining both sides of each specimen using a flaw-cutter at a 15.26 cm (6 inch) radius to produce a randomly oriented nominal 125 rms surface finish. Nominally, .0508 to .0635 cm (0.020 to 0.025 inch) were removed from the flawed side and the opposite side was machined to produce the final specimen thickness and configuration as shown in Figure 5. Specimens were cleaned by vapor degreasing, alkaline cleaning, dried and submitted for inspection.

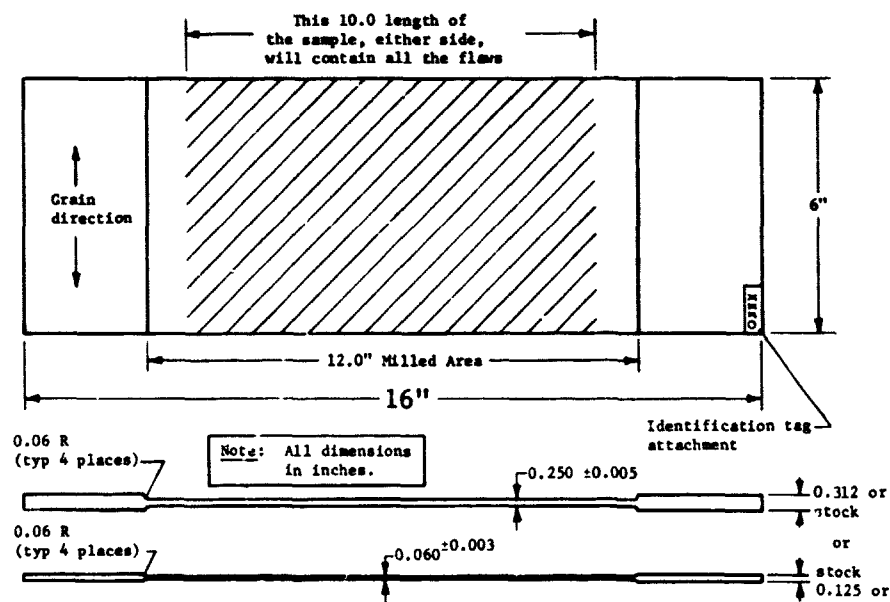


Figure 5. NDT Specimen Configuration

III. NDT METHODS OPTIMIZATION AND PROCEDURES DEVELOPMENT

Nondestructive Test Evaluation

The success of any nondestructive testing program depends on (1) a sound understanding of materials, fabrication techniques, and service demands on the test articles, (2) accurate and precise definition of anomalies to be evaluated by nondestructive testing, (3) definition and understanding of all parameters that will directly and indirectly affect the results of a nondestructive testing technique, (4) fabrication of test samples that are representative of actual fabricated part conditions, (5) use of test samples to establish nondestructive test sensitivity (destructive or functional test verification) and in calibration of test equipment used in production inspection, (6) establishment of well-defined procedures and controls to assure integrity of production inspection, (7) training of production inspection personnel, and (8) establishment of an audit/liaison system to maintain inspection integrity and relevance to production requirements.

4340 steel and 6 Al-4V titanium alloy materials are well characterized and are routinely evaluated by nondestructive testing (NDT) techniques. For purposes of this program, the flaw type as well as the flaw orientation were known and controlled. Calibration specimens had been fabricated for use in establishing optimized procedures. Considerable effort was devoted to procedures optimization to develop procedures which would be suitable for production and would provide a uniform inspection. Calibration specimens were used to evaluate methods and develop procedures. Case 2 specimens contain the smallest crack (0.025 X 0.050 inch) were used to set up each method and to evaluate the apparent signal to noise ratio of the method.

X-Radiography Optimization

Using the specimens as test subjects, optimum exposure values were determined for (1) Kodak Type M, Ready Pak Film, and Kodak Type R, Film and Kodak Industrex Paper. The films provided speed and grain size variations that are representative of commercially available industrial X-ray film now in use. Films were processed using a Kodak Industrial Automatic Processor, Model B, and the paper was processed using an Industrex Processor. Exposure parameters were initially optimized to expose a one foot long (center) section of the specimens, to produce a radiographic film density of 3 and to show the 2T penetrometer hole. This

procedure is typical of normal industrial practices. Variations in voltage, current, exposure time, and collimation were applied to provide the best image of the smallest programmed crack/thickness combination detectable. Kodak Type M was selected due to its superior resolving power at minimum exposure time. An exposure procedure was developed based in the film density, penetrometer resolution and cracks detected. Variations in the ability to resolve cracks were attributed to the crack-focal spot alignment. Intentional variation in alignment on a thin titanium panel resulted in loss of a small (0.152 cm estimated length) crack at greater than 3° angulation and loss of a larger (0.318 cm estimated length) crack beyond 12° angulation. Variation in resolution was attributed to flaw size, shape, tightness and orientation. The techniques which showed the best penetrometer and crack resolution were selected for test specimen evaluation. The finalized techniques are shown in Appendix A of this report.

Liquid Penetrant Optimization

The size flaw that can be detected by a liquid penetrant material depends on (1) its ability to penetrate and fill the crack and on (2) its visibility after processing. The reliability of a liquid penetrant material depends on its tolerance to variations in processing. Various test methods have been developed to compare the performance of penetrant materials. Since a liquid penetrant test is the result of a process, and is dependent, in part, on the host material, development method, etc., an overall evaluation is necessary to determine applicability.

Our previous work with liquid penetrants resulted in selection of the Uresco P-149 material for evaluation. P-149 was used in production applications on the Saturn/Apollo programs and is currently being used on some NASA Space Shuttle Orbiter components. Since our original work with penetrants, two new high sensitivity penetrants have appeared on the open market and were evaluated and compared to P-149.

One material, Sherwin I-319 is a high sensitivity, water washable material. Ease of use is a most desirable feature of this material. When compared with P-149, the I-319 material shows a lower dye concentration as determined by the meniscus method 6, 11 (Figure 6) and lower overall performance on calibration panels.

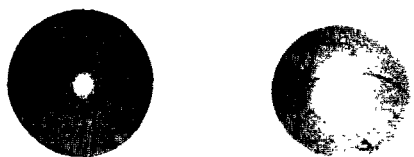


Figure 6. Comparison of P-149 and I-319 Fluorescent Penetrants by the Meniscus Method (P-149 on the Left has Superior Thin Film Sensitivity)



Figure 7. Comparison of P-149 and P6F-4 Fluorescent Penetrants by the Meniscus Method (P6F-4 on the Right has Superior Thin Film Sensitivity)

A second series of materials developed by Rockwell International are high sensitivity, water washable materials and are reported to be biodegradeable. Ease of use and biodegradeable characteristics make these penetrants unique and desirable. When compared with P-149, on the P6F-4 material shows a higher dye concentration as determined by the meniscus method. (Figure 7). Comparison to other penetrants is summarized in Table 4.

Table 4. Results of Penetrant Evaluation by the Meniscus Method

Penetrant	Dimensional Sensitivity	Dimensional Threshold
P-149	1.5 mm	3.0 mm
I-319	2.25	4.75
P6F-1	1.9	5.0
P6F-2	1.75	4.5
P6F-3	1.65	3.25
P6F-4	1.4	2.0

When used on titanium calibration specimens, all cracks were resolved using the P6F-3 and 4 materials. The overall fluorescent background on these specimens was very high compared to P-149. Although these materials were judged to be equal to P-149 for this program. A test procedure was written for use of the P-149 material and was used for all test specimen evaluations. This procedure is shown in Appendix B.

Cleaning of test specimens between evaluations is critical to penetrant evaluation. Panels were ultrasonically cleaned in a trichloroethane bath to remove all penetrant from the previous inspection. Such cleaning was necessary to assure independent test results by different NDT operators. The panel cleaning method is also described in Appendix B.

Ultrasonic Test Optimization

Several methods, test variables and data read-out options are available for ultrasonic inspection. An immersion, shear wave technique with C-scan recording was selected as being most representative of current industry capabilities. Optimization of the shear wave techniques were accomplished by experimental analysis of results obtained by scanning calibration panels. Signal amplitude, signal to noise ratio, and incident angle were evaluated at 2.25, 5 and 10 MHz. 5 MHz was superior for evaluation of panels. Plots of signal amplitude as a function of incident angle were made for incident angles from 12° to 36°. Possible paths of energy reflection were evaluated over this range. An example of a plot of signal response as a function of incident angle is shown in Figure 8.

A 15° incident angle was selected for best overall response and recorded signal output. Recording techniques, test set-up and test controls were optimized by evaluation and comparison of the recorded output obtained. A detailed inspection procedure was written and is shown in Appendix C of this report.

Eddy Current Test Optimization

C-scan evaluation and recording techniques were selected as most representative of state-of-the-art production practices. Titanium and steel differ greatly in eddy current response and were evaluated separately.

Titanium - 6 A⁻⁴V Titanium has a low conductivity (approximately 3% I.A.C.S.) and therefore must be evaluated at high frequencies for best sensitivity. At 3 MHz, the effective depth of eddy current penetration in titanium is approximately 0.076 cm (0.030 inch). 3 MHz was selected as the test frequency. A pencil probe configuration (1/8 inch core) was selected to provide the best sensitivity and discrimination. The NDT Instruments, Vector 111 was selected for its long-term electronic stability. A spring-loaded eddy current scanning probe holder shown in Figure 9 was used to provide minimum lift off variations and minimum probe wear on flat plate. A variation of the probe holder shown in Figure 10 was used for warped specimens. Recording techniques, test set up and test controls were optimized by evaluation and comparison of the recorded output obtained. A detailed inspection procedure was written and is shown in Appendix D.

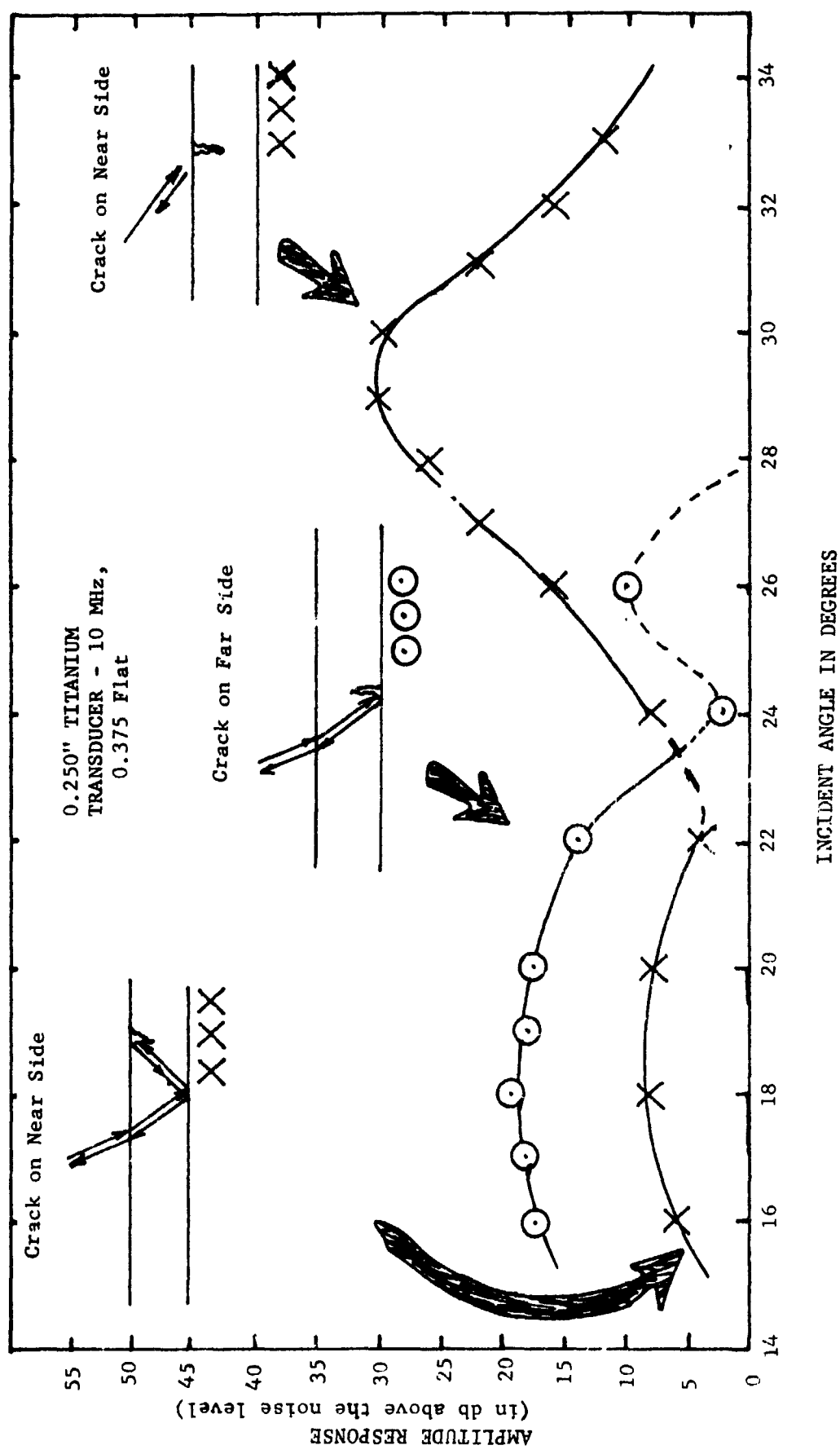


Figure 3. Ultrasonic Shear Wave, Pulse-Echo Reflected Signal Amplitude from a Case 1 Crack as a Function of Incident Angle

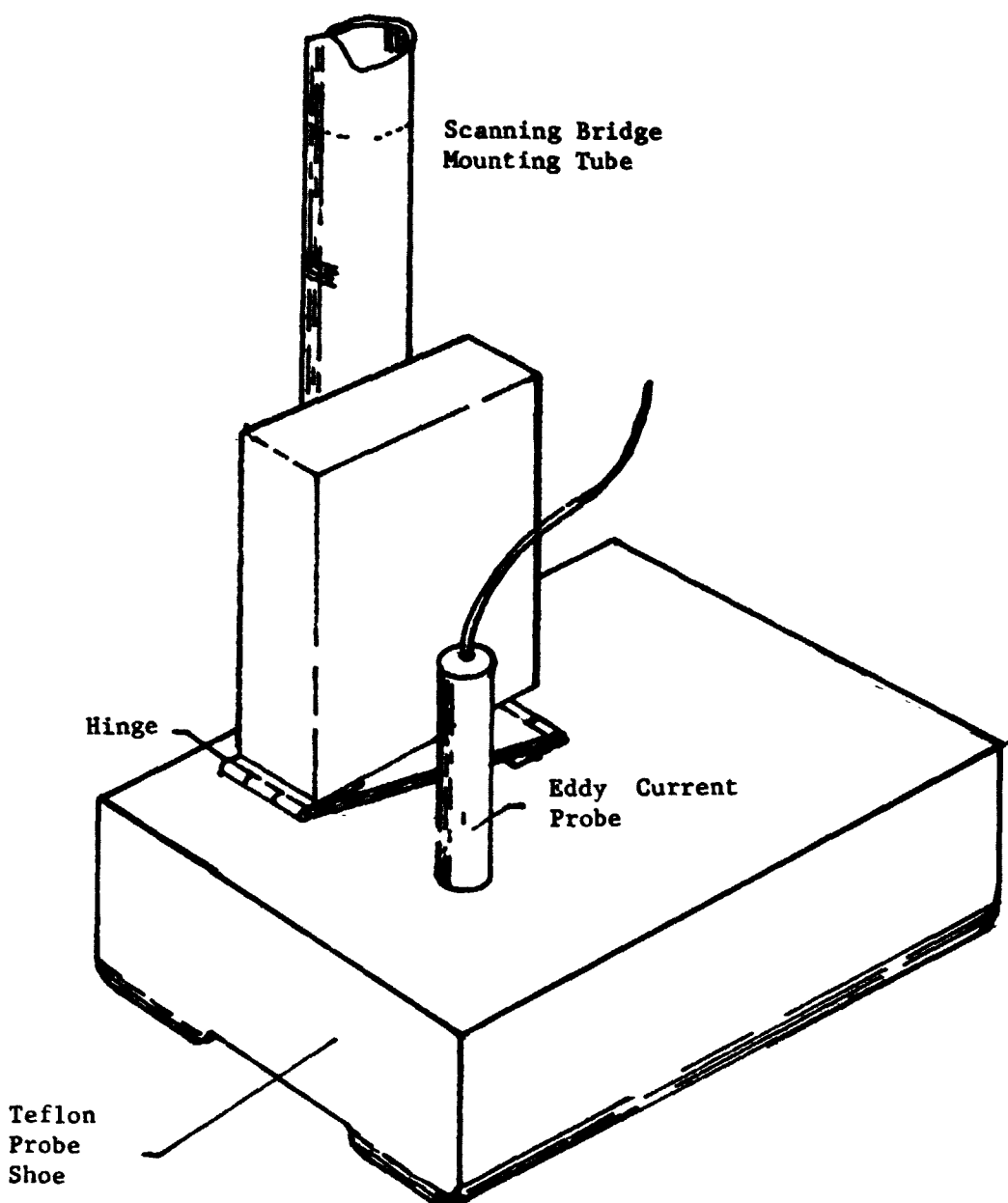


Figure 9 - Spring Loaded Flat Block, Current Scanning Probe Holder

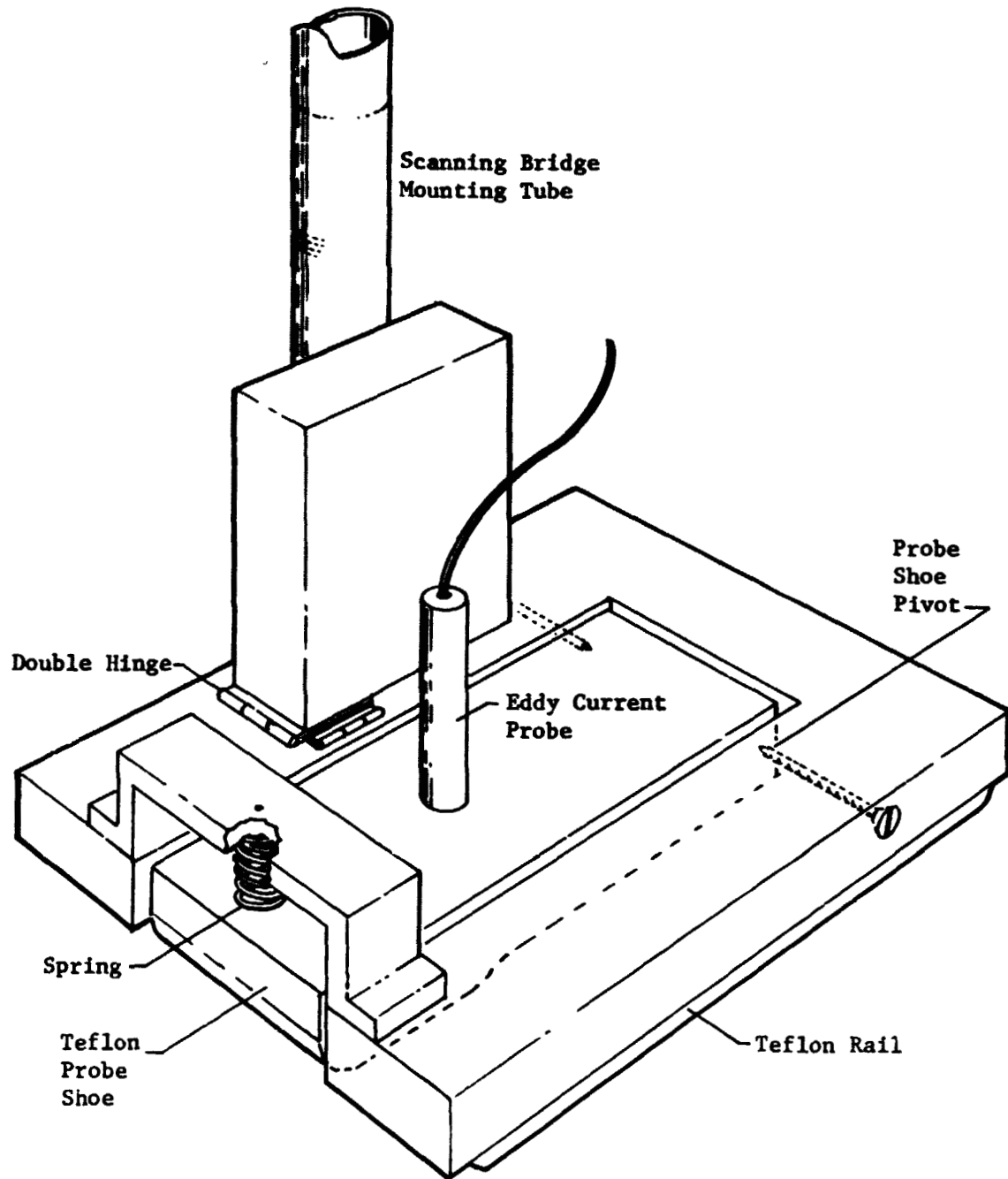


Figure 10 - Spring Loaded Eddy Current Scanning Probe Holder
Used on Warped Panels

Steel - Eddy current inspection of ferromagnetic materials may be accomplished by single coil probe techniques if the magnetic permeability of the material is constant. Specimens were demagnetized and on initial evaluation, good crack detection sensitivity was obtained using a 100 KHz pencil probe with the Vector III and C-scan system used for the titanium panels. This technique was replaced with a 500 KHz differential probe when variations in the specimens were encountered. The 500 KHz probe was held in a spring loaded, flat block scanning fixture as shown in Figure 9. Recording techniques, test set up and test controls were optimized by evaluation and comparison of the recorded output obtained. A detailed Inspection procedure was written and is shown in Appendix E.

Magnetic Particle Test Optimization

Several options for magnetic particle test of steel plates are possible. Best sensitivity is obtained using fluorescent magnetic particle methods. Most uniform reproducibility is obtained using the contact faces in a stationary machine. Our production magnetic particle inspection machine charged with Uresco 228 powder (0.40 ounces per gallon) in kerosene was used as a primary basis for evaluation. Calibration panels were positioned between the machine head such that the heads contacted the sides of the panel. The magnetic particle solution was applied to the calibration specimens followed by a nominally recommended current pulse. The process was repeated for different current densities and the results compared by an iterative visual evaluation. An optimum technique was selected. Calibration specimens were re-evaluated with the optimum techniques using Uresco 210 powder and Magnaflux 14A powder. Little variation in results were obtained. The Uresco 228 powder and optimized magnetization techniques were documented in a test procedure as shown in Appendix F.

NDT evaluation personnel were familiarized with the optimized procedures developed. These procedures were used in all subsequent evaluations of test specimens.

IV. NDT EVALUATION OF TEST SPECIMENS

Flawed test specimens were mixed with blank specimens prepared in like manner. Specimen thickness and surface finish were measured and recorded. Specimens were then submitted for the programmed NDT evaluations.

Sequence 1 - Evaluation of Specimens in the As Machined Condition

All specimens were evaluated by three independent NDT operators who performed independent evaluations without knowledge of actual flaw numbers or distribution and without knowledge of results obtained by other operators.

X-radiography - One set of film was prepared for all specimens with Side A (Side 1) up using the optimized exposure technique. Some variations in exposure time was necessary due to variations in specimen thickness. Film was independently evaluated and results recorded by three operators.

Liquid Penetrant - Penetrant evaluations on both sides of all specimens were performed independently by three operators and the results recorded by each operator. During this sequence a number of unintentional small cracks were revealed along with intentional cracks in test specimens. A large number of unintentional cracks were revealed in thick titanium specimens. Figure 11 shows the pattern of intentional cracks (longest indications) along with a number of unintentional cracks revealed by penetrant. These additional cracks greatly increased the volume of data recording and complicated specimen fracture at the end of the program.

Ultrasonic - Ultrasonic set-up, recording and data analysis were performed independently by three operators on specimens with Side A (Side 7) up.

Eddy Current - Eddy current set-up, recording, and data analysis were performed independently by three operators on both sides of all titanium specimens.

Extreme variations in readout was experienced for eddy current evaluation on steel specimens. Variations were analyzed and attributed to cold work variations induced by the specimen fatigue process and by variations induced during machining.

One set of C-scan recordings were prepared for the steel specimens. These recordings were analyzed by three independent operators.

Magnetic Particle - Magnetic particle evaluations on both sides of all specimens were performed independently by three operators and the results recorded by each operator.



Figure 11. Intentional and Unintentional Cracks Revealed by Penetrant (Actual Size)

Sequence 2 - Evaluation of Specimens in the Post - Etched Condition

State-of-the-art industry practices require etching of machined surfaces prior to performing a high sensitivity penetrant inspection. Specimens were therefore subjected to an etch process to remove approximately 0.0013 cm (0.0005 inch) of material.

Titanium specimens were etched at room temperature in a nitric-hydrofluoric acid (52 oz/gallon, 70% HNO₃ and 6 oz/gallon, 70% HF) mixture. Steel specimens were etched at room temperature in a aqua regia solution (3 parts by volume HCl (concentrated, 1 part HNO₃ (concentrated) and 4 parts H₂O). Following the etch process treatment, specimens were thoroughly rinsed in demineralized water and dried. Specimen surface finish and thickness were measured and recorded.

Liquid Penetrant - Liquid penetrant evaluations were performed on both sides of all specimens. Evaluations were performed independently by three operators and the results recorded by each operator, in accordance with the procedure shown in Appendix B.

Sequence 3 - Evaluation of Specimens in the Post - Proof Loaded Condition

Industry practices were further simulated by proof loading all specimens. Steel specimens were loaded to 80% of the material yield strength ($\sigma_y = 144$ KSI). Thick titanium specimens were loaded to 80% of the material yield strength and thin titanium specimens were loaded to 90% of material yield strength ($\sigma_y = 145$ KSI). Nine specimens were fractured during the proof load cycle. The fractured end pieces were included in the NDT evaluations. Specimens were loaded in less than one minute, held at load for 15 seconds and unloaded rapidly.

All specimens were again evaluated independently by three operators.

X-radiography - One set of film was prepared for all specimens with Side A (Side 1) up using the optimized exposure technique described in Appendix A and accounting for variations in specimen thickness by variation in exposure time. Film was independently evaluated and the results recorded by three operators.

Liquid Penetrant - Penetrant evaluations were performed on both sides of all specimens using the procedures described in Appendix B. Results were evaluated and recorded by each operator.

Ultrasonic - Ultrasonic set-up, recording and data analysis were performed independently by three operators on specimens with Side A (Side 1) up.

Eddy Current - Eddy current set-up, recording and data analysis were performed independently by three operators on both sides of all titanium specimens.

One set of C-scan eddy current recordings was prepared for steel specimens. These recordings were analyzed by three independent operators. Variations in recorded output (noise) on the steel panels was greatly reduced. This reduction was attributed to removal of local cold worked surface material during etching and to relaxation of some non uniform residual stresses during the load cycle.

Magnetic Particle - Magnetic particle evaluations on both sides of all specimens were performed independently by three operators and the results recorded by each operator.

Following verification of all NDT evaluation data, the specimens were submitted for fracture and analysis.

V. SPECIMEN FRACTURE AND CRACK MEASUREMENT

Intentional cracks were located and marked by reference to planned flaw tables. Unintentional cracks were located and marked by visual examination with the aid of penetrant evaluation data. Saw cuts were made from the edges of thin specimens to areas adjacent to the ends of a crack. Cracks were broken open in bending to reveal the actual flaw. An oxyacetylene cutting torch was used to cut slots from the edges of thick specimens to areas adjacent to the ends of a crack. Cracks were then broken open in bending to reveal the actual flaw. Some cracks were lost when the specimen did not break at the crack. In these cases the crack length was measured and recorded but crack depth could not be obtained.

Actual crack length and depth on fractured cracks were measured with the aid of a traveling microscope with an accuracy of ± 0.001 inch. Measurements were recorded in the actual data file by panel number and location. Matching of data to planned flaws was performed by correlation of planned to actual flaw locations. Unintentional flaws were assigned flaw numbers in a progressive 200 numbering series and were correlated to NDT penetrant data by matching NDT locations with actual locations. Actual data on unintentional flaws was not obtained if the flaws could not be located readily by aided visual examination.

Actual crack data measurements were tabulated and entered in the computer for analyses.

VI. DATA ANALYSIS

Actual Crack Data

All actual data and NDT data were input to a computer for compiling and analysis. An actual data file was assembled by ordered panel number and crack numbers. This file was used as the basis of reference for all data sorting and analyses. A tabulation of actual crack data and related crack descriptive information is shown in Tables 5 for titanium and 9 for steel specimens.

Nondestructive Test Data

Nondestructive test data was assembled in data files by panel number and crack number. Numbers entered in the NDT data file are estimates of the actual crack length as observed by the NDT method and measured or estimated to the nearest 0.16 cm (1/16 inch).

Tabulations of NDT observations for titanium specimens are shown in Table 6 for Sequence 1 (As Machined Condition) data, in Table 7 for Sequence 2 (Post Etch Condition) data (Liquid Penetrant Only), and in Table 8 for Sequence 3 (Post Proof Condition) data.

Tabulations of NDT observations for steel specimens are shown in Table 10 for Sequence 1 (As Machined Condition) data, in Table 11 for Sequence 2 (Post Etch Condition) data and in Table 12 for Sequence 3 (Post Proof Condition) data.

Data Ordering

Actual crack data (Tables 5 and 9) were used as the basis for all ordering, calculations and analysis. Cracks were initially ordered by decreasing actual crack length and depth along with the corresponding NDT observations. These data were then assigned file numbers and stored for use in subsequent statistical analyses.

Statistical Analysis

Analysis of data was oriented to demonstrating the sensitivity and reliability of state-of-the-art NDT methods for the detection of small, tightly closed flaws in steel and titanium.

Table 5. Actual Crack Data - Titanium

PANEL NO.	CRACK NO.	CRACK LENGTH	CRACK DEPTH	CRACK POSITION X	CRACK POSITION Y	FINAL FINISH THICKNESS	A/T FINAL	A/2C	AREA (SEMI)
1A	1	.210	.045	7.00	9.00	135	.0490	.00709	
1A	2	.085	.015	3.00	8.00	135	.0490	.00142	
1A	3	.195	.031	4.00	7.00	135	.0490	.00475	
1A	4	.095	.019	1.00	7.00	135	.0490	.00142	
1A	5	.207	.037	1.00	8.00	110	.0560	.00064	
2B	6	.152	.028	3.00	7.00	110	.0560	.00210	
2B	7	.141	.019	4.00	8.00	110	.0560	.00090	
2B	8	.115	.019	1.00	6.00	160	.0740	.00088	
3B	9	.090	.014	1.00	7.00	160	.0740	.00088	
3B	10	.017	.003	1.00	9.00	140	.0610	.00088	
3B	11	.324	.053	1.00	7.00	140	.0610	.00088	
5A	13	.083	.021	2.00	6.00	65	.0720	.00132	
6A	14	.325	.051	1.00	6.00	115	.0620	.00132	
7B	15	.062	.018	2.00	6.00	60	.0630	.00116	
8B	16	.084	.010	4.00	6.00	60	.0630	.00116	
8B	17	.160	.028	3.00	8.00	60	.0630	.00066	
9A	18	.176	.027	1.00	8.00	300	.0640	.00226	
9A	19	.152	.025	3.00	7.00	300	.0640	.00226	
10A	20	.065	.018	5.00	9.00	290	.0650	.00293	
10A	21	.116	.027	4.00	8.00	290	.0660	.00293	
10A	22	.090	.019	1.00	9.00	290	.0660	.00293	
11B	23	.130	.021	1.00	9.00	100	.0630	.00134	
12B	24	.125	.025	2.00	7.00	280	.0700	.00228	
13B	25	.067	.008	2.00	9.00	280	.0700	.00228	
13B	26	.075	.012	4.00	9.00	280	.0700	.00228	
15A	31	.155	.012	2.50	6.00	140	.0670	.00042	
15A	32	.117	.006	4.00	6.00	140	.0670	.00042	
15A	33	.317	.016	2.00	8.00	140	.0670	.00042	
15A	34	.246	.039	3.00	9.00	140	.0670	.00042	
16B	35	.250	.025	1.00	7.00	155	.0630	.00042	
16B	36	.407	.037	3.00	6.00	155	.0630	.00042	
16B	37	.355	.017	4.00	7.00	155	.0630	.00042	
16B	38	.300	.039	2.00	8.00	155	.0630	.00042	
16B	39	.320	.011	3.00	9.00	155	.0630	.00042	
16B	40	.320	.039	1.00	9.00	155	.0630	.00042	
17A	41	.111	.021	2.00	8.00	70	.0630	.00042	
17A	42	.152	.033	4.00	8.00	70	.0630	.00042	
18A	43	.142	.016	3.00	7.00	250	.0600	.00042	
12A	45	.157	.027	2.00	9.00	95	.0630	.00042	
19A	46	.185	.029	4.00	9.00	95	.0630	.00042	
20B	48	.097	.006	1.00	7.00	215	.0640	.00042	
20B	49	.123	.010	3.00	7.00	215	.0640	.00042	
22B	52	.091	.018	2.00	6.00	240	.0620	.00042	
22B	53	.110	.025	4.00	7.00	240	.0620	.00042	
22B	55	.180	.037	1.00	8.00	240	.0620	.00042	
23B	57	.090	.012	2.00	8.00	300	.0790	.00523	
23B	58	.057	.005	3.00	6.00	300	.0790	.00523	
24A	59	.082	.012	1.00	9.00	270	.0710	.00035	
24A	61	.078	.014	2.00	7.00	270	.0710	.00035	
24A	62	.034	.004	7.00	270	.0710			

Table 5. (Continued)

25A	65	.145	.025	3.00	8.00	.056	.118
25A	66	.165	.023	2.00	7.00	.0540	.00611
25A	67	.150	.027	4.00	6.00	.0540	.00285
25A	68	.150	.019	3.00	6.00	.0640	.00.98
26B	70	.144	.019	4.00	8.00	.0680	.00316
27B	74	.144	.019	1.00	9.00	.0630	.00224
28A	75	.260	.021	1.00	9.00	.125	.00215
28A	76	.315	.031	3.00	9.00	.125	.302
28A	77	.300	.023	3.00	8.00	.0660	.318
30A	78	.055	.010	1.00	7.00	.0660	.081
30A	79	.070	.010	4.00	9.00	.255	.0429
30A	80	.070	.006	4.00	7.00	.0650	.359
31A	81	.250	.029	1.00	9.00	.2560	.00616
31A	82	.200	.061	3.00	9.00	.2560	.422
31A	83	.320	.076	4.00	7.00	.2560	.180
31A	84	.352	.057	2.00	7.00	.2560	.279
32A	85	.635	.023	1.00	5.00	.255	.132
32A	86	.045	.003	4.00	7.00	.0660	.127
33A	87	.025	0.	2.00	9.00	.2560	.00569
33A	88	.213	.062	4.00	9.00	.2600	.00644
33A	89	.167	.049	1.00	7.00	.2600	.110
33A	90	.023	0.	3.00	6.00	.2600	.154
33A	91	.023	.010	4.00	6.00	.2590	.00051
35B	93	.067	.010	0.	9.00	.2590	.00055
35B	94	.065	0.	2.00	7.00	.2560	.00033
36B	95	.025	0.	2.00	7.00	.2560	.00767
36B	96	.215	.057	4.00	7.00	.2560	.0778
37A	97	.190	.041	3.00	8.00	.2560	.00216
38B	99	.177	.019	4.00	8.00	.255	.00215
38B	100	.034	0.	3.00	9.00	.255	.00216
39B	101	.182	.049	1.00	7.00	.2480	.00216
39B	102	.187	.047	1.00	9.00	.2490	.00216
42B	103	.235	.043	1.00	6.00	.2490	.00216
42B	104	.235	.043	3.00	6.00	.2490	.00216
42B	105	.216	.049	4.00	9.00	.2490	.00216
43A	106	.195	.018	2.00	8.00	.2500	.00216
43A	107	.167	.068	2.00	6.00	.2570	.00216
45A	111	.235	.045	1.00	9.00	.2470	.00216
45A	112	.262	0.	4.00	9.00	.2470	.00216
45A	113	.205	.031	4.00	8.00	.2470	.00216
45A	114	.227	.015	3.00	7.00	.2470	.00216
45A	115	.207	.041	1.00	6.00	.2470	.00216
46A	116	.183	.058	2.00	9.00	.2500	.00216
46A	117	.085	.021	1.00	8.00	.2500	.00216
46A	118	.215	.068	3.00	8.00	.2500	.00216
46A	119	.175	.058	1.00	7.00	.2500	.00216
46A	120	.242	.052	4.00	6.00	.2500	.00216
47B	121	.255	.053	1.00	7.00	.2520	.00216
47B	122	.275	.060	4.00	7.00	.2520	.00216
47B	123	.262	.041	3.00	8.00	.2520	.00216
47B	124	.220	.047	2.00	9.00	.2520	.00216
49B	125	.200	.064	4.00	6.00	.2590	.00812
49E	126	.125	.060	2.00	9.00	.2590	.01000
				2.00	9.00	.232	.00595
				.207	127		
							5CA

Table 5. (Concluded)

50A	128	.240	-0.	.049	8.00	145	.2610	.175	.00602
50A	129	.240	.043	2.00	7.00	145	.2610	.204	.00924
50A	130	.240	.043	2.00	6.00	145	.2610	.168	.0011
50A	131	.247	0.	.066	3.00	9.00	.2610	.165	.0011
51A	132	.211	.066	2.00	9.00	115	.2550	.259	.01094
51A	133	.165	.057	2.00	8.00	115	.2550	.224	.01739
51A	134	.370	.103	3.00	7.00	115	.2550	.404	.02993
51A	135	.265	.084	3.00	6.00	115	.2550	.329	.01748
52A	136	.130	.049	2.00	8.00	125	.2490	.197	.00500
52A	137	.140	.039	4.00	8.00	125	.2490	.157	.00429
52A	138	.050	0.	1.00	7.00	125	.2490	.097	.00157
53B	140	.080	.025	1.00	6.00	100	.2570	.175	
53B	141	.070	.012	1.00	6.00	100	.2570	.133	
53B	142	.075	0.	4.00	8.00	100	.2570	.171	
53B	143	.080	0.	1.00	9.00	100	.2570	.094	
53B	144	.087	0.	4.00	9.00	100	.2570	.189	
54A	145	.050	0.	2.00	8.00	115	.2510	.047	.00066
54A	146	.225	.021	3.00	6.00	115	.2510	.171	.00371
56C	147	.179	.047	3.00	6.00	200	.2490	.094	.00661
56B	148	.210	.058	2.00	7.00	200	.2490	.233	.00957
56B	149	.212	.058	1.00	9.00	200	.2490	.233	.00966
56B	150	.125	.029	3.00	9.00	200	.2490	.116	.00285
57B	151	.157	.055	3.00	7.00	200	.2480	.141	.00377
57B	152	.130	.047	2.00	8.00	200	.2480	.190	.00480
58A	153	.210	.055	3.00	9.00	250	.2630	.209	.00907
58A	154	.194	.064	1.00	8.00	250	.2630	.143	.00975
58A	155	.202	.057	3.00	8.00	250	.2630	.217	.00904
58A	156	.212	.062	2.00	6.00	250	.2630	.236	.01032
60B	157	.257	.049	1.00	6.00	150	.2430	.202	.00989
60B	158	.182	.033	4.00	6.00	150	.2430	.136	.00472
60B	159	.216	.047	2.00	7.00	150	.2430	.193	.00797
60B	160	.210	.047	1.00	6.00	150	.2430	.193	.00775
60B	161	.125	0.	4.00	8.00				

Table 6. Tabulation of Nondestructive Test Observations for Titanium, Sequence 1

PANEL NUMBER	CRACK NUMBER	X-RADIOGRAPHY			LIQUID PENETRANT			ULTRASONIC			EDDY CURRENT		
		NO. 1	NO. 2	NO. 3	NO. 1	NO. 2	NO. 3	NO. 1	NO. 2	NO. 3	NO. 1	NO. 2	NO. 3
1 1	1	.18	.20	.20	.20	.20	.30	.30	.30	.40	.30	.20	.35
1 1	2	.05	.0	.0	.20	.20	.20	.10	.0	.25	0	0	0
1 1	3	.18	.20	.20	.30	.30	.30	.30	.20	.20	.10	.10	.20
1 1	4	0	0	0	0	0	0	.20	.10	.0	.15	0	0
2 2	5	.20	.20	.20	.30	.30	.30	.20	.10	.0	.20	.20	.25
2 2	6	0	0	0	.15	.15	.15	.25	.0	.15	0	0	0
2 2	7	.10	0	0	.20	.20	.20	.15	.15	.0	.10	.10	.08
3 0	8	0	0	0	0	0	0	0	0	.25	.10	.10	0
3 0	9	0	0	0	0	0	0	0	0	.07	0	0	0
5 0	10	0	0	0	0	0	0	0	0	.07	0	0	0
5 1	11	.28	.30	.30	.40	.40	.40	.30	.40	.50	.15	.10	.35
6 1	13	.18	.10	.20	.30	.30	.30	.15	.25	.30	.15	.15	.35
6 1	14	.30	.0	.40	.40	.40	.40	.20	.40	.50	.30	.20	.50
7 2	15	0	0	0	0	0	0	.10	.07	.10	.15	0	0
8 2	16	0	0	0	.20	.10	.10	.10	.05	.10	.10	.10	.20
8 2	17	0	0	0	.10	.10	.10	.30	.15	.30	.10	.15	.20
9 1	18	0	0	0	.25	.25	.25	.25	.15	.20	.15	.40	.10
9 1	19	0	0	0	.10	.25	.25	.25	.15	.20	.25	.30	.25
10 1	20	0	0	0	0	.10	.10	0	0	0	.05	0	0
10 1	21	0	0	0	0	.15	.15	.15	.10	.10	.05	0	.15
10 1	22	0	0	0	0	.10	.10	.10	.10	.10	.05	0	0
11 2	23	0	.15	.20	.20	.20	.20	.20	.10	.15	.10	.20	.10
13 2	24	0	0	.10	.15	.15	.15	.20	.07	.10	.15	.10	.20
13 2	25	0	0	0	0	.10	.10	.10	0	0	.05	0	0
13 2	26	0	0	0	0	.10	.10	0	0	0	.05	0	0
15 1	27	0	0	0	0	0	0	.20	0	0	0	0	0
15 1	28	0	0	0	0	0	0	.15	0	0	0	0	0
15 1	29	0	0	0	0	0	0	.30	.30	.20	.25	.30	.30
15 1	30	0	0	0	0	0	0	.10	.40	.30	.40	.30	.30
15 1	31	0	0	0	0	0	0	.30	.30	.20	.25	.30	.30
16 2	32	0	0	0	0	0	0	.50	.50	.50	.50	.40	.40
16 2	33	0	0	0	0	0	0	.50	.50	.50	.40	.40	.40
16 2	34	0	0	0	0	0	0	.40	.40	.40	.40	.40	.40
16 2	35	0	0	0	0	0	0	.20	.20	.25	.25	.25	.20
16 2	36	0	0	0	0	0	0	.40	.40	.40	.40	.40	.40
16 2	37	0	0	0	0	0	0	.40	.40	.40	.40	.40	.40
16 2	38	0	0	0	0	0	0	.30	.30	.30	.30	.30	.30
16 2	39	0	0	0	0	0	0	.30	.30	.30	.30	.30	.30
16 2	40	0	0	0	0	0	0	.35	.35	.35	.35	.35	.35
17 1	41	0	0	0	0	0	0	.32	.32	.32	.32	.32	.32
17 1	42	0	0	0	0	0	0	.25	.25	.25	.25	.25	.25

Table 6. (Continued)

Table 6. (Concluded)

Table 7. Tabulation of Nondestructive Test Observations for Titanium, Sequence 2 LIQUID PENETRANT

PANEL NO.	CRACK NO.	NO.1	NO.2	NO.3	PANEL NO.	CRACK NO.	NO.1	NO.2	NO.3	PANEL NO.	CRACK NO.	NO.1	NO.2	NO.3
1 1 1	1 2 3	.25	.30	.30	1 1 1	1 2 3	.15	.20	.20	1 1 1	1 2 3	.15	.20	.20
1 1 1	4 5 6	.25	.30	.30	1 1 1	4 5 6	.15	.20	.20	1 1 1	4 5 6	.15	.20	.20
2 2 2	7 8 9	.25	.30	.30	2 2 2	7 8 9	.15	.20	.20	2 2 2	7 8 9	.15	.20	.20
3 3 0	10 11 12	.25	.30	.30	3 3 0	10 11 12	.15	.20	.20	3 3 0	10 11 12	.15	.20	.20
5 5 0	13 14 15	.25	.30	.30	5 5 0	13 14 15	.15	.20	.20	5 5 0	13 14 15	.15	.20	.20
6 6 2	16 17 18	.25	.30	.30	6 6 2	16 17 18	.15	.20	.20	6 6 2	16 17 18	.15	.20	.20
7 7 2	19 20 21	.25	.30	.30	7 7 2	19 20 21	.15	.20	.20	7 7 2	19 20 21	.15	.20	.20
8 8 2	22 23 24	.25	.30	.30	8 8 2	22 23 24	.15	.20	.20	8 8 2	22 23 24	.15	.20	.20
9 9 1	25 26 27	.25	.30	.30	9 9 1	25 26 27	.15	.20	.20	9 9 1	25 26 27	.15	.20	.20
10 10 1	28 29 30	.25	.30	.30	10 10 1	28 29 30	.15	.20	.20	10 10 1	28 29 30	.15	.20	.20
11 11 1	31 32 33	.25	.30	.30	11 11 1	31 32 33	.15	.20	.20	11 11 1	31 32 33	.15	.20	.20
12 12 1	34 35 36	.25	.30	.30	12 12 1	34 35 36	.15	.20	.20	12 12 1	34 35 36	.15	.20	.20
13 13 1	37 38 39	.25	.30	.30	13 13 1	37 38 39	.15	.20	.20	13 13 1	37 38 39	.15	.20	.20
14 14 1	40 41 42	.25	.30	.30	14 14 1	40 41 42	.15	.20	.20	14 14 1	40 41 42	.15	.20	.20
15 15 1	43 44 45	.25	.30	.30	15 15 1	43 44 45	.15	.20	.20	15 15 1	43 44 45	.15	.20	.20
16 16 1	46 47 48	.25	.30	.30	16 16 1	46 47 48	.15	.20	.20	16 16 1	46 47 48	.15	.20	.20
17 17 1	49 50 51	.25	.30	.30	17 17 1	49 50 51	.15	.20	.20	17 17 1	49 50 51	.15	.20	.20
18 18 1	52 53 54	.25	.30	.30	18 18 1	52 53 54	.15	.20	.20	18 18 1	52 53 54	.15	.20	.20
19 19 1	55 56 57	.25	.30	.30	19 19 1	55 56 57	.15	.20	.20	19 19 1	55 56 57	.15	.20	.20
20 20 1	58 59 60	.25	.30	.30	20 20 1	58 59 60	.15	.20	.20	20 20 1	58 59 60	.15	.20	.20
21 21 1	61 62 63	.25	.30	.30	21 21 1	61 62 63	.15	.20	.20	21 21 1	61 62 63	.15	.20	.20
22 22 1	64 65 66	.25	.30	.30	22 22 1	64 65 66	.15	.20	.20	22 22 1	64 65 66	.15	.20	.20
23 23 1	67 68 69	.25	.30	.30	23 23 1	67 68 69	.15	.20	.20	23 23 1	67 68 69	.15	.20	.20

Table 8. Tabulation of Nondestructive Test Observations for Titanium, Sequence 3

PANEL NUMBER	CRACK NUMBER	X-RADIOGRAPHY			LIQUID PENETRANT			ULTRASONIC			EDDY CURRENT		
		NO. 1	NO. 2	NO. 3	NO. 1	NO. 2	NO. 3	NO. 1	NO. 2	NO. 3	NO. 1	NO. 2	NO. 3
1 1	1	.22	.29	.23	.25	.30	.25	.20	.30	.15	.30	.30	.30
1 1	2	.16	.19	.19	.10	.10	.15	.10	.10	.10	.25	.25	.25
1 0	3	0	0	0	0	0	0	0	0	0	6.00	6.00	6.00
1 0	4	0	0	0	0	0	0	0	0	0	0	0	0
2 0	5	.10	.10	.10	.10	.10	.10	.10	.10	.10	.30	.30	.30
2 0	6	0	0	0	0	0	0	0	0	0	0	0	0
2 0	7	0	0	0	0	0	0	0	0	0	0	0	0
3 2	8	0	0	0	0	0	0	0	0	0	0	0	0
3 2	9	0	0	0	0	0	0	0	0	0	0	0	0
5 0	10	0	0	0	0	0	0	0	0	0	0	0	0
6 1	13	.33	.39	.30	.35	.40	.35	.40	.40	.40	.15	.15	.15
6 1	14	.18	.20	.20	.20	.20	.20	.20	.20	.20	.20	.20	.20
7 2	15	.15	.15	.15	.15	.15	.15	.15	.15	.15	.25	.25	.25
8 2	16	.08	.07	.06	.10	.10	.10	.10	.10	.10	.25	.25	.25
8 2	17	.13	.14	.14	.10	.10	.10	.10	.10	.10	.25	.25	.25
8 2	18	.16	.16	.16	.18	.18	.18	.20	.20	.20	.20	.20	.20
9 1	19	.15	.15	.15	.15	.15	.15	.18	.18	.18	.20	.20	.20
9 1	20	0	0	0	0	0	0	0	0	0	0	0	0
10 1	21	0	0	0	0	0	0	0	0	0	0	0	0
10 1	22	0	0	0	0	0	0	0	0	0	0	0	0
11 2	23	0	0	0	0	0	0	0	0	0	0	0	0
13 2	24	0	0	0	0	0	0	0	0	0	0	0	0
13 2	25	0	0	0	0	0	0	0	0	0	0	0	0
15 1	26	.06	.06	.06	.10	.10	.10	.10	.10	.10	.20	.20	.20
15 1	31	0	0	0	0	0	0	0	0	0	0	0	0
15 1	32	0	0	0	0	0	0	0	0	0	0	0	0
15 1	33	.20	.20	.20	.30	.25	.25	.20	.20	.20	.40	.40	.40
15 1	34	0	0	0	0	0	0	0	0	0	0	0	0
15 2	35	0	0	0	0	0	0	0	0	0	0	0	0
16 0	36	0	0	0	0	0	0	0	0	0	0	0	0
16 0	37	0	0	0	0	0	0	0	0	0	0	0	0
16 2	38	0	0	0	0	0	0	0	0	0	0	0	0
16 2	39	0	0	0	0	0	0	0	0	0	0	0	0
17 1	41	0	0	0	0	0	0	0	0	0	0	0	0
17 1	42	0	0	0	0	0	0	0	0	0	0	0	0

Table 8. (Continued)

Table 8. (Concluded)

Table 9. Actual Crack Data - Steel

PANEL NO.	CRACK NO.	CRACK LENGTH	CRACK DEPTH	CRACK POSITION X	CRACK POSITION Y	FINAL FINISH THICKNESS	FINAL	A/T	A/2C	AREA1 (SEMI)
1A	1	.082	.012	1.00	9.00	45	.0690	.174	.148	.00077
1A	2	.087	.016	1.00	7.00	45	.0690	.232	.184	.00109
1A	3	.084	.018	3.00	8.00	45	.0690	.261	.214	.00119
1A	4	.061	.008	4.00	7.00	45	.0690	.116	.131	.00038
1A	5	.186	.031	1.00	8.00	60	.0550	.564	.167	.00453
2B	6	.174	.023	3.00	7.00	60	.0550	.418	.132	.00314
2B	7	.169	.027	4.00	8.00	60	.0550	.491	.161	.00356
2B	8	.279	.029	2.00	9.00	155	.0650	.439	.104	.00635
5A	9	.280	.027	3.00	7.00	155	.0650	.409	.096	.00594
6A	10	.150	.019	2.00	7.00	55	.0670	.284	.127	.00224
6A	11	.161	.021	2.00	6.00	55	.0670	.313	.130	.00266
7B	12	.222	.029	1.00	6.00	80	.0540	.537	.121	.00506
7B	13	.074	.023	2.00	6.00	60	.0590	.390	.311	.00134
8B	14	.030	.002	4.00	6.00	60	.0590	.034	.067	.00005
8B	15	.077	.010	3.00	6.00	60	.0590	.169	.130	.00060
9A	16	.194	.035	1.00	8.00	60	.0710	.493	.180	.00533
9A	17	.179	.033	3.00	7.00	60	.0710	.465	.184	.00464
10A	18	.031	.004	3.00	9.00	80	.0690	.058	.129	.00010
10A	19	.061	.006	4.00	8.00	80	.0690	.087	.098	.00029
10A	20	.031	.002	1.00	6.00	80	.0690	.029	.065	.00005
11B	21	.035	.004	1.00	9.00	155	.0530	.075	.114	.00011
12B	24	.050	0	4.00	9.00	155	.0700	<u>182</u>	<u>096</u>	<u>.00118</u>
14A	25	.125	.012	2.00	8.00	125	.0680	<u>286</u>	<u>.131</u>	<u>.00216</u>
14A	26	.145	.019	4.00	9.00	125	.0660	<u>.439</u>	<u>.190</u>	<u>.00348</u>
14A	201	.153	.029	1.00	6.00	125	.0660	<u>.695</u>	<u>.126</u>	<u>.01047</u>
14A	202	.142	0	4.00	6.00	125	.0660	<u>.695</u>	<u>.133</u>	<u>.00992</u>
14A	207	.325	.041	2.00	4.00	32	.0590	<u>.627</u>	<u>.121</u>	<u>.00886</u>
15A	28	.308	.041	2.00	6.00	32	.0590	<u>.661</u>	<u>.123</u>	<u>.00974</u>
15A	29	.305	.037	3.00	9.00	32	.0590	<u>.493</u>	<u>.099</u>	<u>.00665</u>
15A	30	.318	.039	1.00	7.00	90	.0640	<u>.219</u>	<u>.059</u>	<u>.00261</u>
16B	31	.292	.029	3.00	6.00	32	.0590	<u>.695</u>	<u>.133</u>	<u>.00667</u>
16B	32	.237	.014	3.00	4.00	90	.0640	<u>.484</u>	<u>.130</u>	<u>.00579</u>
16B	33	.238	.031	2.00	8.00	90	.0640	<u>.484</u>	<u>.113</u>	<u>.00667</u>
16B	34	.274	.031	3.00	9.00	90	.0640	<u>.578</u>	<u>.121</u>	<u>.00889</u>
16B	35	.306	.037	1.00	9.00	90	.0640	<u>.578</u>	<u>.120</u>	<u>.00895</u>
16B	36	.308	.037	1.00	9.00	130	.0610	<u>182</u>	<u>.126</u>	<u>.00667</u>
17B	37	.041	0	3.00	7.00	65	.0700	<u>.586</u>	<u>.198</u>	<u>.00053</u>
18A	39	.207	.041	1.00	7.00	145	.0740	<u>.162</u>	<u>.091</u>	<u>.01124</u>
19A	40	.084	.008	1.00	9.00	145	.0740	<u>.311</u>	<u>.131</u>	<u>.00316</u>
19A	41	.132	.012	2.00	9.00	145	.0740	<u>.162</u>	<u>.091</u>	<u>.00025</u>
19A	42	.175	.023	4.00	9.00	145	.0740	<u>.162</u>	<u>.096</u>	<u>.00118</u>
19A	43	.125	.012	1.00	6.00	65	.0640	<u>.094</u>	<u>.111</u>	<u>.00025</u>
23B	54	.054	.006	3.00	6.00	60	.0570	<u>.035</u>	<u>.035</u>	<u>.00009</u>
24A	55	.030	0	1.00	9.00	60	.0570	<u>.094</u>	<u>.111</u>	<u>.00063</u>
24A	57	.057	.002	2.00	7.00	60	.0570	<u>.035</u>	<u>.035</u>	<u>.00045</u>
24A	58	.100	.008	4.00	9.00	300	.0570	<u>.082</u>	<u>.082</u>	<u>.00025</u>
24A	203	.231	.019	3.00	8.00	60	.0570	<u>.281</u>	<u>.296</u>	<u>.00068</u>
24A	204	.175	0	3.00	8.00	60	.0570	<u>.226</u>	<u>.122</u>	<u>.00126</u>
24A	205	.054	.016	3.00	8.00	60	.0570	<u>.339</u>	<u>.172</u>	<u>.00201</u>
26B	64	.115	.014	3.00	8.00	90	.0520	<u>.0620</u>	<u>.0620</u>	<u>.00291</u>
26B	65	.122	.021	1.00	9.00	90	.0520	<u>.371</u>	<u>.371</u>	<u>.00291</u>
	66									

Table 9. (Continued)

268	.039	1.00	7.00	90	.0620	.00717
268	.075	.004	1.00	90	.0620	.00024
268	.112	.012	4.00	90	.0620	.00105
278	.175	.021	4.00	90	.0690	.00289
28A	.71	.237	.016	1.00	9.00	.00298
28A	.72	.248	.021	3.00	9.00	.00405
28A	.73	.237	.016	3.00	8.00	.00298
30A	.76	.200	.039	4.00	7.00	.00668
30A	.207	.050	0.	4.00	7.00	.00613
30A	.208	.035	0.	4.00	7.00	.00550
30A	.209	.047	0.	4.00	7.00	.00550
30A	.210	.042	.010	4.00	7.00	.00550
31A	.77	.322	0.	.072	2.00	.00550
31A	.79	.332	0.	.072	1.00	.00550
31A	.80	.234	0.	.043	4.00	.00550
32A	.81	.077	.019	1.00	8.00	.00550
32A	.82	.066	.027	4.00	6.00	.00550
33A	.83	.203	.058	2.00	9.00	.00550
33A	.84	.116	.029	4.00	9.00	.00550
33A	.85	.184	.045	1.00	7.00	.00550
33A	.86	.144	.035	1.00	6.00	.00550
33A	.87	.223	.064	3.00	6.00	.00550
33A	.211	.050	0.	1.00	9.00	.00550
35B	.88	.071	.027	1.00	6.00	.00550
36B	.218	.532	.175	5.00	6.00	.00550
36B	.219	.325	.146	5.00	6.00	.00550
37A	.94	.186	.058	3.00	8.00	.00550
38B	.95	.205	.058	1.00	8.00	.00550
38B	.97	.171	.045	3.00	9.00	.00550
39B	.98	.182	.047	1.00	7.00	.00550
39B	.99	.196	.051	1.00	9.00	.00550
43A	103	.210	.062	2.00	8.00	.00550
43A	104	.194	.058	2.00	8.00	.00550
43A	223	.250	.086	4.00	8.00	.00550
43A	224	.060	0.	4.00	8.00	.00550
43A	225	.050	0.	4.00	8.00	.00550
43A	226	.035	0.	4.00	8.00	.00550
43A	227	.185	0.	5.00	8.00	.00550
43A	228	.80	0.	5.00	8.00	.00550
43A	229	.075	0.	5.00	8.00	.00550
43A	230	.020	0.	5.00	8.00	.00550
43A	231	.026	0.	5.00	8.00	.00550
43A	232	.030	0.	5.00	8.00	.00550
43A	233	.025	0.	5.00	8.00	.00550
43A	234	.015	0.	5.00	8.00	.00550
43A	235	.015	0.	5.00	8.00	.00550
44B	105	.195	0.	2.00	6.00	.00550
44B	106	.200	.051	3.00	7.00	.00550
44B	107	.206	.058	2.00	8.00	.00550
44B	235	.070	0.	3.00	8.00	.00550
44B	237	.052	0.	5.00	8.00	.00550
45B	240	.210	0.	3.00	7.00	.00550
45B	240	.035	0.	2.00	6.00	.00550
45B	241	.061	0.	4.00	7.00	.00550
45B	242	.276	0.	5.00	8.00	.00550
45B	243	.130	0.	5.00	7.00	.00550
45B	244	.035	0.	4.00	7.00	.00550
45B	245	.100	0.	4.00	7.00	.00550
46A	110	.287	.088	2.00	9.00	.00550
46A	111	.146	.082	1.00	8.00	.00550
46A	112	.067	0.	3.00	8.00	.00550
46A	113	.202	.057	1.00	7.00	.00550
46A	114	.186	.041	4.00	6.00	.00550
46A	246	.307	.562	.339	.562	.00550

Table 9. (Concluded)

46A	247	.400	.019	.047	.00597
46A	248	.475	.052	.067	.00353
46A	249	.125	.077	.316	.00756
46A	250	.100	.068	.261	.00534
46A	251	.087	.054	.621	.00369
46A	252	.050	.036	.157	.00149
46A	253	.057	.070	.760	.00478
46A	254	.048	.042	.805	.00158
46A	255	.065	.036	.174	.00184
46A	306	.025	.0	.554	.00184
46A	307	.017	.0	.0	.0
46A	256	.072	.0	.0	.0
46A	257	.063	.0	.0	.0
46A	258	.100	.0	.0	.0
46A	259	.177	.0	.0	.0
46A	260	.145	.076	.0	.0
46A	261	.365	.076	.0	.0
46A	262	.070	.010	.0	.0
47B	115	.370	.082	.0	.0
47B	117	.295	.058	.0	.0
47B	118	.330	.080	.0	.0
49B	119	.195	.053	.0	.0
49B	120	.195	.058	.0	.0
50B	264	.286	.0	.0	.0
50B	265	.125	.0	.0	.0
50B	266	.460	.0	.0	.0
50B	267	.068	.0	.0	.0
51A	125	.130	.021	.0	.0
51A	127	.350	.0	.0	.0
51A	128	.262	.094	.0	.0
52A	131	.182	.049	.0	.0
52A	131	.180	.056	.0	.0
53B	134	.075	.018	.0	.0
53B	135	.074	.014	.0	.0
53B	136	.050	.016	.0	.0
54B	138	.060	.006	.0	.0
54B	139	.030	.0	.0	.0
56B	140	.210	.060	.0	.0
56B	141	.210	.068	.0	.0
56B	142	.155	.049	.0	.0
56B	143	.210	.068	.0	.0
57B	144	.210	.056	.0	.0
57B	145	.140	.140	.035	.0
57B	298	.027	.0	.0	.0
57B	299	.027	.0	.0	.0
57B	300	.025	.0	.0	.0
57B	301	.031	.0	.0	.0
57B	302	.133	.039	.0	.0
57B	303	.150	.099	.0	.0
58A	146	.180	.047	.0	.0
58A	147	.175	.058	.0	.0
58A	148	.096	.019	.0	.0
58A	149	.180	.041	.0	.0
58A	304	.060	.0	.0	.0
58A	305	.227	.168	.0	.0
60B	150	.309	.066	.0	.0
60B	151	.282	.051	.0	.0
60B	152	.325	.070	.0	.0
60B	153	.327	.070	.0	.0
60B	154	.300	.058	.0	.0

Table 10. Tabulation of Nondestructive Test Observations for Steel, Sequence I

Table 1C. (Continued)

Table 10. (Concluded)

Table 11. Tabulation of Nondestructive Test Observations for Steel, Sequence 2 LIQUID PENETRANT

PANEL NO.	CRACK NO.	NO. 1	NO. 2	NO. 3	PANEL NO.	CRACK NO.	NO. 1	NO. 2	NO. 3	PANEL NO.	CRACK NO.	NO. 1	NO. 2	NO. 3
1	1	.10	.15	.08	24	1	.10	.05	.10	46	1	.114	.20	.20
1	2	.10	.15	.10	24	1	.20	.13	.13	46	1	.246	.05	.05
1	3	.10	.15	.09	24	1	.10	.15	.15	46	1	.247	.10	.15
1	4	.10	.15	.05	26	2	.65	.15	.20	46	1	.248	.10	.15
2	2	.20	.30	.25	26	2	.65	.15	.20	46	1	.249	.15	.20
2	2	.20	.30	.25	26	2	.67	.25	.30	46	1	.252	.10	.08
2	7	.20	.30	.25	26	2	.68	.10	.10	46	1	.257	.60	.10
5	1	.30	.35	.30	26	2	.69	.15	.10	46	1	.307	.10	0
5	1	.30	.35	.30	27	2	.70	.20	.25	46	1	.307	.67	.10
6	1	.10	.25	.20	28	1	.71	.25	.30	46	1	.258	.20	.05
6	1	.11	.25	.20	28	1	.72	.25	.30	46	1	.259	.0	.20
7	2	.12	.30	.30	28	1	.73	.25	.30	46	1	.262	0	.10
8	2	.13	.10	.10	30	1	.76	.05	.05	47	2	.35	.50	.40
8	2	.14	.07	0	30	1	.76	.05	.05	47	2	.35	.50	.40
8	2	.15	.10	.15	30	1	.76	.07	.07	47	2	.36	.50	.40
9	1	.16	.25	.20	31	1	.77	.35	.40	49	2	.118	.30	.50
9	1	.17	.25	.20	31	1	.79	.35	.50	49	2	.119	.25	.30
10	0	.18	0	0	31	1	.80	.35	.50	49	2	.120	.25	.30
10	1	.19	.07	.08	32	1	.81	.07	.10	50	2	.264	0	.10
10	1	.20	.05	0	32	1	.82	.07	.15	51	1	.125	.15	.20
11	2	.21	.10	.08	33	1	.83	.30	.35	51	1	.127	.40	.40
13	2	.24	.07	.08	33	1	.84	.15	.15	51	1	.128	.30	.40
14	1	.25	.20	.13	33	1	.85	.25	.25	52	1	.129	.20	.25
14	1	.25	.20	.13	33	1	.85	.20	.20	52	1	.131	.20	.20
14	1	.26	.18	.18	33	1	.86	.35	.35	52	1	.131	.20	.25
14	1	.26	.20	.18	33	1	.87	.30	.35	53	2	.134	.10	.10
14	1	.26	.20	.18	33	1	.87	.30	.35	53	2	.135	.10	.10
14	1	.26	.20	.18	33	1	.87	.30	.35	53	2	.135	.10	.10
14	1	.27	.30	.35	35	2	.88	0	.10	53	2	.136	.10	.10
15	1	.28	.30	.35	35	1	.94	.25	.10	54	2	.138	.07	.05
15	1	.29	.30	.35	36	2	.95	.30	.20	54	2	.139	.07	.07
15	1	.30	.30	.35	36	2	.97	.25	.10	55	2	.140	.25	.30
15	1	.30	.30	.35	36	2	.98	.25	.10	55	2	.141	.25	.30
16	2	.31	.30	.35	36	2	.98	.25	.10	56	2	.142	.15	.20
16	2	.32	.30	.35	36	2	.99	.25	.10	56	2	.143	.25	.30
16	2	.32	.30	.35	36	2	.99	.25	.10	56	2	.143	.25	.30
16	2	.33	.30	.35	36	2	.99	.25	.10	57	2	.144	.15	.20
16	2	.33	.30	.35	36	2	.99	.25	.10	57	2	.145	.15	.25
16	2	.34	.30	.35	36	2	.99	.25	.10	57	2	.145	.15	.25
16	2	.35	.30	.35	36	2	.99	.25	.10	57	2	.145	.15	.25
16	2	.36	.30	.35	36	2	.99	.25	.10	57	2	.145	.15	.25
16	2	.36	.30	.35	36	2	.99	.25	.10	57	2	.145	.15	.25
17	2	.37	.08	.08	36	2	.99	.25	.10	57	2	.146	.07	.15
18	1	.39	.25	.35	43	1	.103	.25	.10	58	1	.147	.20	.25
18	1	.40	.10	.10	43	1	.104	.25	.10	58	1	.147	.20	.25
19	1	.41	.15	.18	43	1	.223	.05	.05	58	1	.148	.10	.15
19	1	.42	.20	.20	44	2	.105	.25	.30	58	1	.149	.20	.20
19	1	.43	.15	.18	44	2	.106	.25	.30	58	1	.150	.05	.15
23	1	.43	.15	.18	44	2	.107	.25	.30	58	1	.150	.05	.15
23	1	.44	.10	.10	44	2	.237	.07	.08	58	1	.150	.05	.15
24	0	.55	0	0	45	1	.110	.30	.40	58	1	.150	.40	.30
24	0	.57	0	.08	45	1	.111	.20	.20	60	2	.151	.30	.40
24	1	.58	.10	.13	45	1	.112	.07	.10	60	2	.152	.30	.40
24	1	.203	.08	.20	46	1	.113	.25	.30	60	2	.153	.30	.40
24	1	.54	.08	.07	46	1	.114	.30	.40	60	2	.154	.30	.40

Table 12. Tabulation of Nondestructive Test Observations for Steel, Sequence 3

PANEL NUMBER	CRACK NUMBER	X-RADIOGRAPHY			LIQUID PENETRANT			ULTRASONIC			EDDY CURRENT			MAGNETIC PARTICLE			
		NO. 1	NO. 2	NO. 3	NO. 1	NO. 2	NO. 3	NO. 1	NO. 2	NO. 3	NO. 1	NO. 2	NO. 3	NO. 1	NO. 2	NO. 3	
1 1	1	0.	0.	.08	.10	.10	.10	.05	.10	.13	0.	0.	0.	.10	.10	.10	
1 1	2	.10	0.	0.	.15	.16	.10	.20	.20	.20	.10	.10	.10	.10	.10	.10	
1 0	3	0.	0.	0.	.10	.10	.10	.25	.20	.20	0.	0.	0.	.10	.10	.10	
1 0	4	0.	0.	0.	.09	0.	0.	0.	0.	0.	.08	0.	0.	0.	0.	0.	0.
2 1	5	.18	.20	.18	.25	.20	.25	.30	.40	.40	.40	.25	.30	.30	.20	.15	.18
2 1	6	.18	.18	.25	.20	.25	.25	.30	.40	.40	.40	.25	.30	.30	.20	.15	.18
2 1	7	.15	.15	.18	.25	.20	.25	.30	.40	.40	.40	.25	.30	.30	.20	.15	.17
2 1	8	.30	.25	.30	.35	.30	.35	.35	.50	.65	.65	.30	.30	.30	.25	.25	.30
5 1	9	.30	.30	.30	.35	.30	.35	.35	.50	.65	.65	.30	.30	.30	.25	.25	.30
6 1	10	.18	.20	.20	0.	.18	.20	.20	.30	.30	.30	.10	.10	.10	.20	.15	.16
6 1	11	.25	.20	.20	.20	.18	.20	.20	.30	.30	.30	.10	.10	.10	.20	.15	.16
6 1	12	.30	.30	.30	.35	.30	.35	.35	.50	.65	.65	.30	.30	.30	.25	.25	.30
8 1	13	0.	0.	.10	.10	.10	.10	0.	0.	0.	0.	0.	0.	0.	.10	.10	.10
8 0	14	0.	0.	0.	0.	0.	0.	.75	.05	.06	0.	0.	0.	0.	0.	0.	0.
8 1	15	.10	.10	.10	.20	.20	.20	.10	.12	.10	.10	.28	.28	.28	.10	.05	.10
9 1	16	.20	.20	.20	.25	.20	.25	.20	.30	.30	.30	.50	.50	.50	.20	.20	.20
9 1	17	.20	.20	.20	.20	.18	.20	.20	.30	.30	.30	.40	.40	.40	.20	.20	.21
10 1	18	0.	0.	0.	0.	0.	0.	.07	.08	.08	.08	0.	0.	0.	0.	0.	0.
10 0	19	0.	0.	0.	0.	0.	0.	.10	.10	.10	.10	.20	.20	.20	.10	.05	.05
11 0	20	0.	0.	0.	0.	0.	0.	0.	0.	0.	0.	0.	0.	0.	0.	0.	0.
13 0	21	0.	0.	0.	0.	0.	0.	0.	0.	0.	0.	0.	0.	0.	0.	0.	0.
13 0	24	0.	0.	0.	0.	0.	0.	0.	0.	0.	0.	0.	0.	0.	0.	0.	0.
14 1	25	0.	0.	0.	0.	0.	0.	0.	0.	0.	0.	0.	0.	0.	0.	0.	0.
14 1	26	.10	0.	0.	.15	0.	0.	.25	.20	.20	.20	.10	.10	.10	.25	.25	.16
14 1	27	.15	.10	.10	.25	.20	.20	.20	.30	.30	.30	.10	.10	.10	.25	.25	.17
14 1	28	.30	.30	.30	.35	.30	.35	.35	.50	.65	.65	.30	.30	.30	.30	.30	.16
15 1	29	.30	.30	.30	.35	.30	.35	.35	.50	.65	.65	.30	.30	.30	.30	.30	.16
15 1	30	.30	.30	.30	.35	.30	.35	.35	.50	.65	.65	.30	.30	.30	.30	.30	.16
16 1	31	0.	0.	0.	0.	0.	0.	.30	.30	.30	.30	.30	.30	.30	.30	.30	.16
16 1	32	0.	0.	0.	0.	0.	0.	.30	.30	.30	.30	.30	.30	.30	.30	.30	.16
16 0	33	0.	0.	0.	0.	0.	0.	.30	.30	.30	.30	.30	.30	.30	.30	.30	.16
16 1	34	0.	0.	0.	0.	0.	0.	.30	.30	.30	.30	.30	.30	.30	.30	.30	.16
16 1	35	0.	0.	0.	0.	0.	0.	.30	.30	.30	.30	.30	.30	.30	.30	.30	.16
16 1	36	0.	0.	0.	0.	0.	0.	.30	.30	.30	.30	.30	.30	.30	.30	.30	.16
17 0	37	0.	0.	0.	0.	0.	0.	.07	.05	.05	.05	0.	0.	0.	.30	.30	.15
18 1	38	.20	.20	.20	.25	.20	.25	.25	.35	.35	.35	.30	.30	.30	.25	.25	.15
19 0	39	0.	0.	0.	0.	0.	0.	.10	.10	.10	.10	.15	.15	.15	.10	.15	.15
19 0	40	0.	0.	0.	0.	0.	0.	.20	.20	.20	.20	.35	.35	.35	.15	.15	.15
19 1	41	0.	0.	0.	0.	0.	0.	.13	.13	.13	.13	.20	.20	.20	.20	.20	.15
19 1	42	0.	0.	0.	0.	0.	0.	.20	.20	.20	.20	.25	.25	.25	.20	.20	.20
19 1	43	0.	0.	0.	0.	0.	0.	.10	.20	.20	.20	.15	.15	.15	.10	.15	.15
23 0	54	0.	0.	0.	0.	0.	0.	.07	.05	.05	.05	0.	0.	0.	.12	.12	.12
24 0	55	0.	0.	0.	0.	0.	0.	0.	0.	0.	0.	0.	0.	0.	.20	.20	.20
24 1	57	0.	0.	0.	0.	0.	0.	.07	.05	.07	.07	0.	0.	0.	.05	.05	.05
24 0	58	0.	0.	0.	0.	0.	0.	.10	.08	.12	.07	0.	0.	0.	.10	.10	.10
24 1	203	0.	0.	0.	0.	0.	0.	.10	.07	.07	.07	0.	0.	0.	.10	.10	.10
24 1	204	0.	0.	0.	0.	0.	0.	.15	.05	.15	.15	0.	0.	0.	.15	.15	.15
24 0	205	0.	0.	0.	0.	0.	0.	.10	.07	.07	.07	0.	0.	0.	.10	.10	.10
26 0	64	0.	0.	0.	0.	0.	0.	.08	.06	.08	.08	0.	0.	0.	.15	.15	.15
26 1	65	0.	0.	0.	0.	0.	0.	.15	.15	.15	.15	.20	.20	.20	.20	.20	.20
26 1	66	0.	0.	0.	0.	0.	0.	.10	.10	.10	.10	.20	.20	.20	.20	.20	.20
26 1	67	0.	0.	0.	0.	0.	0.	.23	.23	.23	.23	.25	.25	.25	.25	.25	.25
26 0	68	0.	0.	0.	0.	0.	0.	.08	.08	.08	.08	.10	.10	.10	.10	.10	.10
26 0	69	0.	0.	0.	0.	0.	0.	.15	.15	.15	.15	.15	.15	.15	.15	.15	.15
27 1	70	0.	0.	0.	0.	0.	0.	.20	.18	.18	.18	.20	.20	.20	.20	.20	.20

Table 12. (Continued)

Table 12. (Concluded)

Analyses were separated to evaluate the influences of surface finish, etching and proof loading. Flaw size parameters of primary importance in the use of NDT data for fracture control are crack length ($2C$) and crack depth (a). Analyses were directed to determine the flaw size that would be detected by NDT inspection with a high probability and confidence.

To establish detection probabilities from the data available, traditional reliability methods were applied. Reliability is concerned with the probability that a failure will not occur when an inspection method is applied. One of the ways to measure reliability is to measure the ratio of the number of successes to the number of trials (or number of chances for failure). This ratio times 100% gives us an estimate of the reliability of an inspection process and is termed a point estimate. A point estimate is independent of sample size and may or may not constitute a statistically significant measurement. Statistically significant analysis must take into account both the sample size and the success of the observations in the sample.

If we assume a totally successful inspection process (no failures) we may use standard reliability tables to select a sample size. A 95% confidence level was selected for processing all combined data, and analyses were based on these conditions. For data analysis at a 95% confidence level, 60 successful inspection trials with no failure are required to establish a valid sampling and hence a statistically significant data point. For large crack sizes where detection reliability would be expected to be high, this criteria would be expected to be reasonable. For smaller crack sizes where detection reliability would be expected to be low, the required sample size to meet the 95% confidence level criteria would be very large.

Calculation of Confidence Limits

To establish a reasonable sample size and to maintain some continuity of data we held the sample size constant at 60 NDT observations (trials). We then applied confidence limits to the data generated to provide a basis for comparison and analysis of detection successes, and to provide an estimate of the true proportion of cracks of a particular size that can be detected. Confidence limits are statistical determinations based on sampling theory and are values (boundaries) within which we expect the true reliability value to be if an infinitely large sample is taken. For a given sample size, the higher our

confidence level, the wider our confidence. Simply expressed this means that the more we know about anything, the better our chances are of being right. It is a mathematical probability relating the true value of a parameter to an estimate of that parameter and is based on history repeating itself.

The statistics that are used to determine confidence limits are dependent upon the distribution of whatever characteristic we are measuring. Data based on success/failure criteria can be best described statistically by applying the binomial distribution. The normal, Chi-square and Poisson distributions are sometimes used as approximations to the binomial and are selected on the basis of available sample size. If the sample size is held constant, confidence limits may be applied to these data to establish uncertainties in the true reliability values. A binomial distribution analysis was applied to the data to find the lower or one-sided confidence limit based on the proportion of successes in each sample group.

Lower confidence limits were calculated by standard statistical methods¹² and is compatible with the method described by Yee et al¹³ in an independent NASA program. The lower confidence level, p_l , is obtained by solving the equation:

$$G = \sum_{i=0}^{n-1} \binom{N}{i} p_l^i (1-p_l)^{N-i}$$

Where G is the confidence level desired,
N is the number of tests performed,
n is the number of successes in N tests,
And p_l is the lower confidence level.

Lower confidence limits were determined at a confidence level of 95% ($G=.95$) using 60 trials ($N=60$) for all calculations. The lower confidence limits are plotted as (-) points on all graphical presentations of data reported herein.

Data Plotting

In plotting data graphically, we have attempted to summarize the results of our studies in a few rigorous analyses. Plots were generated by referring to the tables of ordered values by actual flaw dimension, i.e., crack length.

Starting at the longest crack length, we counted down 60 inspection observations and calculated a point estimate of detection reliability (successes divided by trials). A single data point was plotted as a "o" at the largest crack (length in this group). This plotting technique biases data in the conservative direction. The lower confidence limit at a 95% confidence level ($G=.95$) was calculated for this data group and plotted as an (-) at the largest crack length in the group. We then backed up 57 observations (19 cracks), counted down 50 observations, repeated calculation of the point estimate of detection reliability and lower confidence limit for this data group, and plotted the resultant values ("o" and "-") at the largest crack length in this data group. The process was repeated for the remaining observations in each inspection operation. By use of the overlapping sampling technique, the total amount of data required could be reduced. The overlapping method is applicable since all observations are independent and hence may be included in any data sampling group. An added advantage is the "smoothing" of the curve resulting from such a plotting technique.

Plots of detection reliabilities at the 95% confidence level for NDT methods as applied to titanium specimens are shown in Figures 12 through 19. Plots of detection reliabilities at the 95% confidence level for steel specimens are shown in Figures 20 through 29. Plots shown are for planned crack data only. Unintentional flaw data was discarded after an initial run due to problems incurred in matching, verifying and correlating actual data to NDT observations.

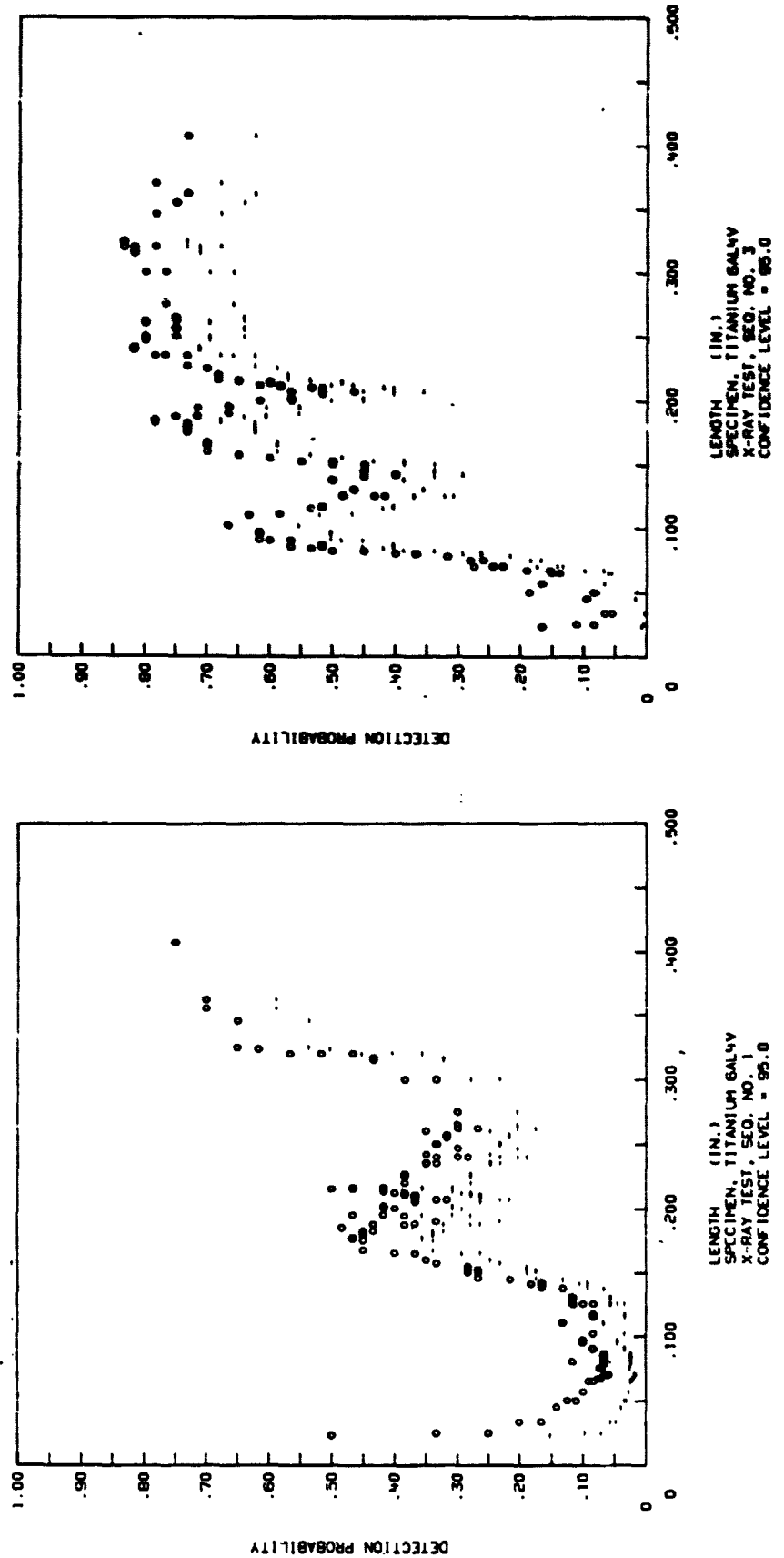


FIGURE 12. Crack Detection Probability of the X-radiographic Inspection Method for Titanium Specimens Plotted by Actual Crack Length at 95% Confidence

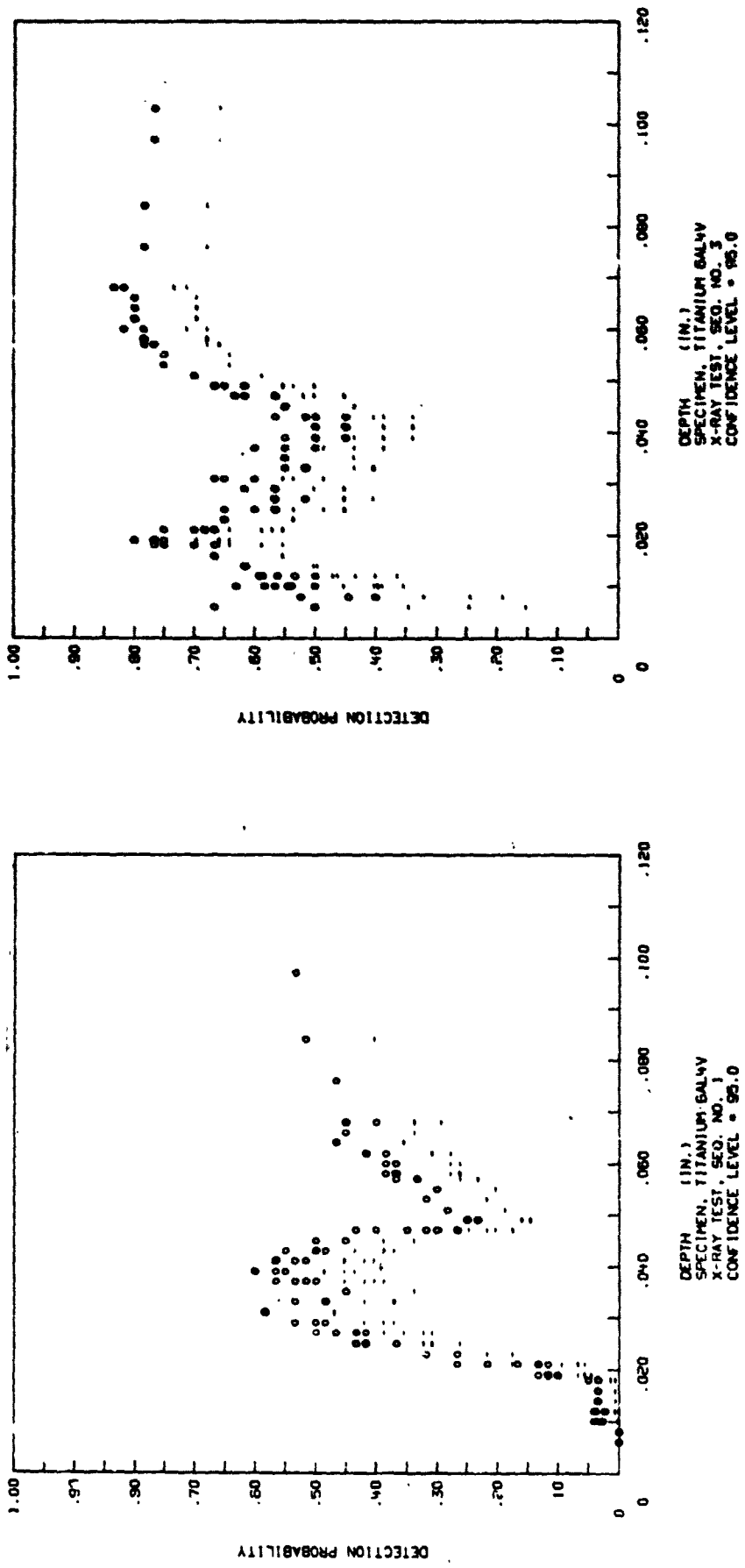


FIGURE 13. Crack Detection Probability of the X-radiographic Inspection Method for Titanium Specimens Plotted by Actual Crack Depth at 95% Confidence

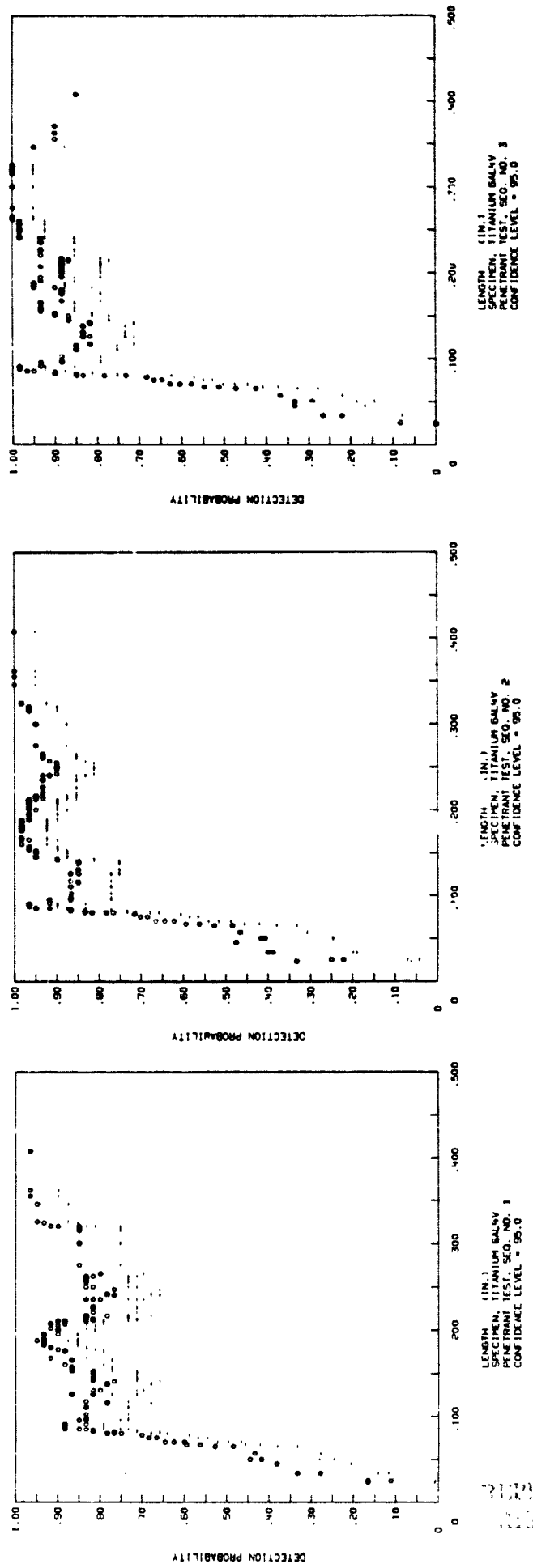


FIGURE 14. Crack Detection Probability of the Penetrant Inspection Method for Titanium Specimens
Plotted by Actual Crack Length at 95% Confidence

REPRODUCIBILITY OF THIS
ORIGINAL PAGE IS POOR

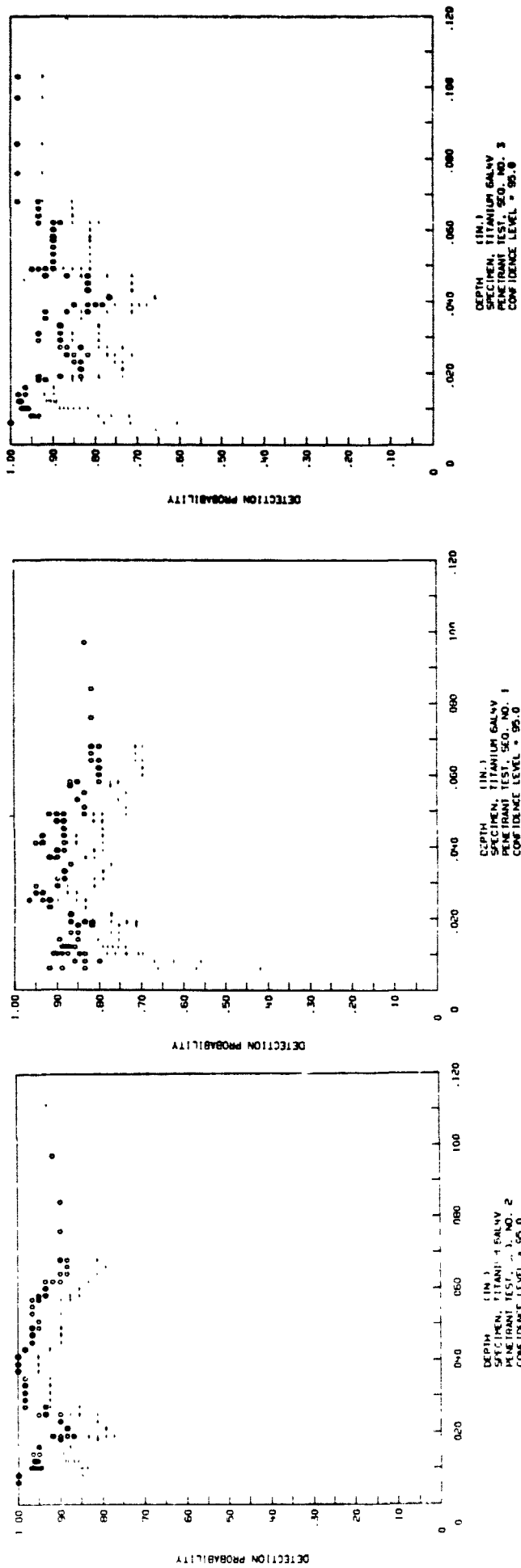


FIGURE 15. Crack Detection Probability of the Penetrant Inspection Method for Titanium Specimens
Plotted by Actual Crack Depth at 95% Confidence

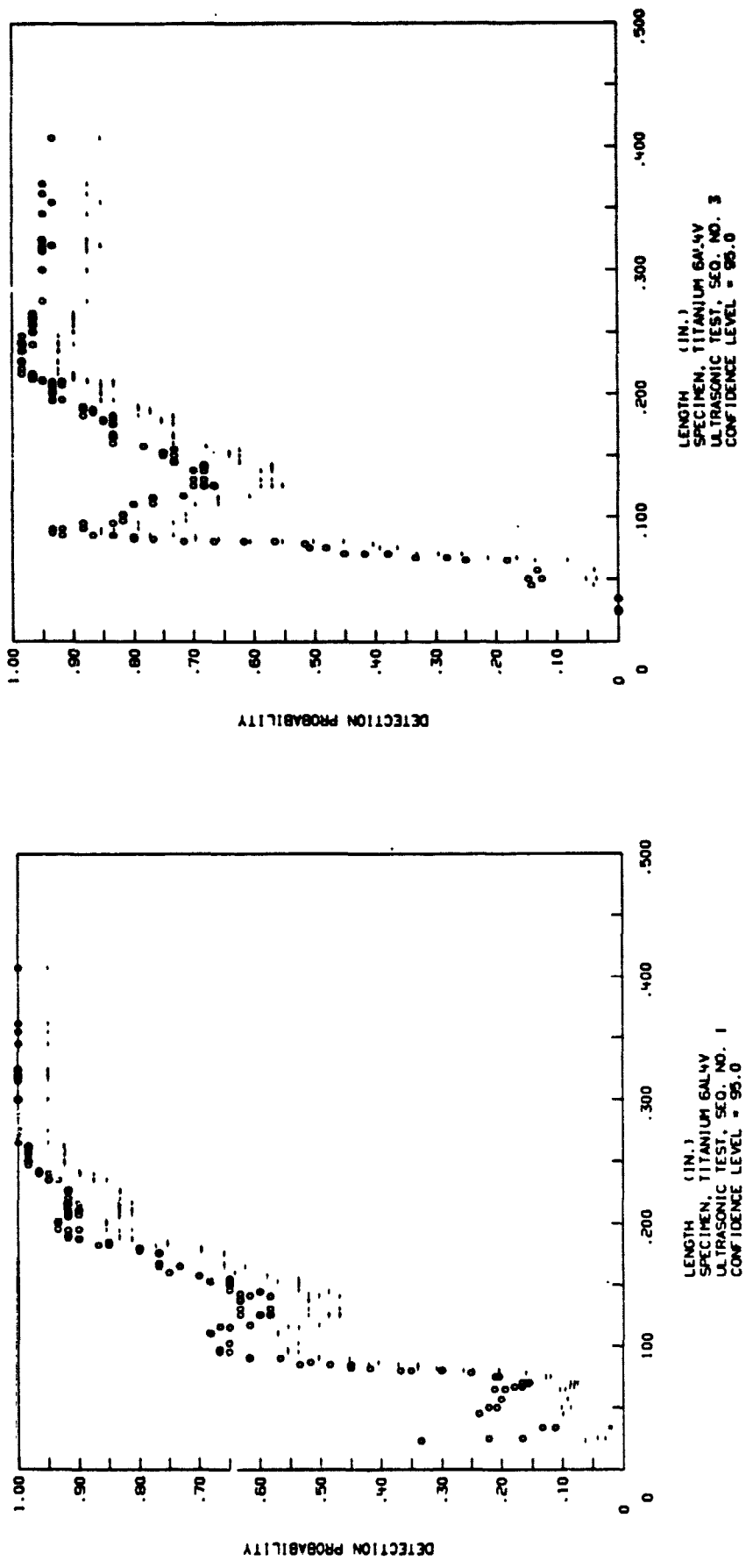


FIGURE 16. Crack Detection Probability of the Ultrasonic Inspection Method for Titanium Specimens Plotted by Actual Crack Length at 95% Confidence

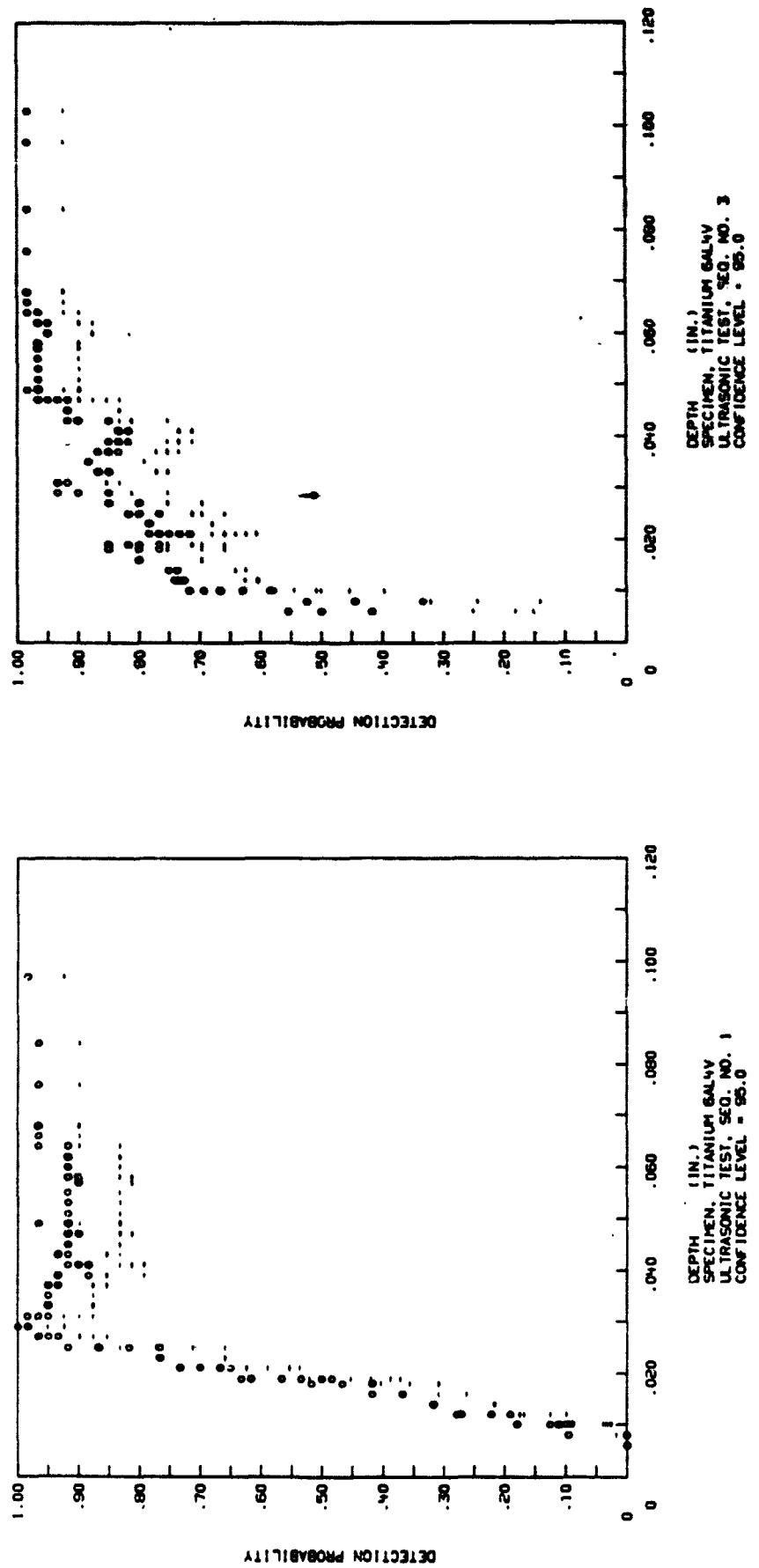


FIGURE 17. Crack Detection Probability of the Ultrasonic Inspection Method for Titanium Specimens
Plotted by Actual Crack Depth at 95% Confidence

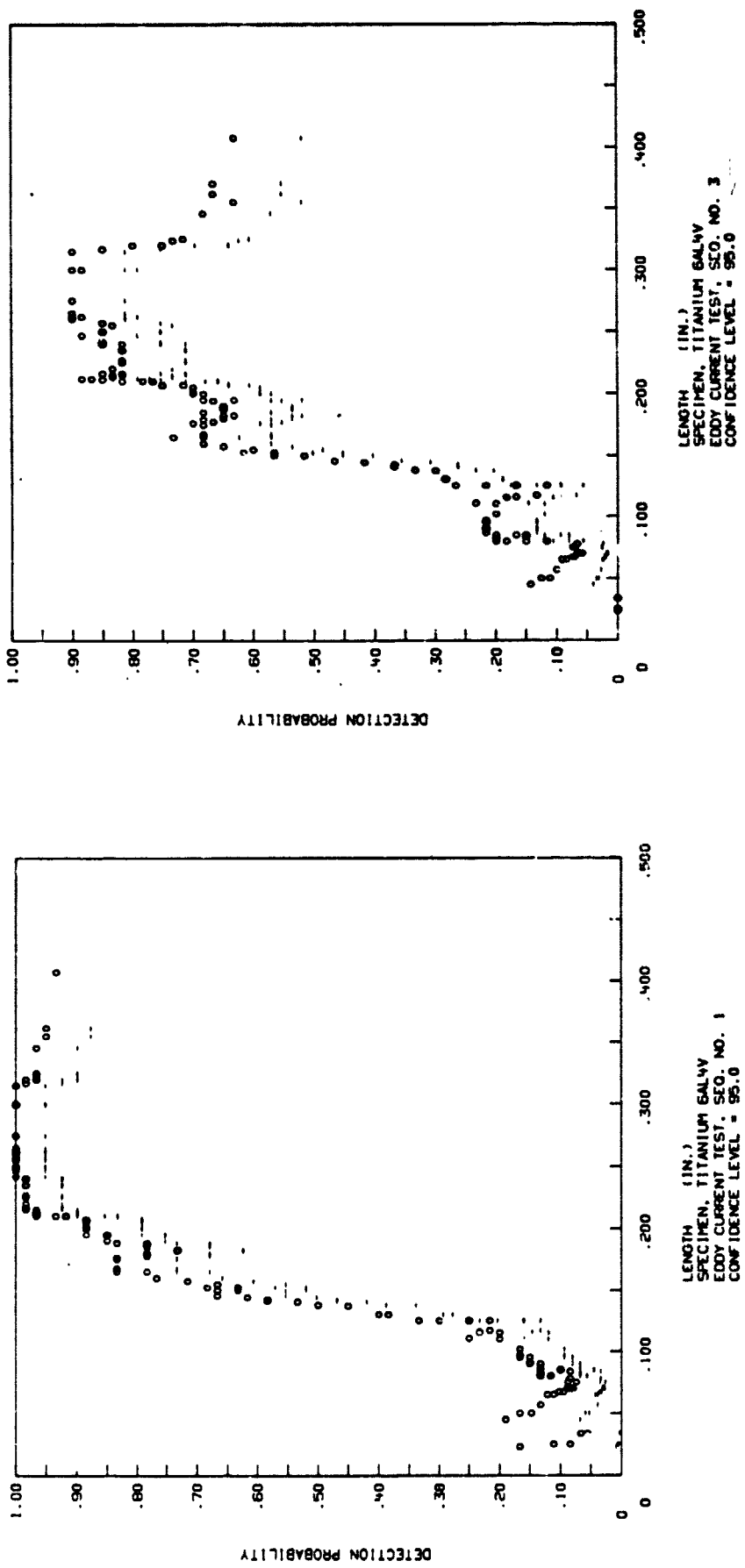


FIGURE 18. Crack Detection Probability of the Eddy Current Inspection Method for Titanium Specimens
Plotted by Actual Crack Length at 95% Confidence

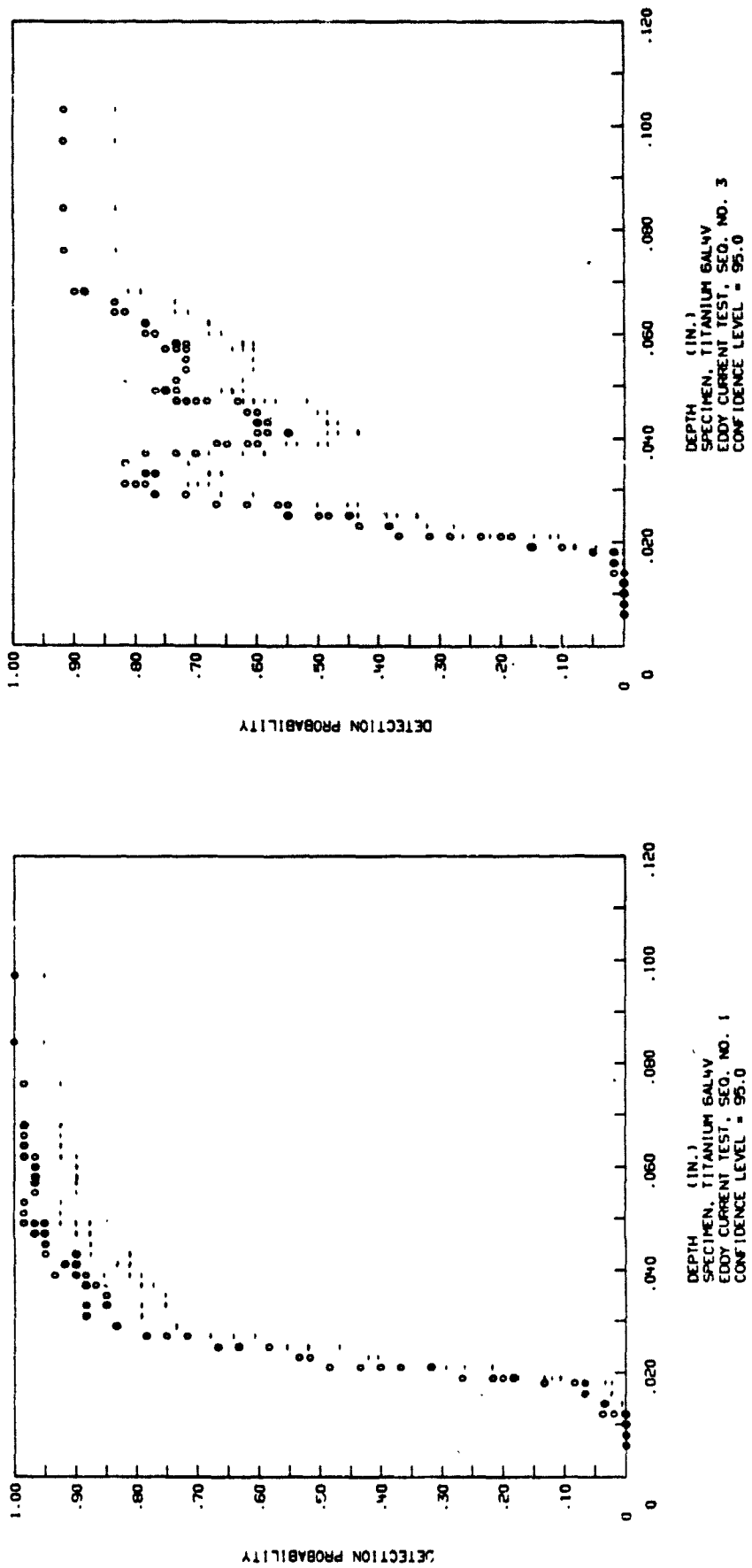


FIGURE 19. Crack Detection Probability of the Eddy Current Inspection Method for Titanium Specimens Plotted by Actual Crack Depth at 95% Confidence

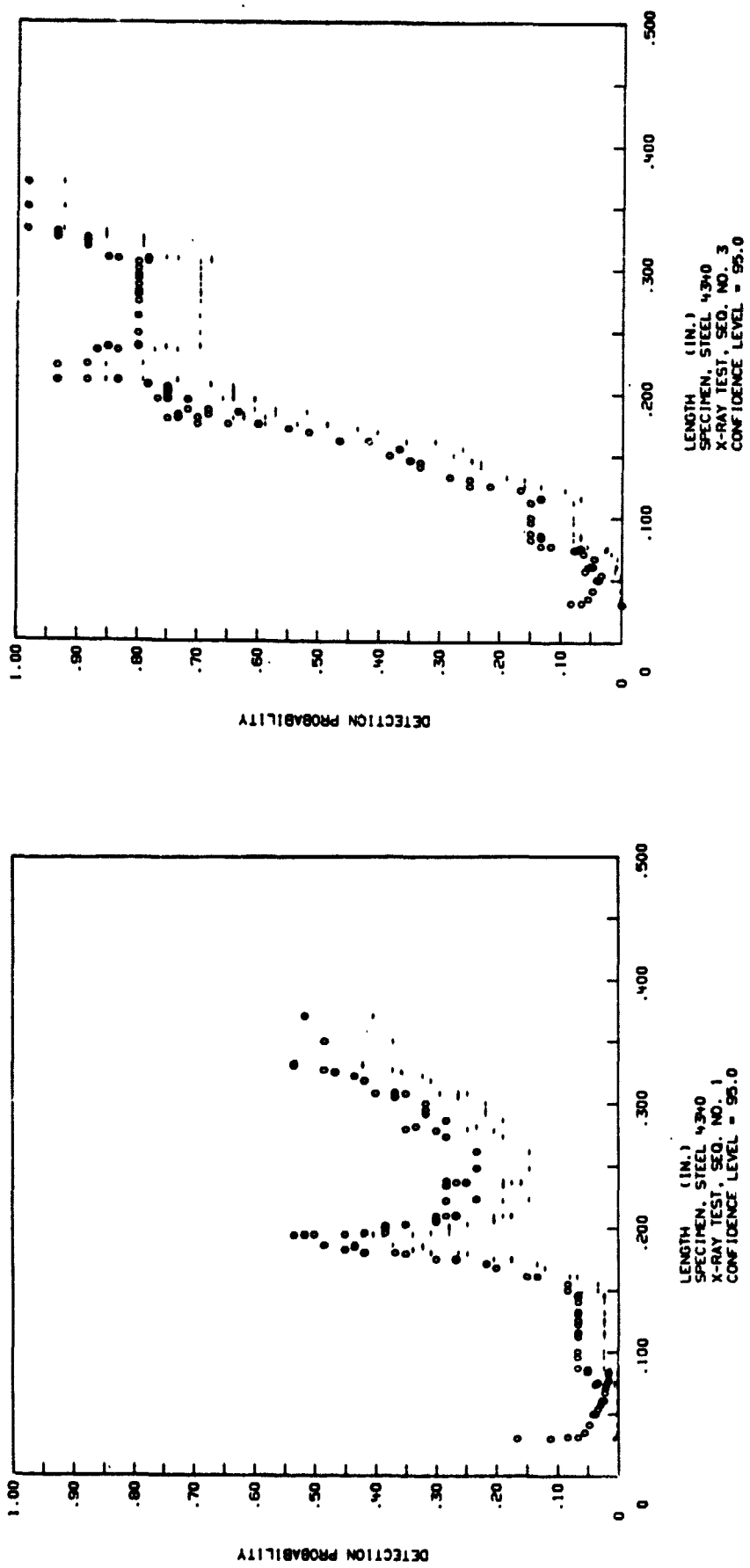


FIGURE 20. Crack Detection Probability of the X-radiographic Inspection Method for Steel Specimens
Plotted by Actual Crack Length at .95% Confidence

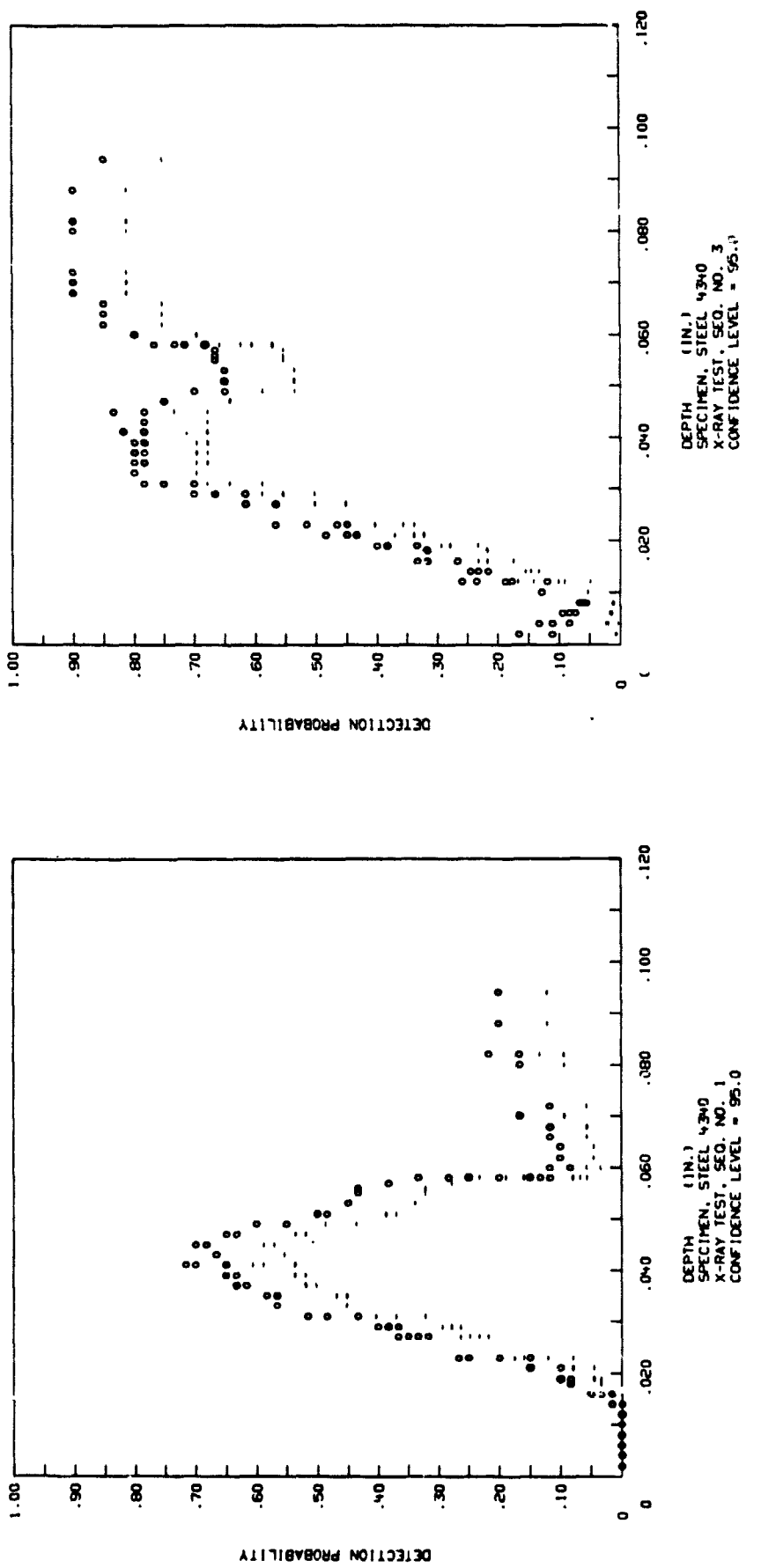


FIGURE 21. Crack Detection Probability of the X-ray Radiographic Inspection Method for Steel Specimens Plotted by Actual Crack Depth at 95% Confidence

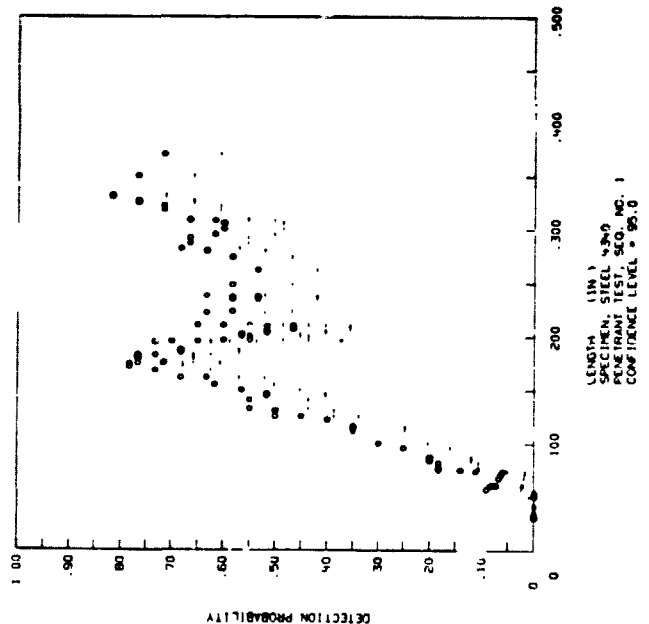
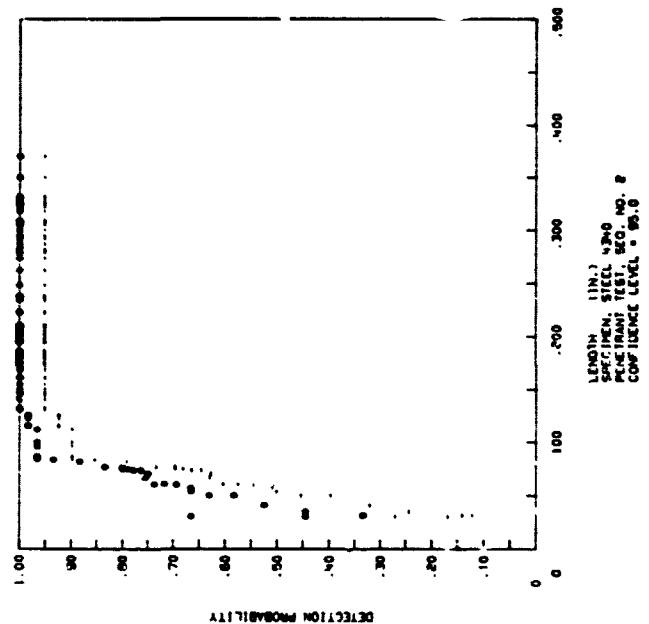
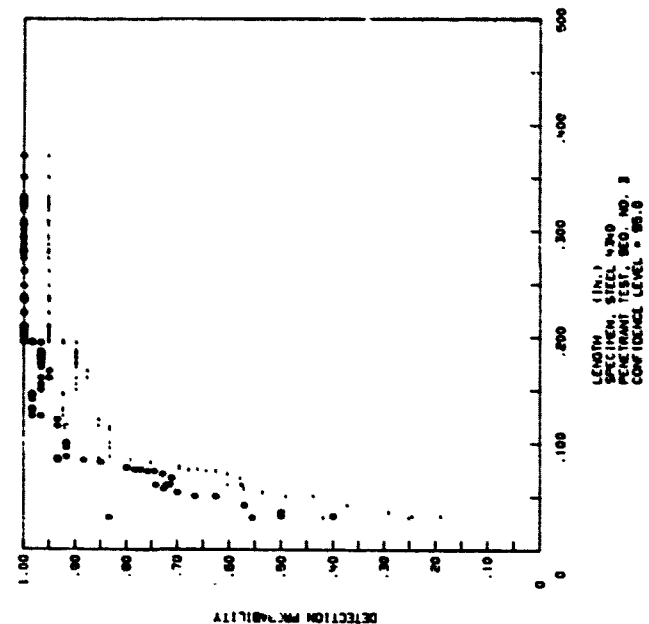


FIGURE 22. Crack Detection Probability of the Penetrant Inspection Method for Steel Specimens Plotted by Actual Crack Length at 95% Confidence

REPRODUCIBILITY OF THE
ORIGINAL PAGE IS POOR

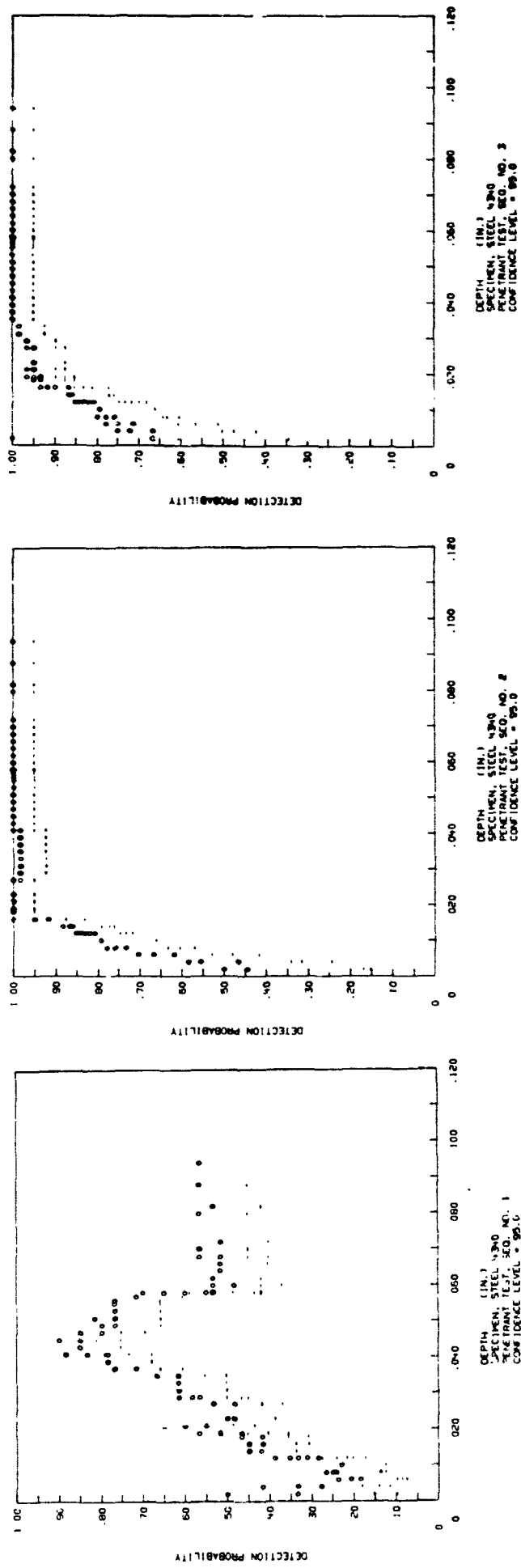


FIGURE 23. Crack Detection Probability of the Penetrant Inspection Method for Steel Specimens Plotted by Actual Crack Depth at 99% Confidence

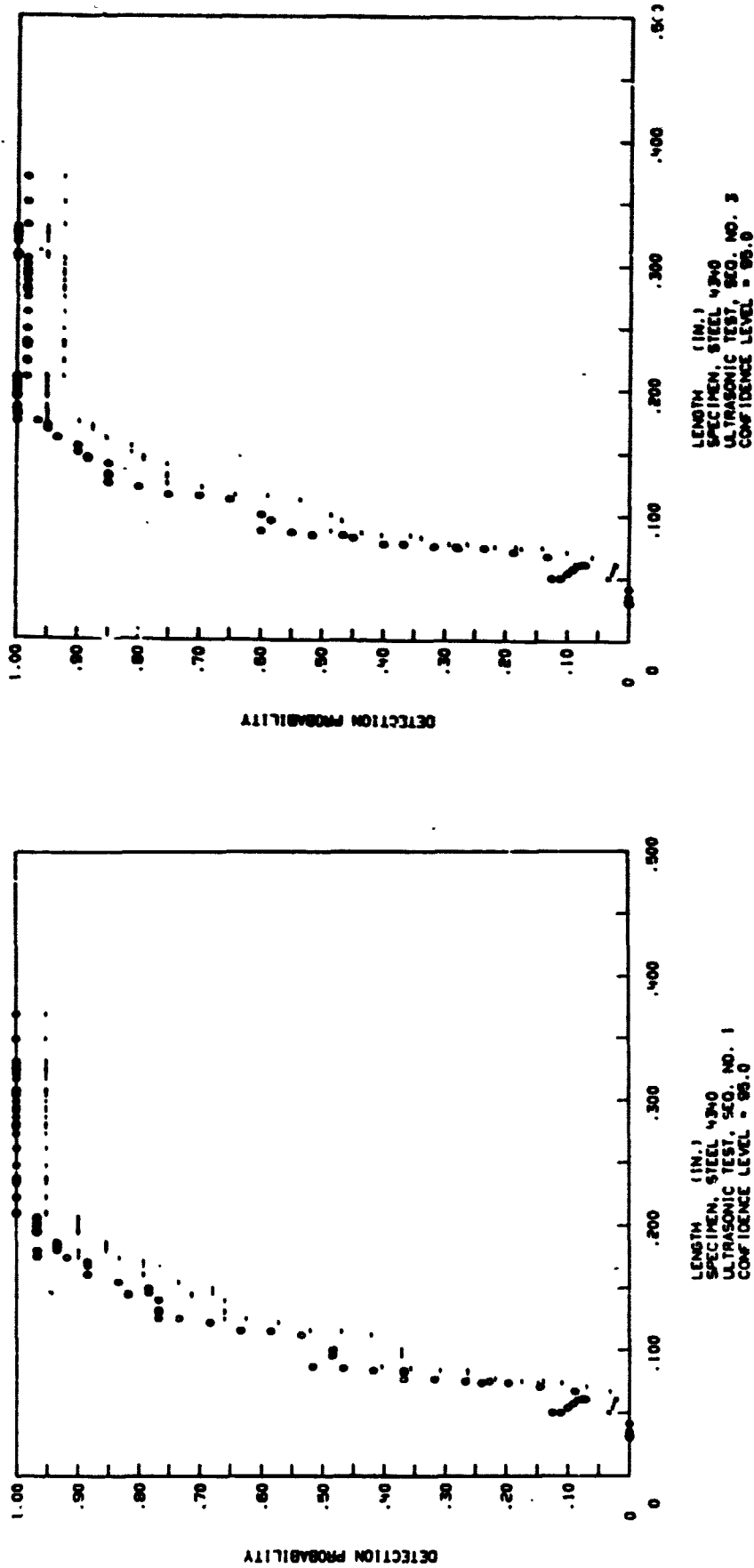
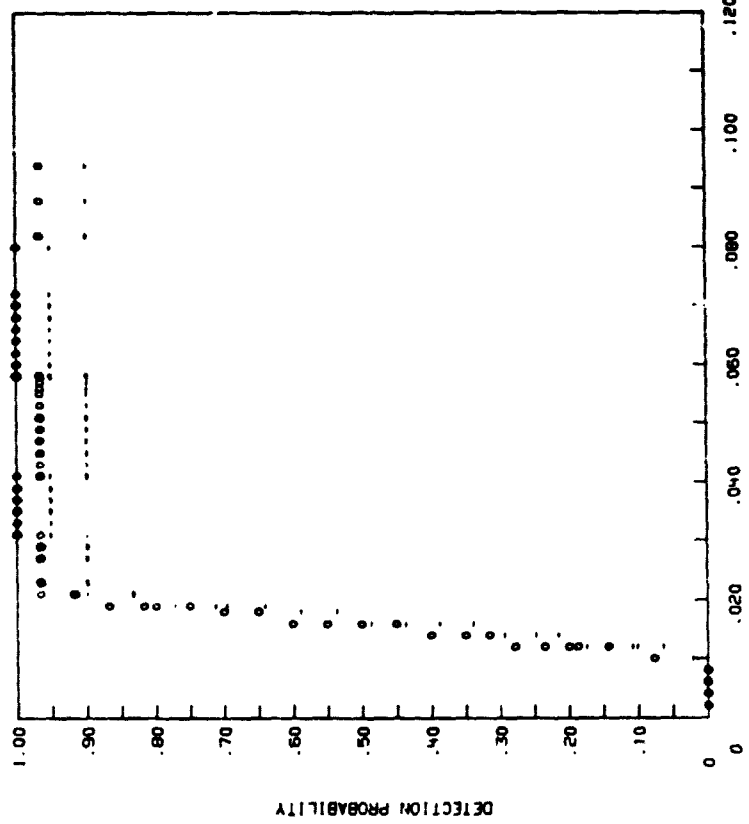
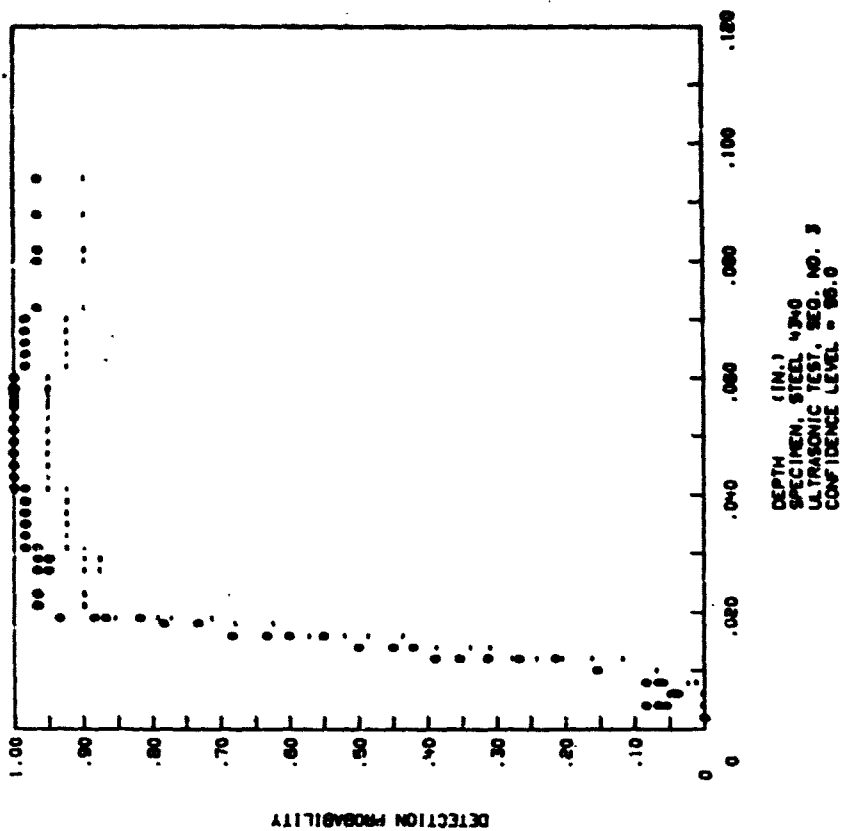


FIGURE 2b. Crack Detection Probability of the Ultrasonic Inspection Method for Steel Specimens Plotted by Actual Crack Length at 95% Confidence



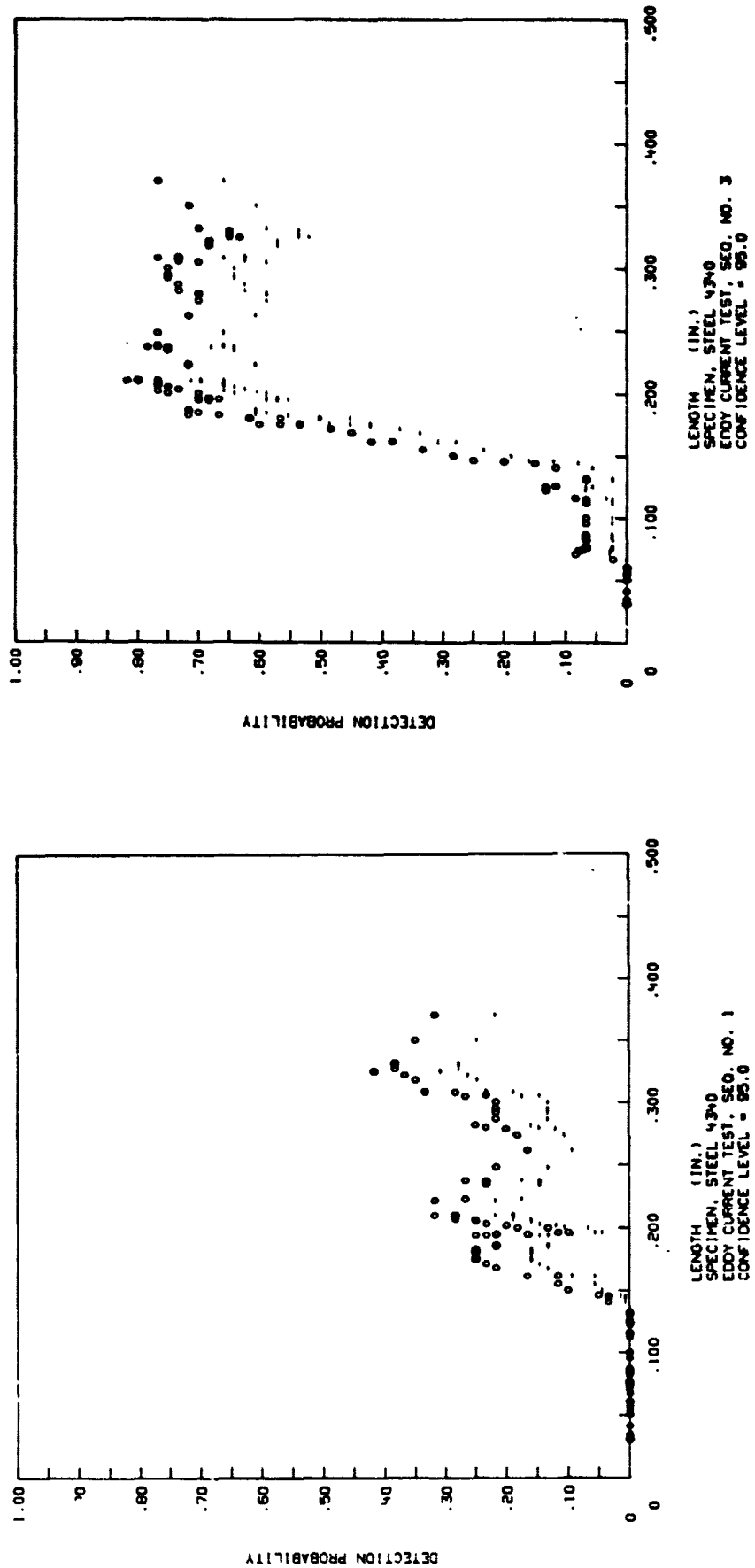


FIGURE 26. Crack Detection Probability of the Eddy Current Inspection Method for Steel Specimens Plotted by Actual Crack Length at 95% Confidence

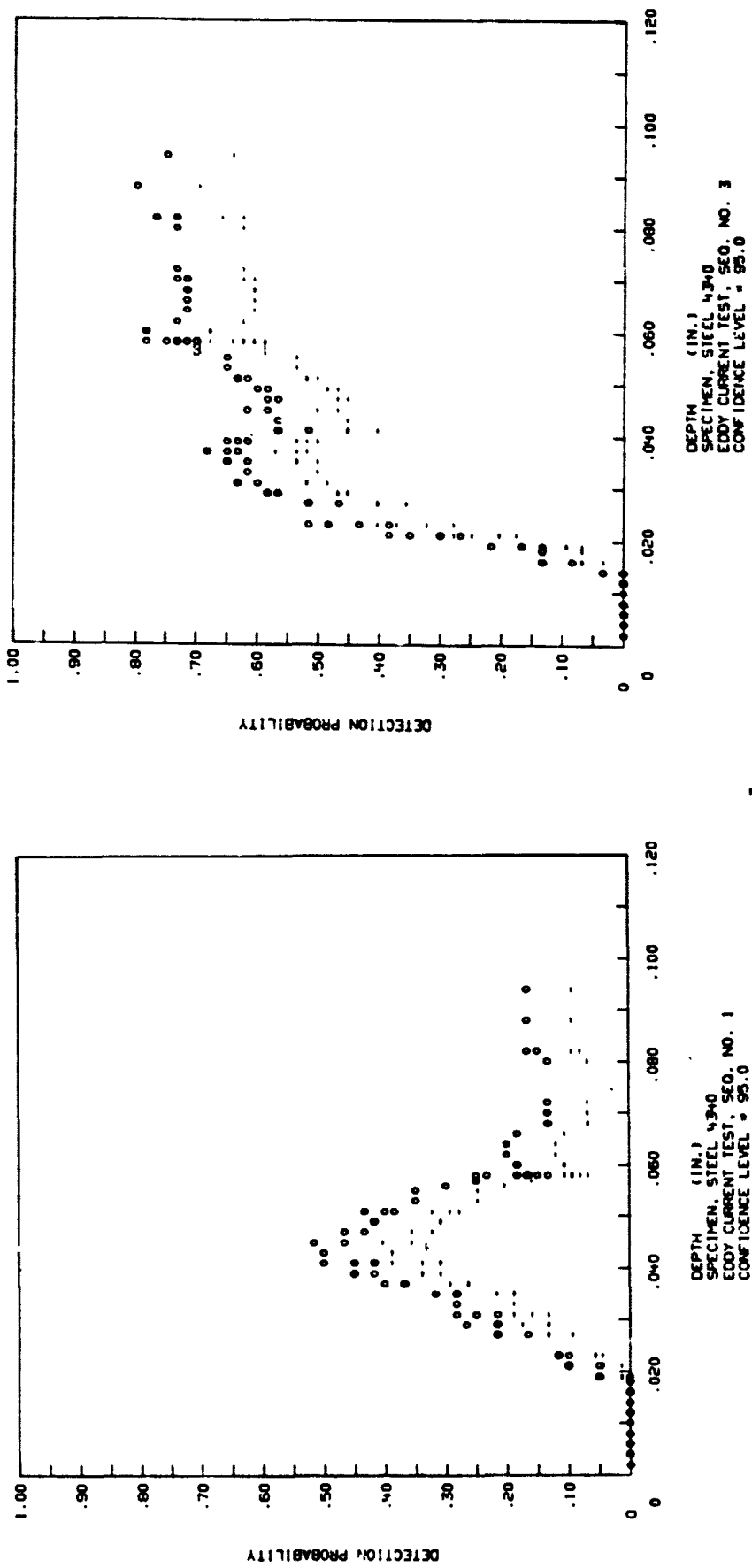


FIGURE 27. Crack Detection Probability of the Eddy Current Inspection Method for Steel Specimens Plotted by Actual Crack Depth at 95% Confidence

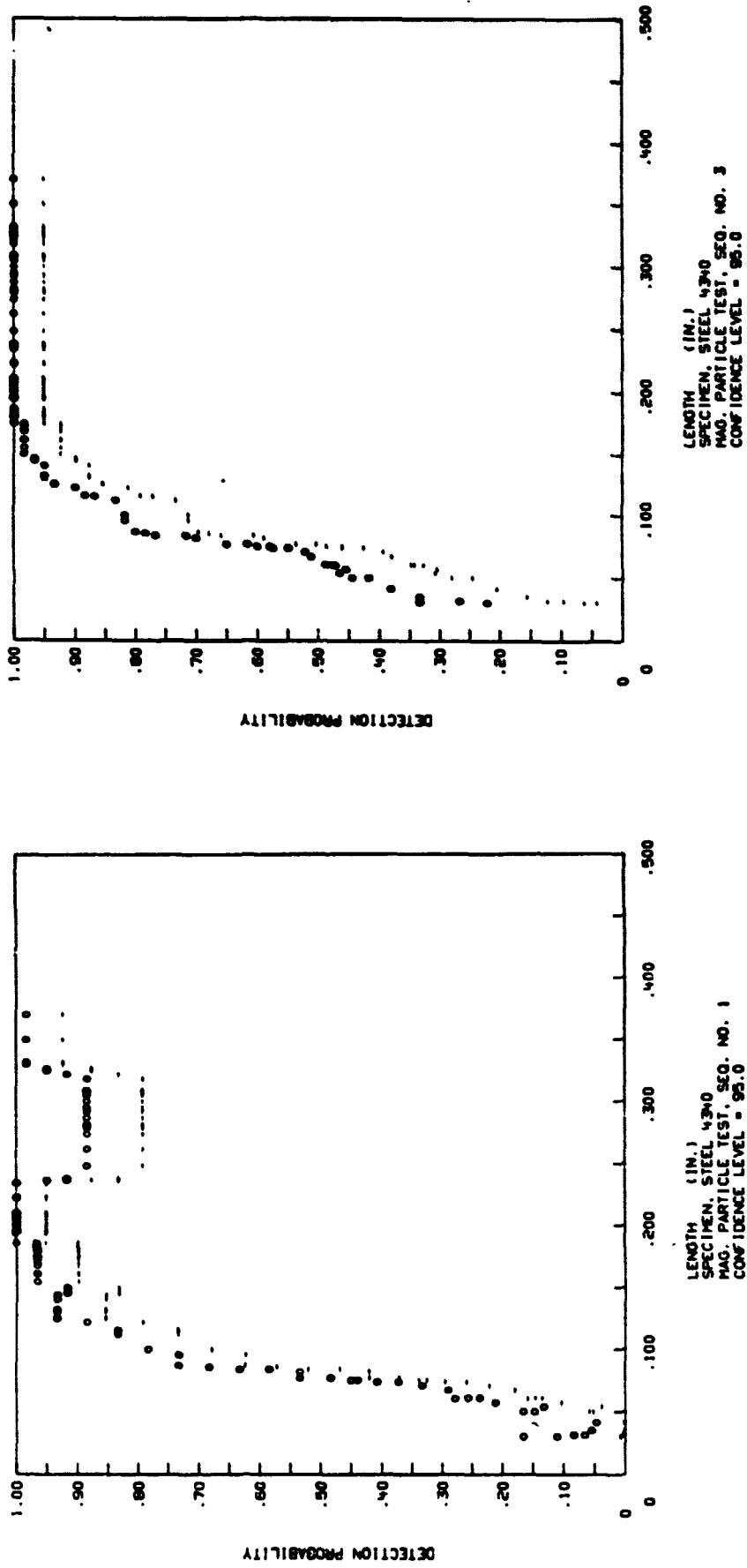


FIGURE 28. Crack Detection Probability of the Magnetic Particle Inspection Method for Steel Specimens Plotted by Actual Crack Length at 95% Confidence

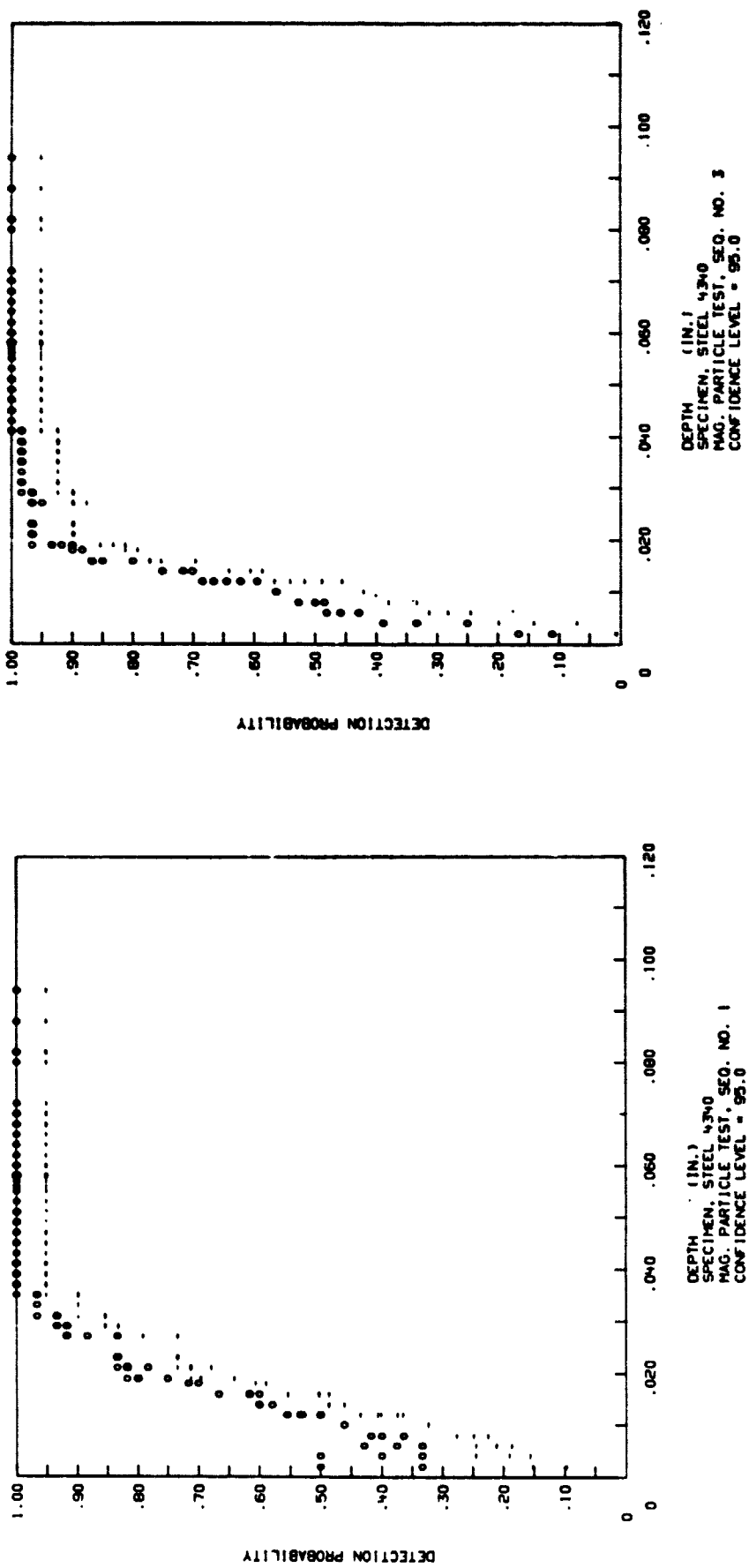


FIGURE 29. Crack Detection Probability of the Magnetic Particle Inspection Method for Steel Specimens
Plotted by Actual Crack Depth at 95% Confidence

VII. RESULTS, CONCLUSIONS AND RECOMMENDATIONS

Plots of NDT data difference from those previously obtained^{6, 8} due to the overlapping plotting method used. Data plotted by this method provide a more accurate display of detection anomalies as a function of specific crack and specimen factors.

Titanium Specimen Results

The influence of specific cracks on detection probability are evident in analysis of X-radiographic data for titanium panels. Detection by the X-radiographic technique is improved after etching and proof loading. The cyclic nature of the data plots are attributed to the effects of flaw closure for specific cracks. The overall improvement in detection for this method is attributed primarily proof loading of the specimens with some visible evidence of plastic flow around the cracks.

Detection of cracks by the penetrant method in titanium panels is also cyclic with crack length and is attributed to variations in crack closure. An improvement in detection was realized after etching to remove flowed material. A decrease in detection was obtained after proof loading. This is attributed to plastic flow around the cracks and a resultant increase flaw width. Penetrant material can be more easily washed out of open flaws. Flaw opening variations in turn influence the penetrant process and human factors associated with the process application.

The cyclic nature of the data is also reflected by ultrasonic detection as a function of crack length. An overall improvement in detection is evident after etching and proof loading. A decrease in detection at longer crack lengths is evident after proof loading. This decrease is attributed to a combination of human factors and an increase in energy scattering at the crack after deformation due to proof loading.

A decrease in detection by the eddy current method was realized after proof loading. This is attributed to the increased opening at the cracks and resultant overall decrease in eddy current signal amplitude as obtained by the small diameter pencil probe.

Steel Specimen Results

X-ray detection for steel specimens was also improved by proof loading. The improvement is attributed to increased crack opening.

Penetrant detection was improved greatly by etching steel specimens and decreased slightly after proof loading. The decrease is attributed to penetrant variation with increased crack opening.

Ultrasonic data shows an overall improvement in detection after proof loading with some decrease at the longer crack lengths. The decrease is attributed to increased scatter due to distortion of the crack by proof loading.

Eddy current detection prior to etching and proof loading is poor. Eddy current inspection was extremely difficult due to large variations in the balance point within and between specimens. These variations were attributed to cold working of the surface layer of the specimens due to machining with resultant variations in conductivity and magnetic permeability. Variations were removed by etching and proof loading which resulted in an increase in detection probability.

Detection by the magnetic particle technique is also believed to be affected by the cold worked surface layer on specimens in the as-machined condition. An improvement in detection was obtained after etching and proof loading.

Conclusions

Results of this work differ from those reported previously for steel and titanium alloy materials¹⁰. Differences are due to differences in specimens used for evaluation. The influence of the specimen and crack are emphasized by data obtained during this study. The importance and influence of specimens on reliability demonstration is evident and must be accounted for in extrapolation of this data and in application to varying hardware configurations.

The overall results show that a high detection probability can be achieved if proper NDT techniques are selected and properly applied.

Recommendations

Data obtained in this program provides a better understanding of the capabilities of various NDT techniques and emphasizes areas where more understanding is required before general predictions can be made for detection reliability. Areas identified where further understanding is required include:

- The influence of specimen surface preparation or detection.
- The influence of crack closure on detection.
- The influence of service life (loading and flaw shape) on detection.
- The influence of crack geometry (length versus depth) on detection.
- The influence of methods variation on detection.
- The influence of signal response (signal to noise, calibration, etc.) on detection.

A basis for understanding has been established and some direction has been indicated for achieving a goal of consistent and reliable flaw detection by nondestructive testing techniques.

References:

1. Paul F. Packman, ASM/AE's Fourth Annual Forum: Prevention of Failure through Nondestructive Inspection, Tarpon Springs, Florida, June 14-16 1976.
2. Robert W. Neuschaefer and James B. Beal: "Assessment of and Standardization for Quantitative Nondestructive Testing," NASA TM-X- 64706, September 30, 1972.
3. B.G.W. Yee, F. H. Chang, J. C. Couchman and P. F. Packman, Assessment of NDT Reliability Data, NASA CR-50001, October 1975.
4. Donald E. Pettit and David W. Hoeppner: Fatigue Flaw Growth and NDT Evaluation for Preventing Through-Cracks in Spacecraft Tankage Structures. NASA CR-128560, September 25, 1972.
5. R. T. Anderson, T. J. DeLacy and R. C. Stewart: Detection of Fatigue Cracks by Nondestructive Testing Methods. NASA CR-128946, March 1973.
6. Ward D. Rummel, Paul H. Todd, Jr., Sandcr A. Frecka, and Richard A. Rathke: The Detection of Fatigue Cracks by Nondestructive Testing Methods. NASA CR-2362, February 1974.
7. C. R. Bishop, Nondestructive Evaluation of Fatigue Cracks, Rockwell International, Space Division, SD-73-SH-0219, September, 1973.
8. Ward D. Rummel, Richard A. Rathke, Paul H. Todd, Jr., and Steve J. Mullen, The Detection of Tightly Closed Flaws by Nondestructive Testing (NDT) Methods, NTIS-N-76-14475, October 1975.
9. P. F. Packman, H. S. Pearson, J. S. Owens, and G. B. Marchese, The Applicability of a Fracture Mechanics Nondestructive Testing Design Criterion. TR-68-32. AFML, May, 1968.
10. E. L. Caustin, B-1 USAF/Rockwell International NDI Demonstration Program, Rockwell International B-1 Division, 1972-1973.

11. James R. Alburger: "Theory and Application of Liquid Tracers," Nondestructive Testing, Vol. XX, No. 2, 1962, p 91.
12. Alexander McFarlane Moog: Introduction to the Theory of Statistics. McGraw-Hill Book Company, Inc, 1950, pp 233-237.
13. B.G.W. Yee, J. C. Couchman, F. H. Chang, and D. F. Packman: "Assessment of NDE Reliability Data." CR-134834. General Dynamics Corporation, Fort Worth Division, September 1975.

MARTIN MARIETTA

APPENDIX A

QUALITY LABORATORIES INSTRUCTION

Division	Number
DENVER	X-22
Subject	Page
DETECTION OF TIGHTLY CLOSED FLAWS BY RADIOGRAPHIC INSPECTION IN STEEL AND TITANIUM	1 Of 7
	Issued
	Revised
	Approved <i>[Signature]</i>

1.0 SCOPE

To establish the technique for performing X-radiography of fatigue cracked panels using a selected optimum technique.

2.0 REFERENCES

- 2.1 Technical Proposal -Volume I Detection of tightly closed flaws by Nondestructive Testing (NDI) methods in steel and titanium.
- 2.2 Military Standard 000453A Inspection, Radiographic.
- 2.3 Quality Technical Instruction (QTI) 401, Section II Radiographic Inspection

3.0 EQUIPMENT AND MATERIALS

- 3.1 Norelco MG 150 Industrial X-ray unit.
- 3.2 Kodak X-Omat Processor Model M3.
- 3.3 MacBeth Quantalog Transmission Densitometer, Model TD-100A.
- 3.4 Viewer, High Intensity, General Electric Model BY-Type I or equivalent.
- 3.5 Penetrameters - In accordance with Military Standard 000453A Figure 1.
- 3.6 Magnifiers, 5X and 10X Pocket Comparator or equivalent.
- 3.7 Misc. radiographic accessories.
- 3.8 Coding Sheet E-232D.

4.0 PERSONNEL

Personnel performing radiographic inspection shall qualify to SNT-TC-1A Level II or Level III.

5.0 PROCEDURE

- 5.1 An optimum technique using Kodak, Type M Industrial X-ray film shall be used to perform the radiography of fatigue cracked panels (Attachments #1 and #2).

DIVISION		DATE	NUMBER	PAGE	OF
	DENVER		X-22	2	7

The rationale for the techniques is based on the results as demonstrated by the radiographs and techniques employed for the radiography of fourteen calibration panels.

- 5.2 Refer to Attachment #1 (Titanium) and/or Attachment #2 (Steel) for the optimum setup and exposure data necessary to produce the proper radiograph.
- 5.3 Place the film in direct contact with the machined surface (Side B) of the panel being radiographed.
- 5.4 Prepare and place the required identification and accessories on the film and/or panel. (Figure #1).
NOTE: The panel will be placed on the exposure table in a manner such that the panel number will always be on the radiation source side and in the upper left hand corner. The (8) symbol will always identify the center line of the panel.
- 5.5 The appropriate penetrometer (Military Standard 000453A, 0.06 for the thin panels, 0.25 for the thick panels) shall be radiographed with each panel for the duration of the exposure.
- 5.6 The penetrometers shall be placed on the machined portion of the panel. (Figure #1).
- 5.7 The radiographic density of the machined area of panel shall not vary more than + 30 percent or -15 percent from the density at the penetrometer location.
- 5.8 Align the direction of the central beam of radiation perpendicular and to the center of the panel being radiographed.
NOTE: Make sure that the X-ray tube head is level in both the X and Y Axis.
- 5.9 Expose the film at the selected optimum technique from Attachment #1 (Titanium) Attachment #2 (Steel).
- 5.10 Process the exposed film through the automatic processor (Attachment #1).
- 5.11 The radiographs shall be free from blemishes which may mask fatigue cracks or interfere with radiographic interpretation.
- 5.12 The density of the radiographs shall be checked with a densitometer and shall be within a range of 2.5 to 4.0 (3.5 optimum).
- 5.13 Using a viewer with the proper illumination and with the aid of magnification, interpret the radiographs to determine the number of fatigue cracks in each panel radiographed. Each crack shall be marked by encirclement with wax pencil of a contrasting color.
- 5.14 The radiographic interpreter will record the location of the fatigue cracks on Coding Sheet E-232D.

DIVISION	DATE	NUMBER	PAGE	OF
DENVER		X-22	3	,

NOTE: A transparent grid overlay technique will be used to conveniently and accurately locate flaws. (Figure #2 - Grid Pattern Layout).

- 5.14.1 Determine the location of cracks by placing the transparent grid over the radiograph with center line (8) over the symbol (\$) on the radiograph and aligning it with the panel edges (parallel).
- 5.14.2 Locate cracks by counting the squares in the (Y) direction 6, 7, 9, or 10 and then the (X) direction 1,2,3,4, or 5 and record the location on coding sheet E-232D.

6.0 SAFETY

- 6.1 The use of radiographic equipment shall be in accordance with the safety provisions specified in Martin Marietta Corporation, Denver Division Radiological Safety Manual and Quality Laboratory Instruction X-11.
- 6.2 Radiographic personnel shall wear a film badge at all times while operating the X-ray equipment.

ATTACHMENT #1

Type of Film - Eastman Kodak Type M

Exposure Parameters: Optimum Technique - Titanium

(A) Kilovoltage

.060-35
.250-55

(B) Milliamperes

.060-8
.250-8

(C) Exposure Time

.060-15 min.
.250-26 min.

(D) Target/Film Distance

24" inches

(E) Geometry of Exposure

Perpendicular

(F) Film Holders/Screens

Ready Pack/No screens

(G) Development Parameters

Kodak Model M3 X-Omat Processor
Development Temperature of 80°F.

(H) Radiographic Density

2.5 to 4.0
(3.5 optimum)

(I) Other pertinent parameters/remarks

Radiographic Equipment

Norelco MG150

Beryllium Window

.7 mm focal spot

ATTACHMENT #2

Type of Film - Eastman Kodak Type M

Exposure Parameters: Optimum Technique - Steel

- (A) Kilovoltage
 - .060-55
 - .250-100
- (B) Milliamperes
 - .060-8
 - .250-4
- (C) Exposure Time
 - .060-10 min.
 - .250-15 min.
- (D) Target/Film Distance
 - 24 inches
- (E) Geometry of Exposure
 - Perpendicular
- (F) Film Holders/Screens
 - Ready Pack/No screens
- (G) Development Parameters
 - Kodak Model M3 X-Omat Processor
 - Development Temperature of 80° F.
- (H) Radiographic Density
 - 2.5 to 4.0
 - (3.5 optimum)
- (I) Other pertinent parameters/remarks
 - Beryllium Window
 - Radiographic Equipment
 - Norelco MG150
 - .7mm focal spot

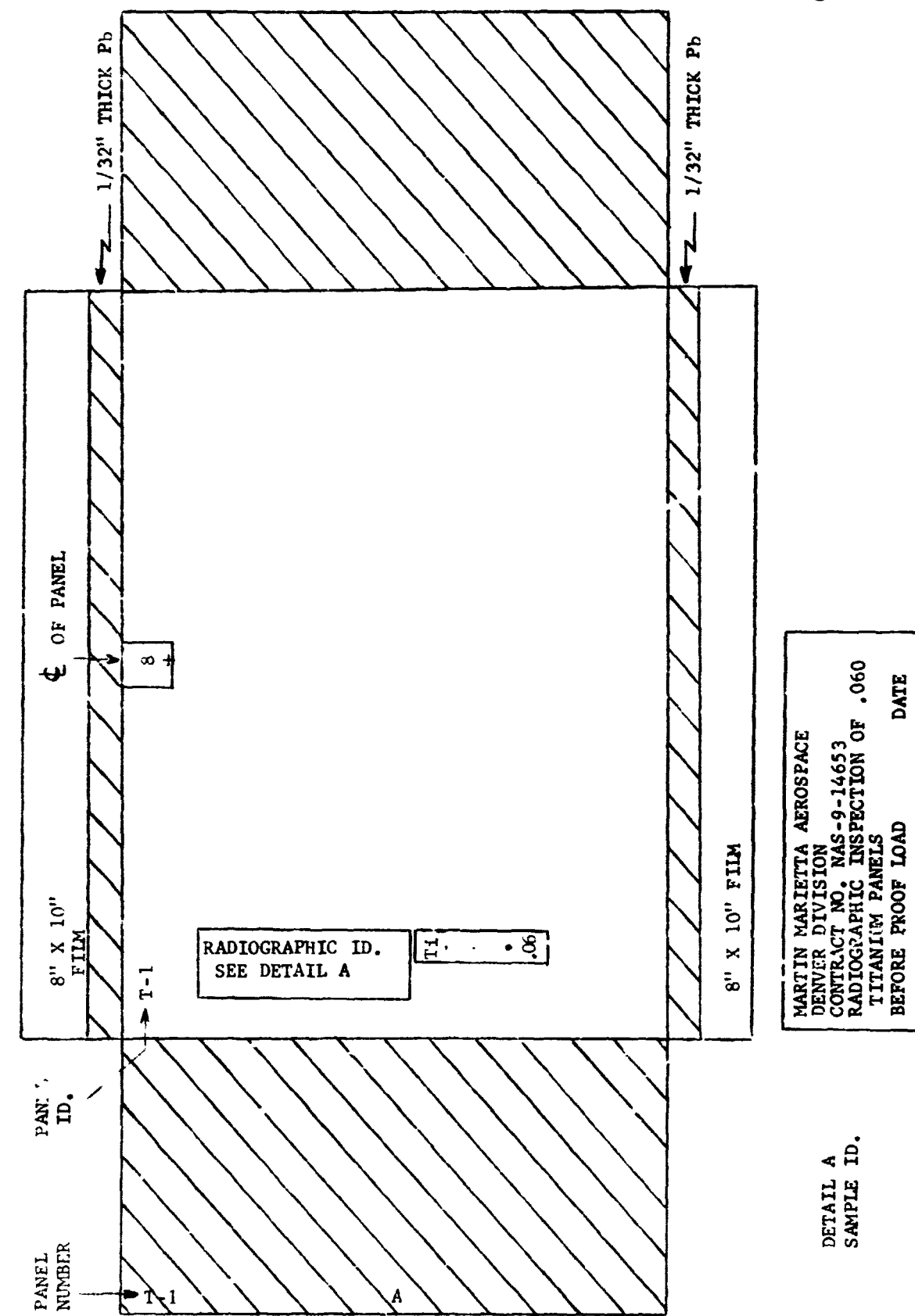


FIGURE 1

QUALITY LABORATORIES INSTRUCTION

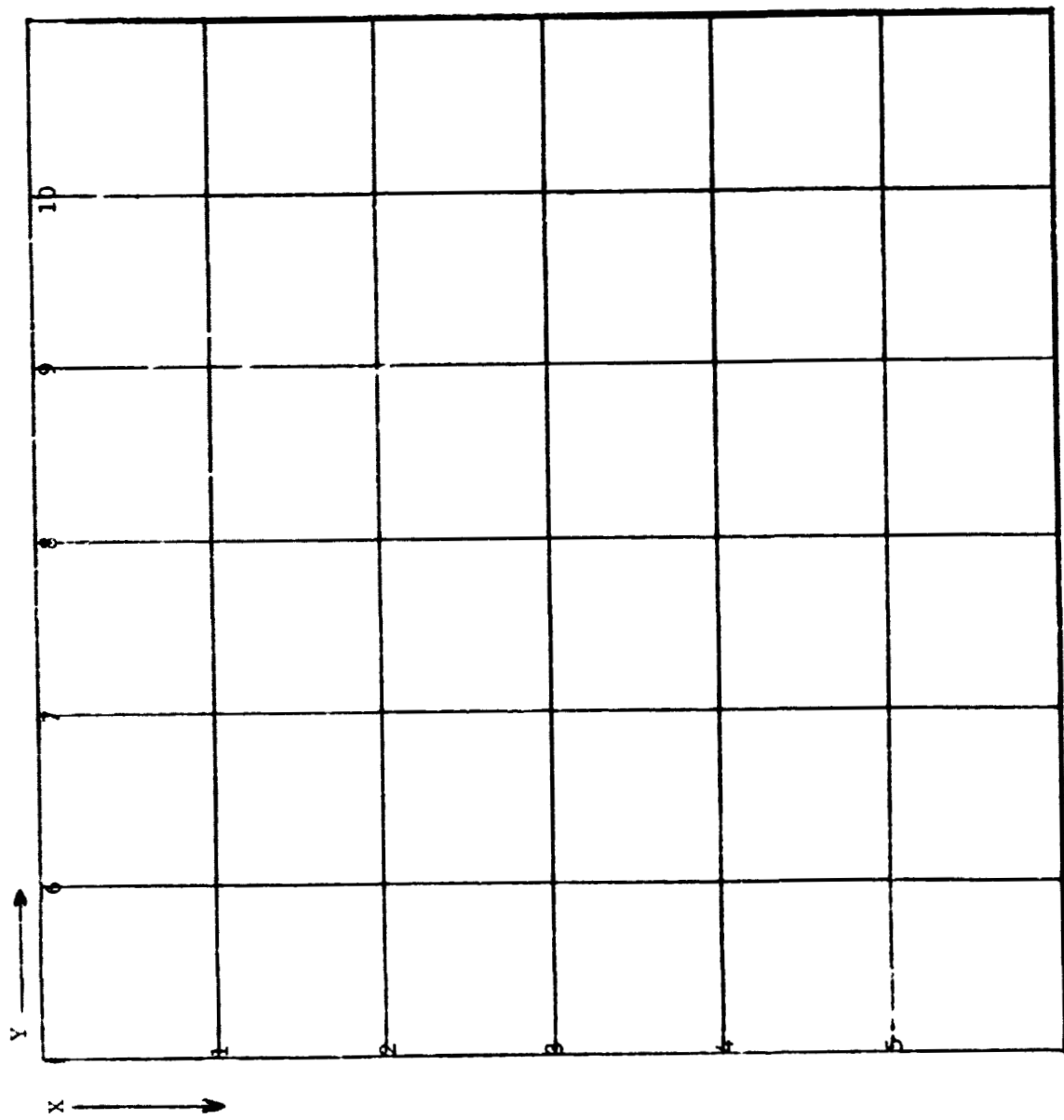


FIGURE 2
SAMPLE - GRID PATTERN LAYOUT

X-22
Page 7 of 7

APPENDIX B

MARTIN MARIETTA**QUALITY LABORATORIES INSTRUCTION**

Division	Number
DENVER	
Subject	Page 1 Of 3
LIQUID PENETRANT INSPECTION PROCEDURE FOR FATIGUE CRACK DETECTION	Issued
	Revised
	Approved
	<i>Mark J. Russell</i>

1.0 SCOPE

- 1.1 This procedure describes liquid penetrant inspection of titanium and steel plate for detecting fatigue cracks.

2.0 REFERENCES

- 2.1 Uresco Corporation Data Sheet No. PN-100
- 2.2 Non-destructive Testing Training Handbooks Pl-4-2, Liquid Penetrant Testing, General Dynamics Corporation, 1967.
- 2.3 Nondestructive Testing Handbook, McMasters Ronald Press, 1959, Volume I, Sections 6,7 and 8.

3.0 EQUIPMENT AND MATERIALS

- 3.1 Uresco P-149 High Sensitive Fluorescent Penetrant
- 3.2 Uresco K-410 E Spray Remover
- 3.3 Uresco D499C Spray Developer
- 3.4 Cheese Cloth
- 3.5 Ultraviolet light source (Magnaflux Black-Ray B-100 with General Electric H-100, FL4, Projector flood lamp and Magnaflux 3901 filter.
- 3.6 Quarter inch paint brush
- 3.7 Isopropyl Alcohol
- 3.8 Rubber Gloves
- 3.9 Ultrasonic Cleaner (Branson Ultrasonic Power Pack Model 610)
- 3.10 Light Meter, Weston Model 703, Type 3A
- 3.11 Trichloroethane

PRODUCIBILITY OF THIS
FINAL PAGE IS POOR

DIVISION	DATE	NUMBER	PAGE	OF
DENVER			2	3

4.0 PERSONNEL

- 4.1 The liquid penetrant inspection shall be performed by technically qualified personnel.

5.0 PROCEDURE

5.1 Clean panels to be penetrant inspected by immersing in trichloroethane in the ultrasonic cleaner and running for 1 hour; stack on tray and air dry for 15 minutes.

5.2 Lay panels flat on work bench and apply P-149 penetrant using a brush to the areas to be inspected. Allow a dwell time of 30 minutes.

5.3 Turn on the ultraviolet light and allow a warm up of 15 minutes.

5.3.1 Measure the intensity of the ultraviolet light and assure a minimum reading of 125 foot candles at 15" from the filter. (or 1020 micro watts per cm²)

5.4 After the 30 minute penetrant dwell time, remove the excess penetrant remaining on the panel as follows:

5.4.1 With dry cheese cloth, remove as much penetrant as possible from the surfaces of the panel.

5.4.2 With cheese cloth, dampened with K-410E, wipe remainder of surface penetrant from the panel.

5.4.3 Inspect the panel under ultraviolet light. If surface penetrant remains on the panel, repeat step 5.4.2.

NOTE: The check for cleanliness shall be done in a dark room with no more than two foot candles of white ambient light.

5.5 Spray developer D-499C on the panels by spraying from the pressurized container. Hold the container 6 to 12 inches from the area to be inspected. Apply the developer in a light, thin coat sufficient to provide a continuous film on the surface to be inspected.

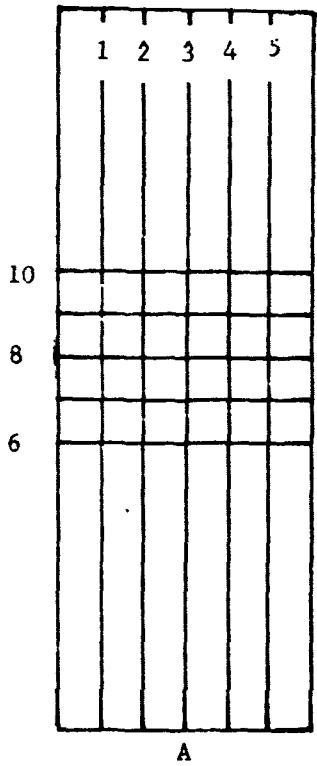
NOTE: A heavy coat of developer may mask possible defects.

5.6 After the 30 minute bleed out time, inspect the panels for cracks under black light. This inspection will again be done in a dark room.

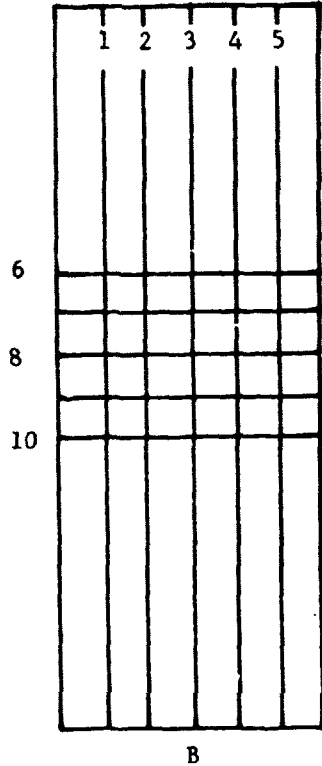
5.7 Using wire grid frame locate and record the grid coordinate of each crack on the NDT raw data coding sheet E232D-Mod.

DIVISION		DATE	NUMBER	PAGE	OF
	DENVER			3	3

5.8 Panel orientation and grid pattern layout



A



B

5.9 After readout is completed repeat Paragraph 5.1 and turn off ultraviolet light.

Division	Number
DENVER	Page 1 Of 7
Subject	Issued
ULTRASONIC INSPECTION FOR FATIGUE CRACK PROGRAM PANELS	Revised
	Approved: <i>[Signature]</i>

1.0 SCOPE

- 1.1 This procedure covers ultrasonic inspection for detecting fatigue cracks in thin titanium and steel plate.

2.0 REFERENCES

- 2.1 Manufacturer's instruction manual for the UM-715 Reflectoscope instrument.
- 2.2 Nondestructive Testing Training Handbook, P1-4-4, Volumes I, II and III, Ultrasonic Testing, General Dynamics 1967.
- 2.3 Nondestructive Testing Handbook, McMasters, Ronald Press, 1959, Volume II, Sections 43-48.

3.0 EQUIPMENT

- 3.1 UM-715 Reflectoscope, Automatic Industries
- 3.2 10N Pulser/Receiver, Automation Industries
- 3.3 E-550 Transigate, Automation Industries
- 3.4 5MHz, .375 inch dia., flat, I30506 Transducer, Harisonic, S/N-N123
- 3.5 SR 150 Budd, Ultrasonic Bridge
- 3.6 319DA Alden, Recorder
- 3.7 Calibration Panel and Reference Panels

4.0 PERSONNEL

- 4.1 The ultrasonic inspection shall be performed only by technically qualified personnel.

5.0 PROCEDURE

- 5.1 Set up equipment per attached set-up sheet.

DIVISION	DATE	NUMBER	PAGE	OF
DENVER			2	7

- 5.2 Submerge the appropriate case 1 reference panel in the tank of water and position the transducer to produce a maximum reflected signal from the appropriate flaw.

NOTE: Before submerging the steel panels in water, add to the water a rust inhibitor. (.015% Sodium Chromate and .015% Sodium Nitrite, by wt.)

- 5.2.1 The appropriate flaw shall be the smallest detectable flaw in the case panels (i.e. flaw #2 in the Thick Titanium Case 1 Panel - see Figure 2.).

- 5.3 Adjust the sensitivity control for a signal amplitude as shown in photographs 1 and 2 for the respective flaw orientations.

- 5.4 Scan the reference panel at the sensitivity setting established in paragraph 5.3 for both near surface and far surface flaw conditions. Compare these recordings to the reference recordings 1 and 2 and make any necessary adjustments.

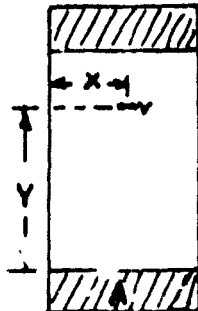
- 5.5 Submerge and scan the production panels two at a time, inspecting only from side A to obtain similar recordings.

- 5.6 When removing panels from water, thoroughly dry by wiping with cheese cloth.

- 5.7 On the data sheet, note the locations of each crack giving "X" and "Y" coordinates as noted by grid locators shows in Figure 1.

Figure 1 Orientation and Dimensioning of the Panels.

Side I



DIVISION DENVER	DATE	NUMBER	PAGE 3 OF 7
--------------------	------	--------	-------------

ULTRASONIC SET-UP SHEET

Method: Shear Wave Pulse/Echo @ 14.9° incident angle in water for Titanium and 15.1° for Steel. This angle was found to be optimum for detecting flaws lying on the near and far side of the panel with a single scan.

Instrument: UM-715 Reflectoscope with ION Pulser/Receiver and E-550 Transigate.

Pulse Length: Minimum

Pulse Tuning: Tuned for Maximum response

Reject: 12:00 O'clock

Sensitivity: Titanium: 1×10
Steel: 2×10

Frequency: 5 MHz

Gate Start: ~ 4

Gate Length: ~ 3

Transducer: 5 MHz, .375" dia., Flat, I30506, S/N N-123 Harisonic

Water Path: 2.5 inches

Write Level: + Auto Reset

Part: Flat, 0.250" and 0.060" thick, titanium and Steel Fatigue Crack Panels.

NOTE: When inspecting thin steel panels increase the angle slightly but not to exceed 15.75° and adjust gate accordingly.

Specific information for final Sensitivity and Gate settings:

The following sweep and marker settings are required to obtain the presentations shown in Photos 1 and 2 when the transducer is looking at flaw #2 of Panel # Case 1 of the Thick Ti Panel group.

Markers:

very coarse: 2
coarse: fccw
fine: fccw

Sweep Delay:

very coarse: 2
coarse:
fine: fccw

Sweep:

very coarse: .1
coarse: 1
fine: Min.

DIVISION	DENVER	DATE	NUMBER	PAGE	OF
----------	--------	------	--------	------	----

4 7

Photo 1 is with flaw #2 up (near side) and Photo #2 is with flaw #2 down (far side)

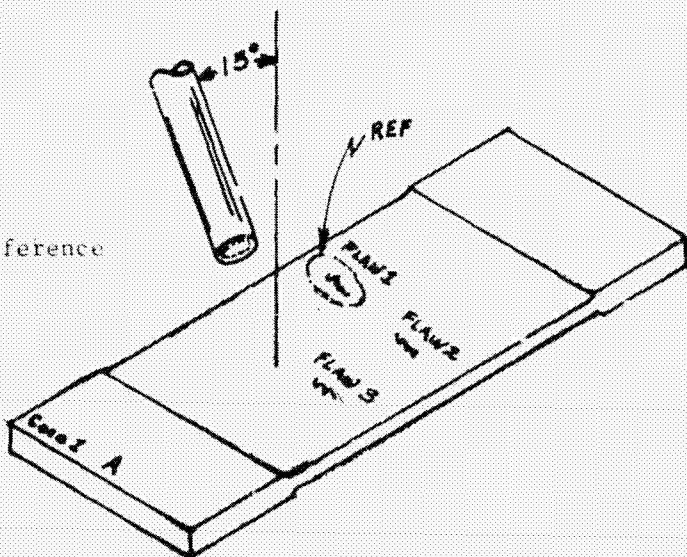


Figure 2: Thick Titanium Reference Panel, Case 1

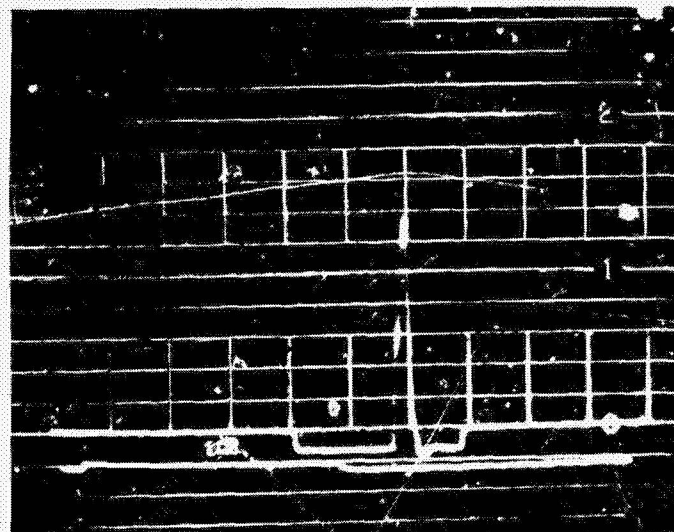
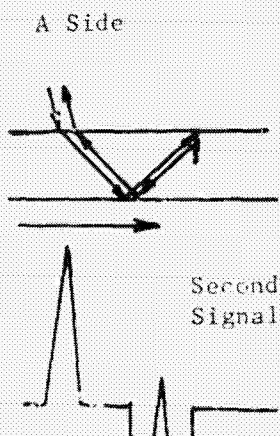
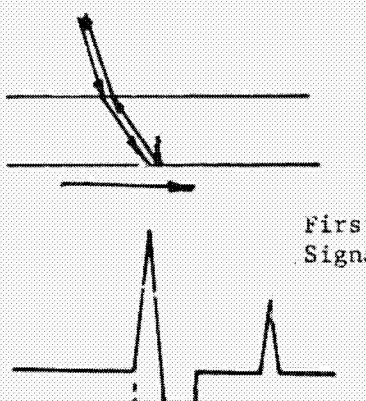


Photo #1 "A" scan presentation of flaw #2 contained in Case 1, Thick, Titanium, Reference Panel when flaw #2 is at near surface to the transducer.

DIVISION	DENVER	DATE	NUMBER	PAGE 5	OF 7
----------	--------	------	--------	-----------	---------

B Side



First
Signal

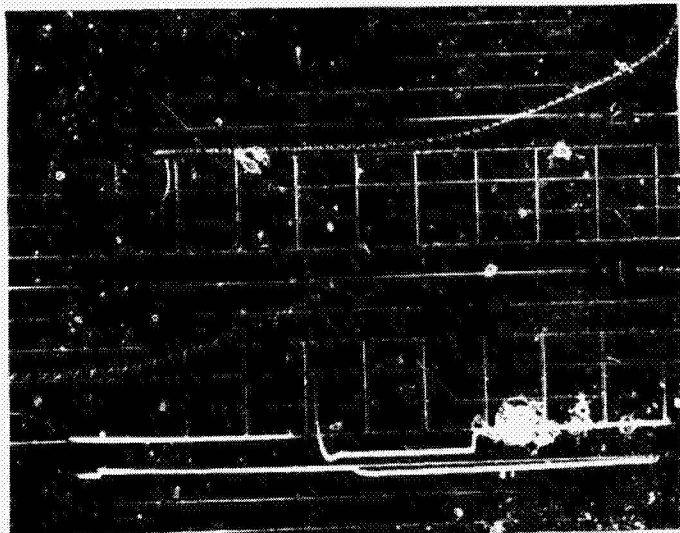


Photo #2 "A" scan presentation of flaw #2 contained in Case 1, Thick, Titanium, Reference Panel when flaw #2 is at far surface from transducer.

DIVISION	DENVER	DATE	NUMBER	PAGE 6 OF 7
----------	--------	------	--------	----------------

Side B



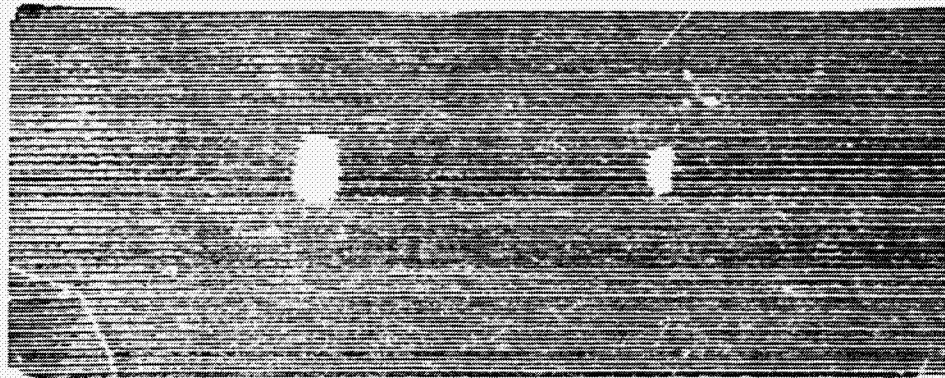
Recording #1: "C" scan presentation of flaws contained in Case 1, Thick, Titanium Reference Panel with flaws at far surface.



Side A

Recording #2: "C" scan presentation of flaws contained in Case 1, Thick Titanium Reference Panels with flaws at near surface.

DIVISION	DENVER	DATE	NUMBER	PAGE 7	OF 7
----------	--------	------	--------	-----------	---------



Recording #3: "C" scan presentation of flaws contained in Case 1, Thick, Steel Reference Panel with flaws at near surface (Side A).



Recording #4: "C" scan presentation of flaws contained in Case 1, Thick Steel Reference Panel with flaws at far surface (Side b)

APPENDIX D

MARTIN MARIETTA**QUALITY LABORATORIES INSTRUCTION**

Division	Number
DENVER	
Subject	Page
EDDY CURRENT INSPECTION AND C-SCAN RECORDING OF TITANIUM PANELS	1 Of
	Issued
	Revised
	Approved
	<i>Walter Schumel</i>

1.0 SCOPE

- 1.1 This procedure covers eddy current C-scan inspection detecting fatigue flaws in titanium panels.

2.0 REFERENCES

- 2.1 Manufacturer's instruction manual for the NDT instruments Model Vector 111 Eddy Current Instrument.
- 2.2 Nondestructive Testing Training Handbooks, P1-4-5, Volumes I and II, Eddy Current Testing, General Dynamics, 1967.
- 2.3 Nondestructive Testing Handbook, McMasters, Ronald Press, 1959, Volume II, Sections 35-41.

3.0 EQUIPMENT

- 3.1 NDT Instruments Vector 111 Eddy Current Instrument.
- 3.1.1 3 MHz pencil probe for Vector 111.
- 3.2 SR 150 Budd, Ultrasonic Bridge.
- 3.3 319DA Alden, Recorder.
- 3.4 Special Probe (3-axis motion) Scanning Fixture.
- 3.5 Dual DC Power Supply; 0-25V, 0-1A (HP Model 6227B or equivalent).
- 3.6 NDE Thin Titanium reference panel No. 17.
- 3.7 NDE Thick Titanium reference panel case No. 1.
- 3.8 Special Eddy Current Recorder Controller (SECR) circuit.

4.0 PROCEDURE

- 4.1 Connect 3 MHz probe to Vector 111 instrument. Use wire loop cable support to prevent probe cable from contacting large metal masses.
- 4.2 Turn instrument power on and set SENSITIVITY COURSE control to position 1.
- 4.3 Check batteries by operating power switch to BAT position. Batteries should be checked every two hours of use. Meter should read above 70.

DIVISION	DATE	NUMBER	PAGE	OF
DENVER			2	

4.4 Connect C-scan/Recorder Controller Circuit

4.4.1 Set Power Supply for +16 volts and -16 volts.

4.4.2 Set U/S-E/C switch to E/C.

4.4.3 Set OP AMP switch to OPR.

4.4.4 Set RUN/RESET switch to RESET.

4.5 Set up NDT panel scanning support fixture as follows:

4.5.1 Clamp an end scan plate of the same thickness as the NDT panel to the support fixture. One panel will be scanned at a time.

4.5.2 Align the end scan plate, using one panel so that the direction of the scan probe will be perpendicular to the long dimension of the panel.

4.5.3 Use shims or clamps to provide smooth scan transition between panel and end plates. Use weights on thin panels as required.

4.6 Set Vector 111 controls to the following preliminary values:

"X" 345.0

"R" 416.0

SENSITIVITY, COURSE 6, FINE 10.

MANUAL/AUTO switch to MAN.

4.7 Set the Recorder controls for scanning as follows:

Index Step Increment - .020 inch

Carriage Speed - .029

Scan Limits - set to scan 1½ inches beyond the panel edge.

Bridge switch - OFF

Scan Switch - OFF

4.8 Postion the 3 MHz pencil probe in the tracking shoe. Use a smooth panel for these preliminary probe offset and lift-off compensation adjustments. Extend the probe until it touches the panel. Using a .003 inch non-conductive shim, determine the meter deflection due to the shim (temporarily reduce gain if response is greater than 80 scale units) remove shim. Carefully pull probe out of holder (i.e. away from panel) until meter indicates 30 to 50% of shim deflection value. (Probe is properly spaced away from panel to prevent probe tip wear). Return gain to previous setting.

4.9 Using the scale control on Vector 111, verify that the LED indicator on SECR circuit goes off for a meter indication of 39 to 40. Adjust the E/C reference pot on SECR if needed.

DIVISION	DATE	NUMBER	PAGE OF
DENVER			3

- 4.10 Place the appropriate reference panel in scanning fixture and position the panel to correspond with the indicated reference mark. Use hold-down blocks for thin panels. Place end-scan plates in position. Verify that the tracking shoe makes contact with the panel.
- 4.11 Using the .003 inch shim and with probe at 3-8 location, adjust only the X control for lift-off null. When the difference between "shim in" and "shim out" indications is within one scale division, lift-off is compensated.
- 4.12 Position the scan probe near the center (X dimension) of the panel. Manually move the bridge through the Y grid range of 6 to 10 and set the Scale control so that the average (background) indication is 36 to 36 (set at 38 or slightly less if possible). If a flaw is encountered the meter indication should be greater than 40, but the background should be not greater than 38.
- 4.13 Position the bridge so that the scan probe is at Y grid marker number 10. Place BRIDGE switch to ON and SCAN switch to ON.
- 4.14 Initiate the Recorder/Scan function.
- 4.15 Annotate recording with panel number, side, "X" and "R" settings, date, test method and operator.
- 4.16 Set BRIDGE and SCAN switches to OFF.
- 4.17 Verify recording just obtained corresponds to the appropriate reference panel recordings shown herein.
- 4.18 Perform steps 4.10 through 4.16 to scan remaining panels. At the completion of inspection on the NDT panels, repeat steps 4.11 through 4.17 using the appropriate reference panel.
- 4.19 Evaluate recordings for flaws and enter panel, flaw location, side and length data on applicable data coding sheet. Observe correct orientation of reference edge of each panel side when measuring location of flaws. Also enter data for test method, sequences, operator and material.

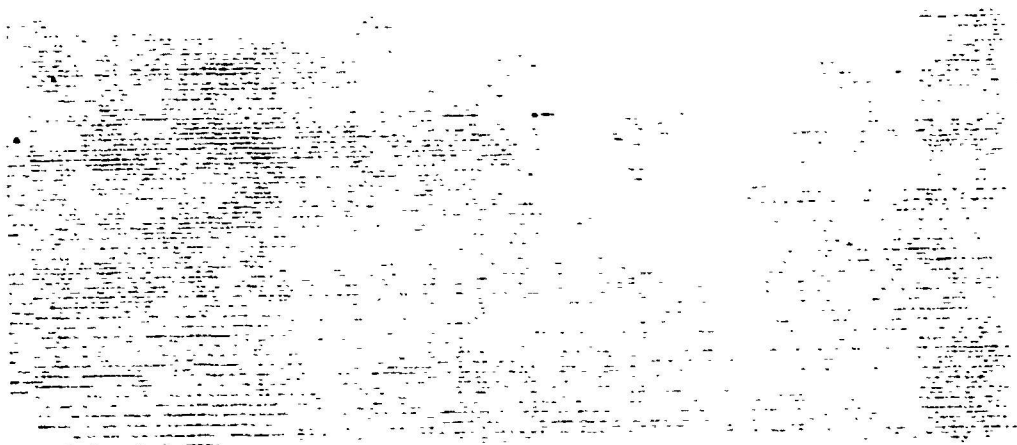
5.0 PERSONNEL

- 5.1 Only qualified personnel shall perform inspection.

6.0 SAFETY

- 6.1 Operation should be in accordance with Standard Safety Procedure used in operating any electrical device.

DIVISION		DATE	NUMBER	PAGE	OF
	DENVER			4	



Thin Titanium No. 17



Thick Titanium, Case No. 1

NDE TITANIUM REFERENCE PANELS

MARTIN MARIETTA

APPENDIX E

QUALITY LABORATORIES INSTRUCTION

Division	Number
DENVER	
Subject	Page 1 Of Issued
EDDY CURRENT INSPECTION AND C-SCAN RECORDING OF STEEL PANELS	Revised

Ward, Personnel

1.0 SCOPE

1.1 This procedure covers eddy current C-scan inspection detecting fatigue flaws in steel panels.

2.0 REFERENCES

- 2.1 Manufacturer's instruction manual for the NDT instruments Model Vector 111 Eddy Current Instrument.
- 2.2 Nondestructive Testing Training Handbooks, P1-4-5, Volumes I and II, Eddy Current Testing, General Dynamics, 1967.
- 2.3 Nondestructive Testing Handbook, McMasters, Ronald Press, 1959, Volume II, Sections 35-41.

3.0 EQUIPMENT

3.1 NDT Instruments Vector 111 Eddy Current Instrument.

3.1.1 500 KHz differential probe for Vector 111.

3.2 SR 150 Budd, Ultrasonic Bridge.

3.3 '9DA Alden, Recorder. REPRODUCIBILITY OF 1.
ORIGINAL PAGE IS POOR

3.4 Special Probe (Flat Block) Scanning Fixture.

3.5 Dual DC Power Supply; 0-25V, 0-1A (HP Model 6227B or equivalent).

3.6 NDE Steel reference panel Case No. 3.

3.7 Special Eddy Current Recorder Controller (SECR) circuit.

4.0 PROCEDURE

4.1 Connect 500 KHz differential probe to Vector 111 instrument.

4.2 Turn instrument power on and set SENSITIVITY COURSE control to position 1.

4.3 Check batteries by operating power switch to BAT position. Batteries should be checked every two hours of use. Meter should read above 70.

DIVISION	DATE	NUMBER	PAGE OF
DENVER			2

4.4 Connect C-scan/Recorder Controller Circuit

- 4.4.1 Set Power Supply for +16 volts and -16 volts.
- 4.4.2 Set U/S-E/C switch to E/C.
- 4.4.3 Set OP AMP switch to OPR.
- 4.4.4 Set RUN/RESET switch to RESET.

4.5 Set up NDT panel scanning support fixture as follows:

- 4.5.1 Clamp an end scan plate of the same thickness as the NDT panel to the support fixture. One panel will be scanned at a time.
- 4.5.2 Align the end scan plate, using one panel so that the direction of the scan probe will be perpendicular to the long dimension of the panel.
- 4.5.3 Use shims or clamps to provide smooth scan transition between panel and end plates. Use weights on thin panels as required.

4.6 Set Vector 111 controls to the following preliminary values:

"X" 410
 "R" 450
 SENSITIVITY, COURSE 4, FINE 0.
 MANUAL/AUTO switch to MAN.

4.7 Set the Recorder controls for scanning as follows:

Index Step Increment - .020 inch
 Carriage Speed - .029
 Scan Limits - set to scan 1½ inches beyond the panel edge.
 Bridge Switch - OFF
 Scan Switch - OFF

4.8 Position the probe in the tracking shoe of the scanning fixture so that the probe tip is recessed about .002 to .004 inch from the scan surface. Rotate the probe so that only one core at a time senses a flaw as the scan bridge moves incrementally.

4.9 Place the Reference panel in the scan fixture. Position the probe at the mid-point of the panel (i.e. 3-8 location). Adjust the X and R controls (and Scale control as required) for null condition.

4.10 Using the Scale control verify that the LED indicator on the SECR circuit goes off for a meter indication of 39 to 40. Adjust the E/C reference pot (on SECR) if required.

4.11 Manually move the probe through the Y grid range from 6 to 10 and set the Scale control for background indication of 30 to 36. (Background set point should be such that the recording does not have excessive background). Background set point should never exceed 38.

DIVISION	DATE	NUMBER	PAGE	OF
DENVER			3	

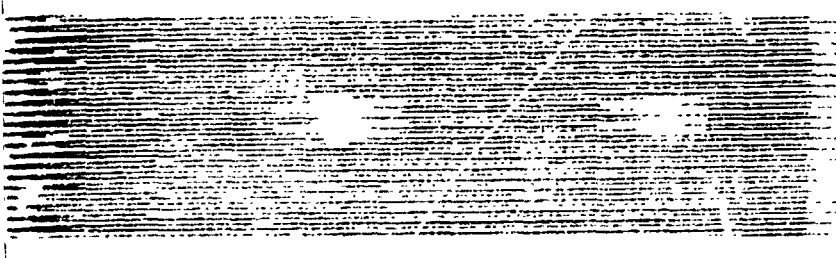
- 4.12 Position the bridge so that the probe is at Y grid number 10. Place BRIDGE and SCAN switches to ON.
- 4.13 Initiate the Recorder/Scan function. If background is excessive, perform step 4.15 then step 4.11 for lower background set point.
- 4.14 Annotate the recording with panel number, X and R settings, date, test method and operator.
- 4.15 Set BRIDGE and SCAN switches to OFF.
- 4.16 Verify recording just obtained corresponds to Reference panel recording shown herein.
- 4.17 Perform steps 4.9 through 4.15 to scan remaining panels. At the completion of inspection on the NDT panels, repeat steps 4.9 through 4.16 using the Reference panel.
- 4.18 Evaluate recordings for flaws and enter panel, flaw location side and length data on applicable data coding sheet. Observe correct orientation of reference edge of each panel side when measuring location of flaws. Also enter data for test method, sequence, operator and material.

5.0 PERSONNEL

- 5.1 Only qualified personnel shall perform inspection.

6.0 SAFETY

- 6.1 Operation should be in accordance with Standard Safety Procedure used in operating any electrical device.



NDE Steel Reference Panel Case No. 3

APPENDIX F

MARTIN MARIETTA**QUALITY LABORATORIES INSTRUCTION**

Division	Number
DENVER	
Subject	Page 1 Of 3
FLUORESCENT MAGNETIC PARTICLE INSPECTION FOR FATIGUE CRACK DETECTION	Issued
	Revised
	Approved <i>[Signature]</i>

1.0 SCOPE

- 1.1 This procedure describes magnetic particle inspection of steel plate specimens for detecting fatigue cracks.

2.0 REFERENCES

- 2.1 Nondestructive Testing Handbook P1-4-3, Magnetic Particle Testing, General Dynamics Corporation, 1967.
- 2.2 Nondestructive Testing Handbook, McMasters Ronald Press, 1959, Volume II Sections 30-32.
- 2.3 Principles of Magnetic Particle Testing, Carl E. Betz, Magnaflux Corporation, 1966.
- 2.4 MIL-I-6868, Inspection Process, Magnetic Particle.

3.0 EQUIPMENT AND MATERIALS

- 3.1 Stationary Magne-Tech Model 3509A, Uresco.
- 3.2 Demagnatizing Machine, Model 3534D, Uresco.
- 3.3 Field Strength Indicator, Uresco
- 3.4 Test Meter Kit, Uresco.
- 3.5 Gaussmeter, RFL Industries
- 3.6 Black light, Spot Type, Uresco
- 3.7 Ultraviolet Light Meter, Model S-221, Ultra-Violet Products, Inc.
- 3.8 Weston N. 703 Light Meter.
- 3.9 Ultrasonic Cleaner, Power Pack Model 610, Branson
- 3.10 Trichloroethane
- 3.11 Kerosene VV-K-220, Water White Deodorized.
- 3.12 Fluorescent Particle Powder #228, Uresco.
- 3.13 Wire screen grid for locating flaws.

DIVISION DENVER	DATE	NUMBER	PAGE 2	OF 3
<p>4.0 PERSONNEL</p> <p>4.1 The magnetic particle inspection shall be performed by technically qualified personnel.</p> <p>5.0 SOLUTION PREPARATION</p> <p>5.1 Mix 0.40 ounces of 228 (Uresco) Powder to 1 gallon of Kerosene, Federal Standard VV-K-220.</p> <p>5.2 Run the pump for a minimum of 30 minutes, and stir bath to put powder clinging to the sides and bottom of tank into suspension.</p> <p>5.3 Fill a 100-ml ASTM graduated centrifuge tube to the 100 ml mark with suspension directly from the hose. Demagnetize the suspension if considered necessary and let it stand for 30 minutes to precipitate or until the solid matter is apparently all down.</p> <p>5.4 Read the volume of precipitate in the graduate. The volume shall be 0.20 to 0.30 ml.</p> <p>5.5 If the particle volume does not meet 5.4 above add the appropriate amount of liquid or powder to bring the particle concentration into agreement with 5.4.</p> <p>6.0 PROCEDURE</p> <p>6.1 Assure all equipment and solutions conform to the requirements for the use specified (i.e., calibration, qualification, certification, etc.).</p> <p>6.2 Clean panels to be inspected by placing them in the ultrasonic cleaning unit (3.9) and covering them with trichloroethane.</p> <p>6.3 Turn on the ultrasonic cleaning unit and allow panels to be cleaned for (1) one hour.</p> <p>6.4 Stack panels on end and air dry for fifteen (15) minutes.</p> <p>6.5 Turn on ultraviolet light and allow a warm up time of fifteen (15) minutes.</p> <p>6.5.1 Measure the intensity of the ultraviolet light and assure a minimum reading of 1020 micro watts per cm^2 at 15" from the filter.</p> <p>6.6 Place the part between the contact plates and at 45° from the vertical with current flaw parallel to the 6" dimension and passing through the center 8 inches of the plate. (This is a circular magnetization method).</p> <p>6.7 Set the head pressure at 60 psi.</p>				

DIVISION DENVER	DATE	NUMBER	PAGE OF 3 3
--------------------	------	--------	----------------

6.8 With the part properly positioned on the magnetizing machine, set the current dial to the following settings:

<u>PANEL</u>	<u>DIAL SETTINGS</u>	<u>CURRENT READING</u>
Thin	74	2,200 amps.
Thick	76	3,000 amps.

6.9 Apply a flow of suspension, from the prepared solution, by hose to the positioned part. Assure the part is thoroughly saturated.

6.10 Remove the flow and immediately apply the current by pushing the energize button. Apply three (3) shots of current.

NOTE: The period of current flow is pre-set for approximately 1/2 second.

6.11 Examine the part under black light for fatigue cracks.

NOTE: This inspection will be done in a darkened area having no more than two foot candles of ambient light.

6.12 Using the wire grid (3.13) locate and record the grid coordinate for each crack.

6.13 After readout is complete remove panel from the magnetizing machine.

6.14 Place panel within the demagnetization coil (3.2) and unit on.

6.15 With the current still applied, slowly pull the part through and away from the coil until the part is at least 24" from the coil.

6.16 Check the part for evidence of magnetism using the Magnetic Field Indicator (3.3). If the indicator registers the presence of a magnetic field, repeat paragraphs 6.14 and 6.15 until there is no magnetic field indication.

6.17 After panels have been demagnetized clean the panels per paragraphs 6.2 through 6.4.